SCHOOL OF CIVIL ENGINEERING

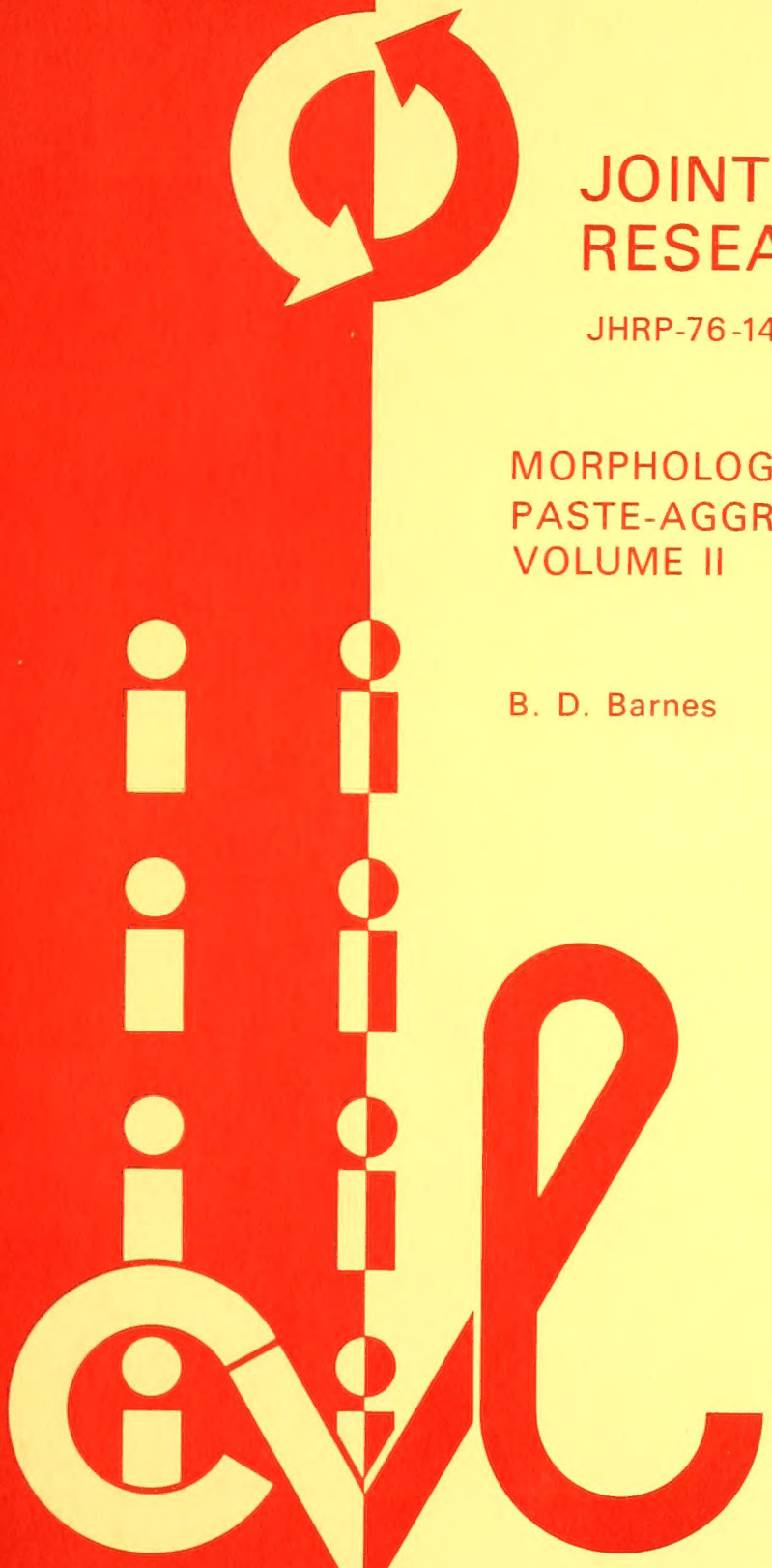

JOINT HIGHWAY RESEARCH PROJECT

JHRP-76-14

MORPHOLOGY OF THE PASTE-AGGREGATE INTERFACE VOLUME II

B. D. Barnes

PURDUE UNIVERSITY
INDIANA STATE HIGHWAY COMMISSION

TECHNICAL REPORT STANDARD TITLE PAGE

1. Report No.	2. Government Accession No.	3. Recipient's Catalog No.
JHRP-76-14		

4. Title and Subtitle	5. Report Date
MORPHOLOGY OF THE PASTE-AGGREGATE INTERFACE, VOLUME II	March 1976
	6. Performing Organization Code

7. Author(s)	8. Performing Organization Report No.
Bobby David Barnes	JHRP-76-14

9. Performing Organization Name and Address	10. Work Unit No.
Joint Highway Research Project Civil Engineering Building Purdue University W. Lafayette, Indiana 47907	11. Contract or Grant No. HPR-1(13) Part II
	13. Type of Report and Period Covered
12. Sponsoring Agency Name and Address Indiana State Highway Commission State Office Building 100 North Senate Avenue Indianapolis, Indiana 46204	Final Report
	14. Sponsoring Agency Code

15. Supplementary Notes

Prepared in cooperation with the U. S. Department of Transportation, Federal Highway Administration.
From the study, "Fundamental Studies of Portland Cement Concrete"

16. Abstract

The results of this study provide extensive new information on the nature and morphology of the interfacial zone between cement paste and aggregate and on crack development in concrete.

A thin "duplex film" of $Ca(OH)_2$ backed with a layer of C-S-H gel particles deposits directly on the aggregate surface; a few large $Ca(OH)_2$ crystals then develop and extend into the cement paste. A secondary deposit of thick $Ca(OH)_2$ crystals deposits later and effectively ties the duplex film to the cement paste.

An unusual pattern of cement hydration in which C_3S grains apparently dissolve out from within thin hydration product shells is confirmed, but this appears to have little effect on cracking.

These features occur for all types of portland cement examined irrespective of w:c ratio.

In mortars, fine cracks (ca. 1 um) were found within a zone of 40 um from the aggregate prior to loading and likely existing before drying. On compressive loading these extended near the interface until high stress levels initiated unstable crack propagation. Previous investigators apparently were unable to observe these fine preexisting cracks because of the inadequate resolving power of the methods used.

17. Key Words	18. Distribution Statement
Cement Paste; Concrete; Cement Hydration; Concrete Cracking	No restrictions. This document is available to the public through the National Technical Information Service, Springfield, Virginia 22161

19. Security Classif. (of this report)	20. Security Classif. (of this page)	21. No. of Pages	22. Price
Unclassified	Unclassified	175	

Form DOT F 1700.7 (8-69)

Final Report

MORPHOLOGY OF THE PASTE-AGGREGATE INTERFACE

VOLUME II

by

Bobby David Barnes
Graduate Instructor in Research

Joint Highway Research Project

Project No.: C-36-61E

File No.: 5-14-5

Prepared as Part of an Investigation

Conducted by

Joint Highway Research Project
Engineering Experiment Station
Purdue University

in cooperation with the

Indiana State Highway Commission

and the

U.S. Department of Transportation
Federal Highway Administration

The contents of this report reflect the views of the author who is responsible for the facts and the accuracy of the data presented herein. The contents do not necessarily reflect the official views or policies of the Federal Highway Administration. This report does not constitute a standard, specification, or regulation.

Purdue University
West Lafayette, Indiana
March 16, 1976

APPENDIX VII

FIGURES

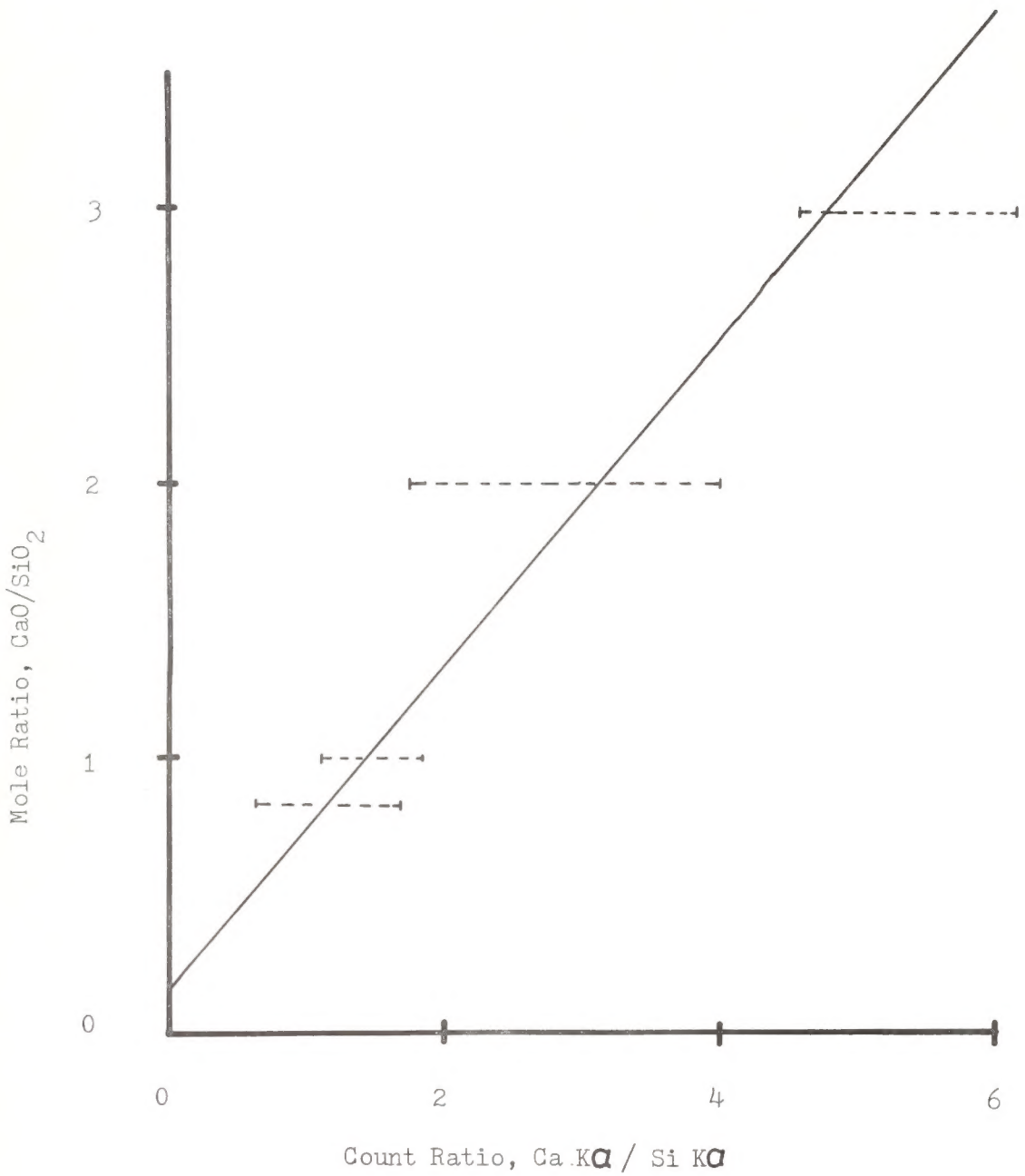

Figure 1. Calibration for CaO/SiO_2 Ratio

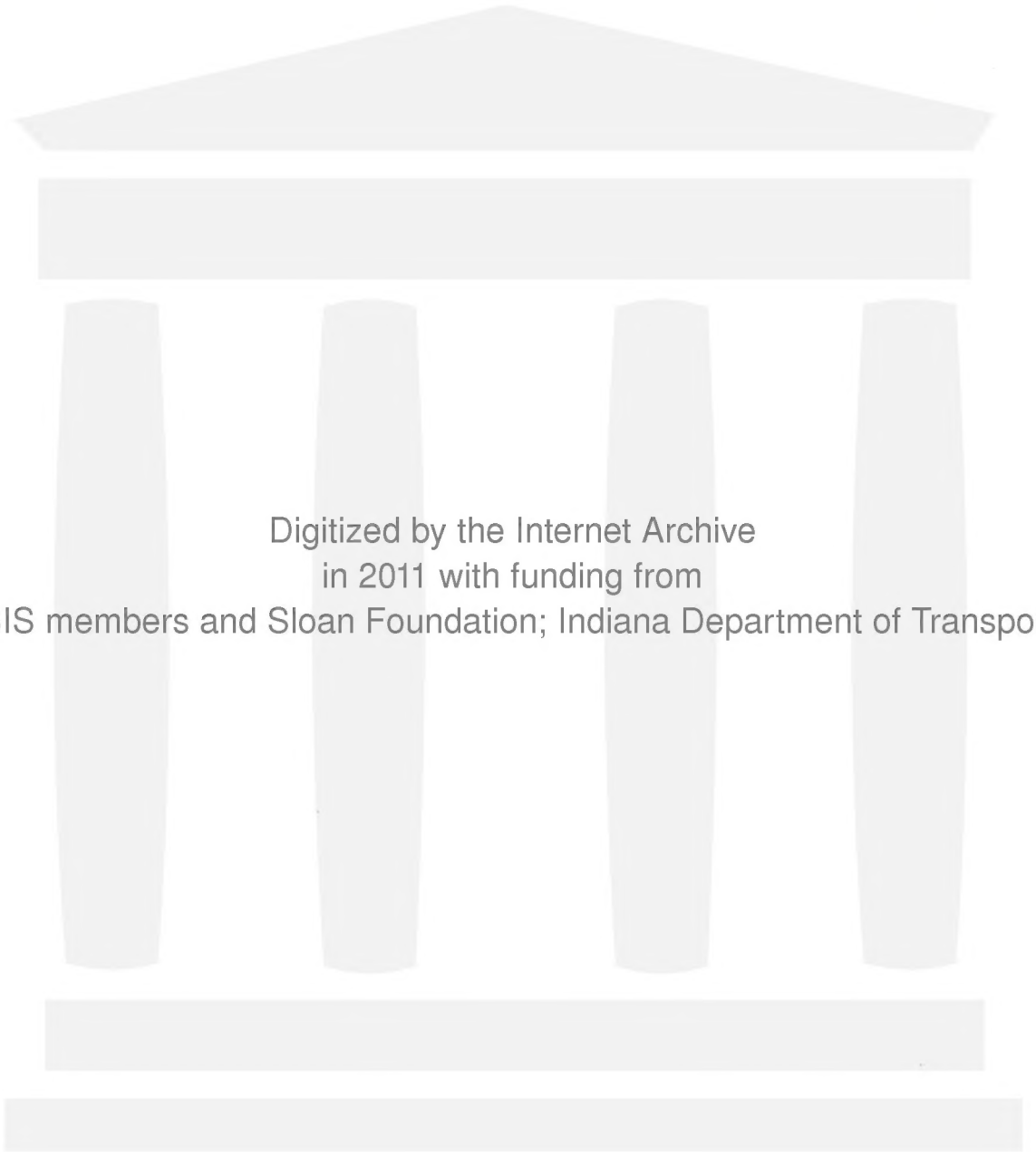

Digitized by the Internet Archive
in 2011 with funding from
LYRASIS members and Sloan Foundation; Indiana Department of Transportation

http://www.archive.org/details/morphologyofpast02barn

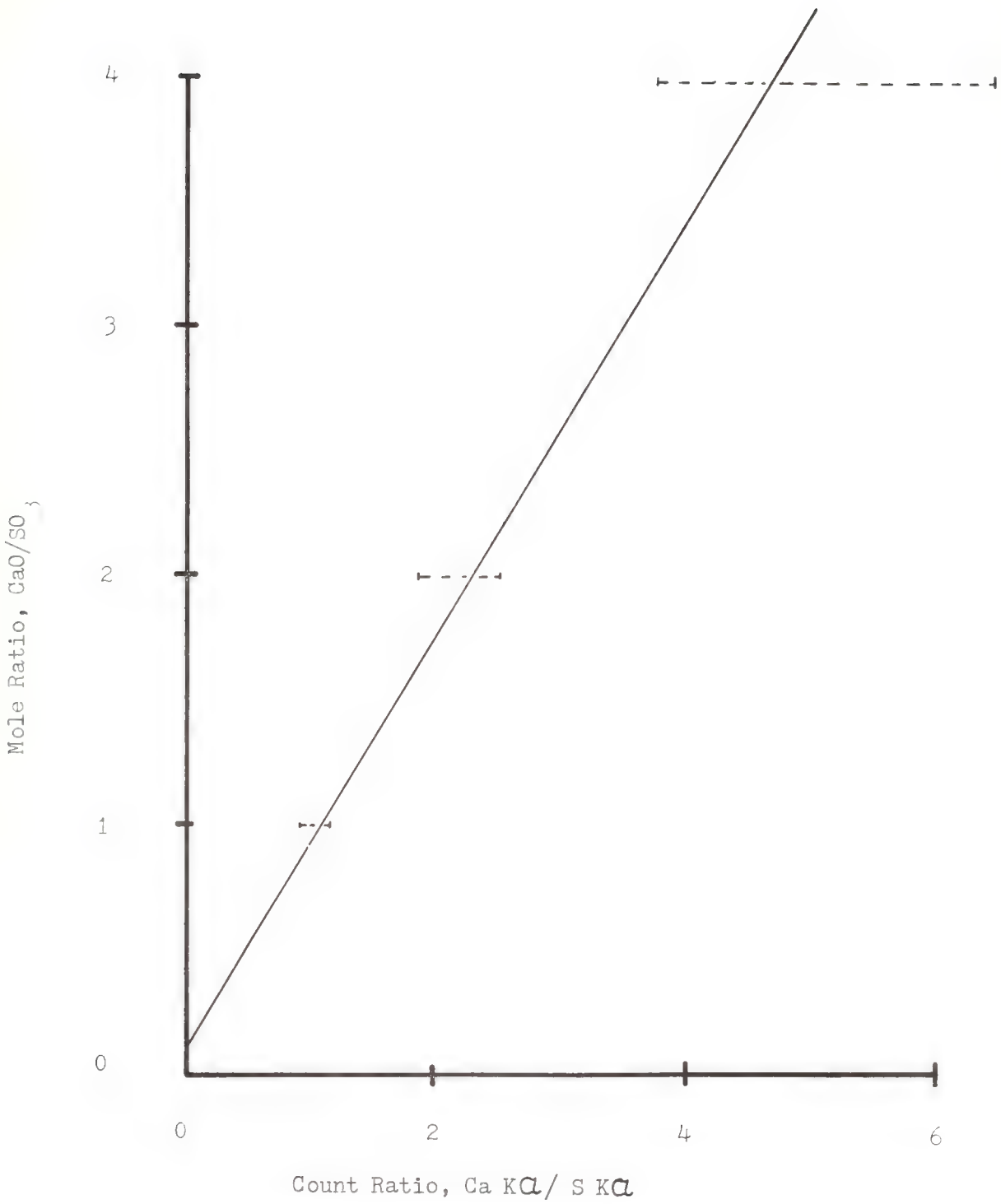

Figure 2. Calibration for CaO/SO_3 Ratio

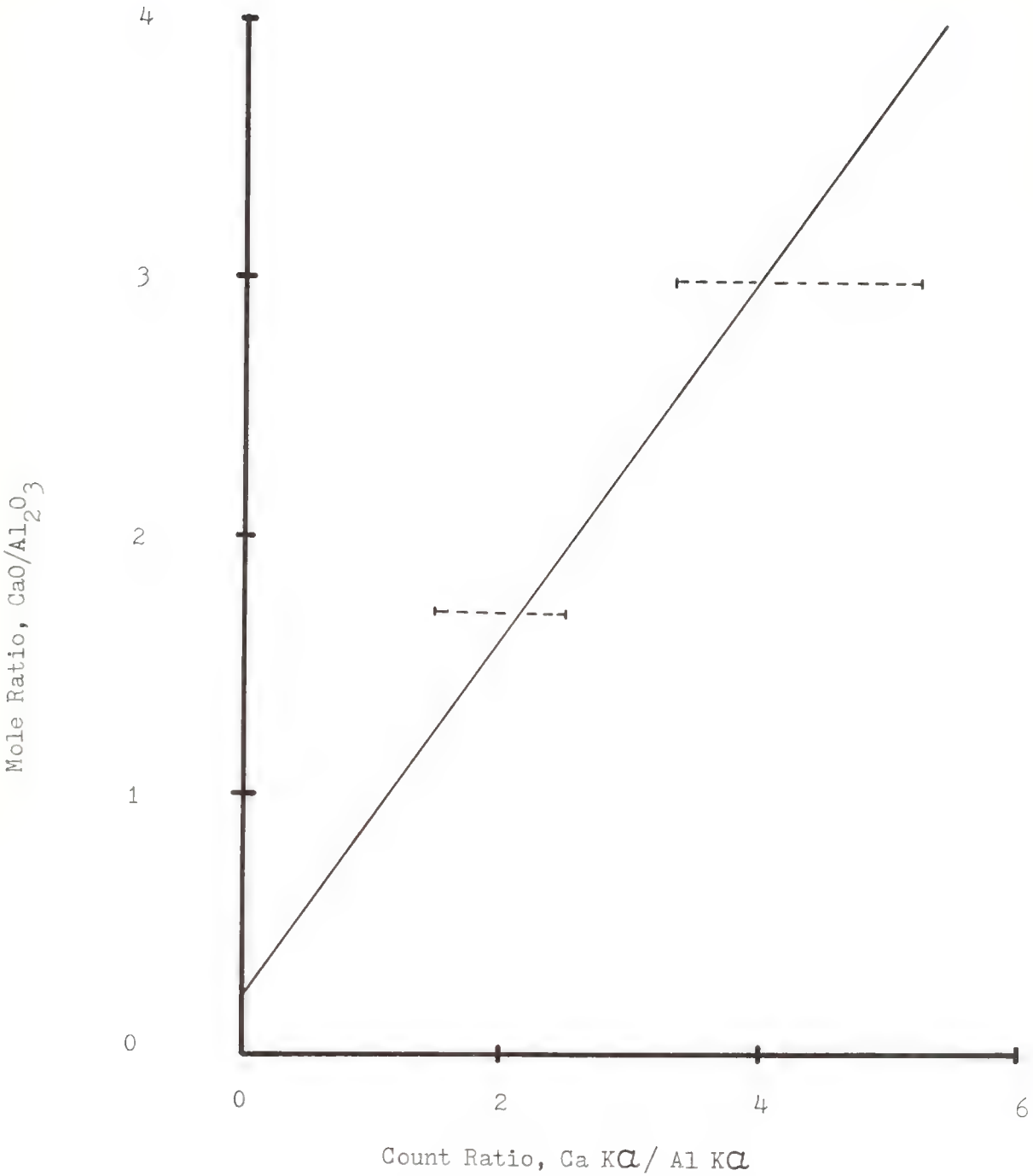

Figure 3. Calibration Curve for CaO/Al_2O_3

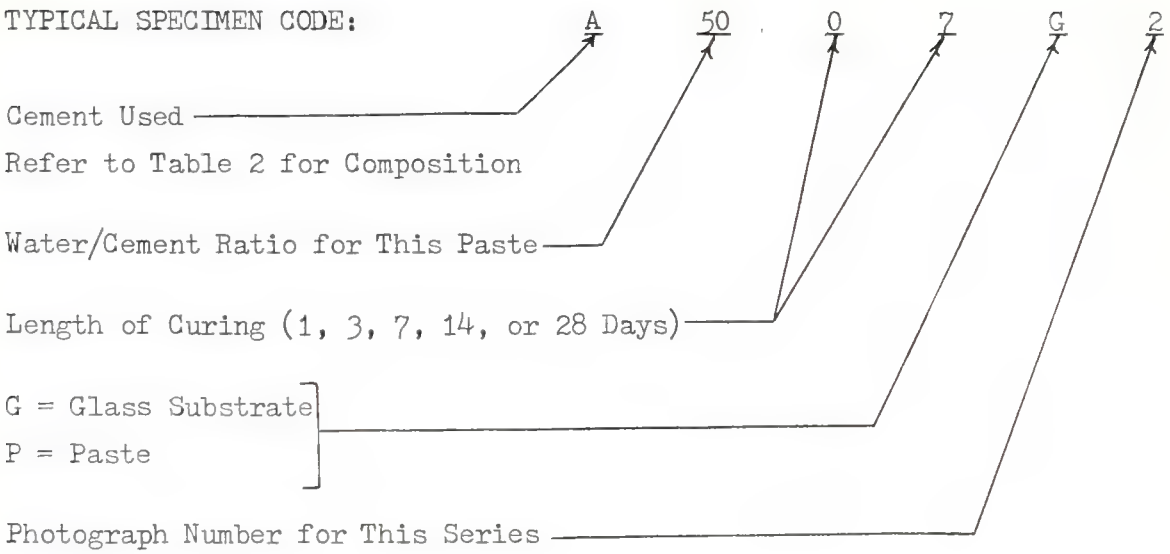

For Example: C6528P9

Means cement of composition C (Portland-Blast Furnace Slag) was used. The w/c ratio was 0.65. The time of hydration was 28 days. This is a picture of the paste.

Figure 4. Coding Key for Type I Specimens

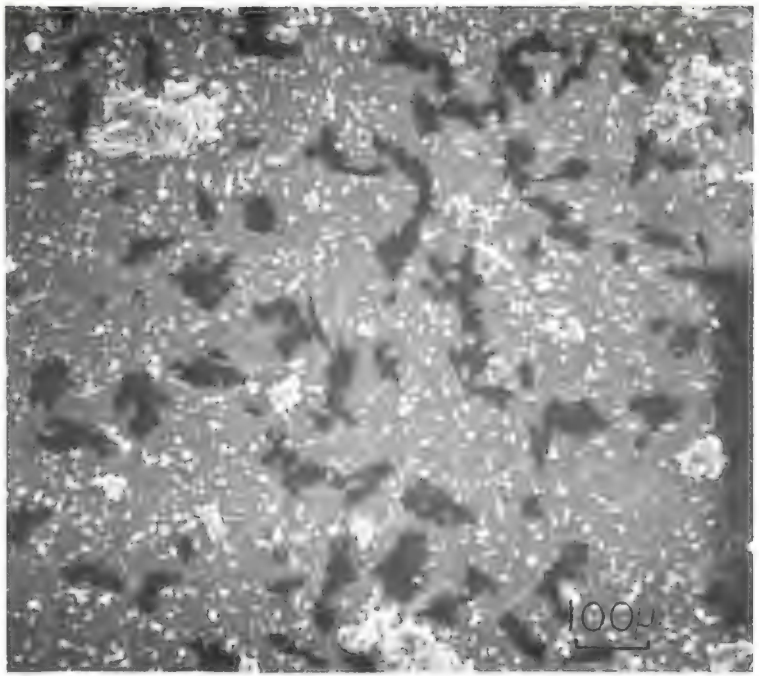

Figure 5. Low Magnification View of Hydration Products on Glass Substrate (A5001G1)

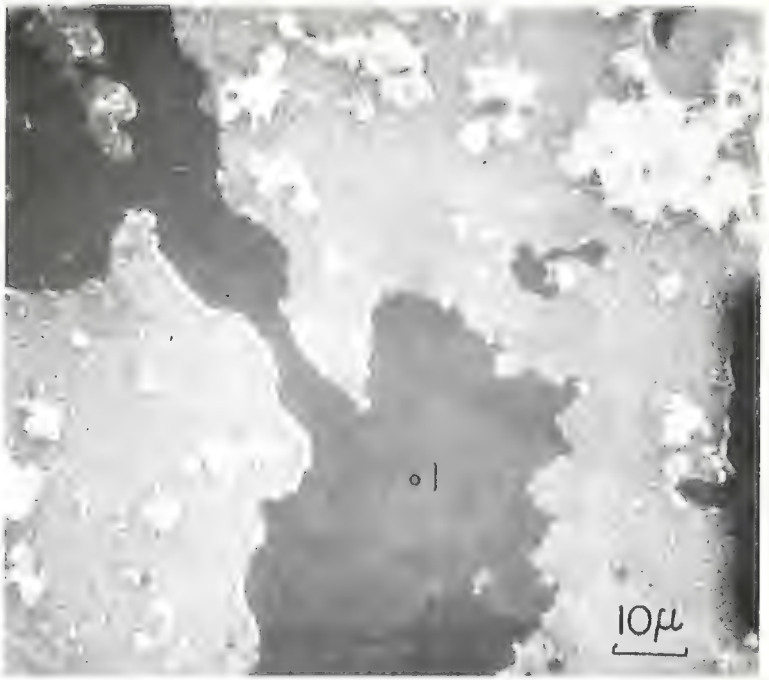

Figure 6. Enlargement of Material on Glass Substrate (A5001G2)

No.	C/S	C/A	C/$\bar{S}$
1	0.11	0.88	No SO_3

Figure 7. Close-up View of Grey Film Adhering to Substrate (A5001G3)

No.	C/S	C/A	C/$\bar{S}$
1	0.29	No A	No $\bar{S}$

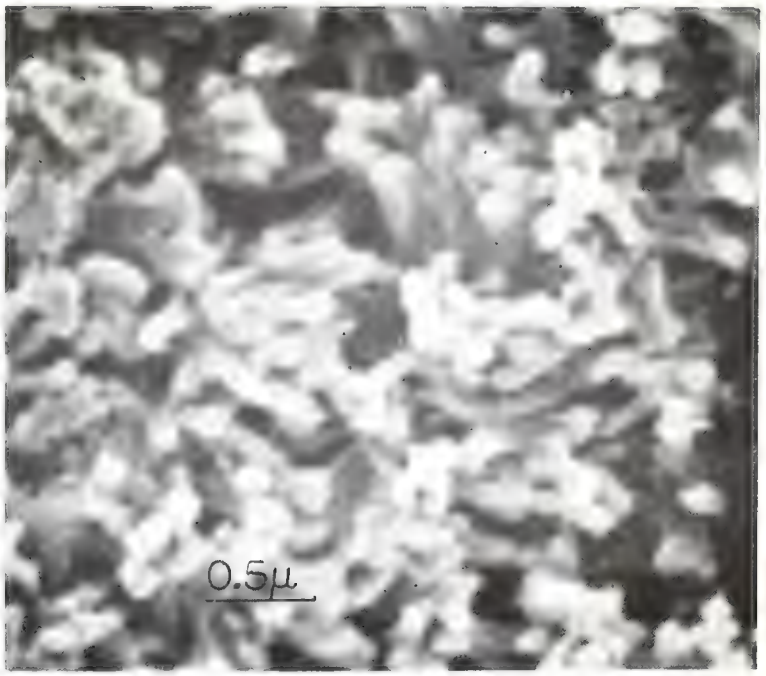

Figure 8. High Magnification of C-S-H Gel Shown in Figure 7 (A5001G4)

No.	C/S	C/A	C/$\bar{S}$
1*	0.28	No A	No $\bar{S}$

* Area EDXA

Figure 9. Low Magnification View of Hydration Products and Small Cement Grains on Glass (B5001G1)

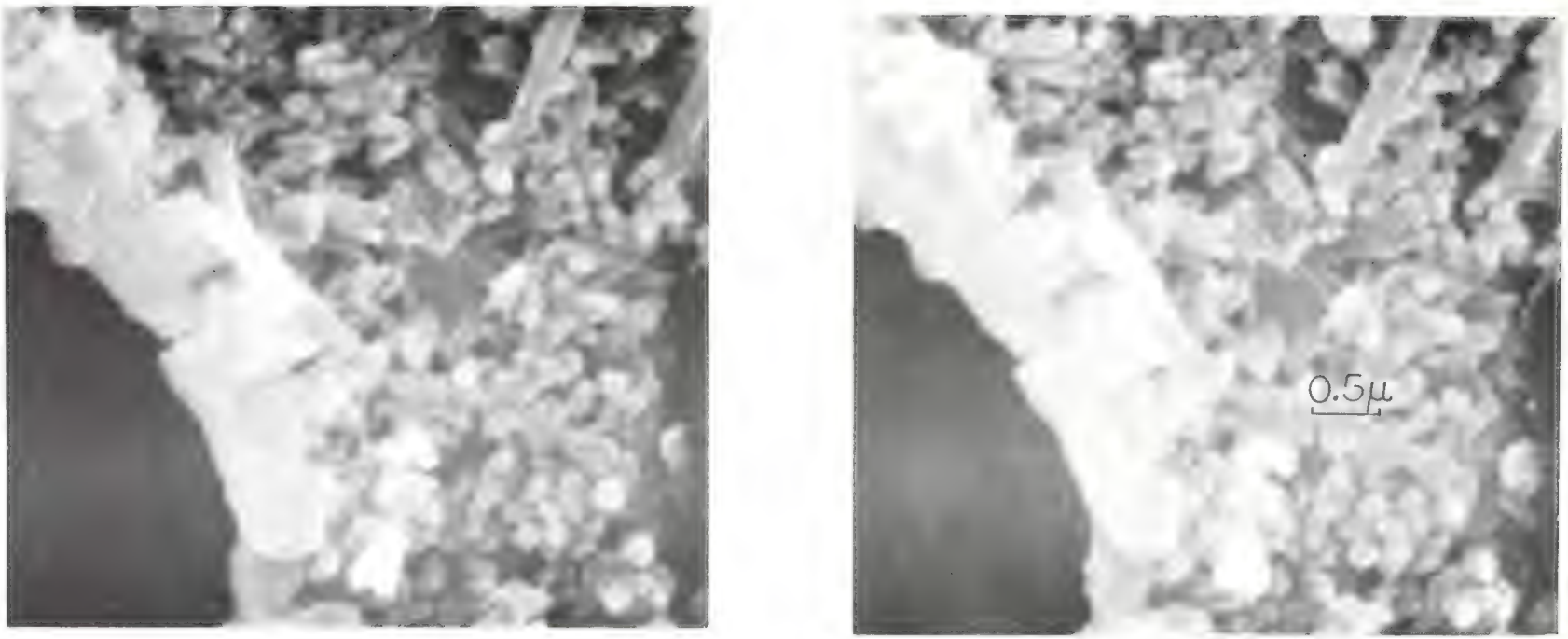

Figure 10. High Magnification Stereomicrograph of Duplex Film on Glass (B6501G2)

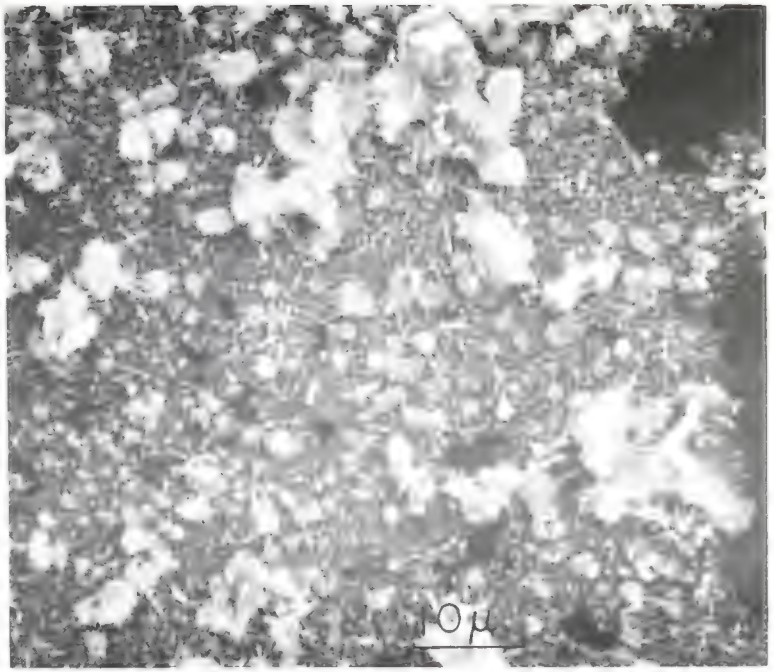

Figure 11. Numerous Small Cement Grains Lying on Duplex Film (C5001G2)

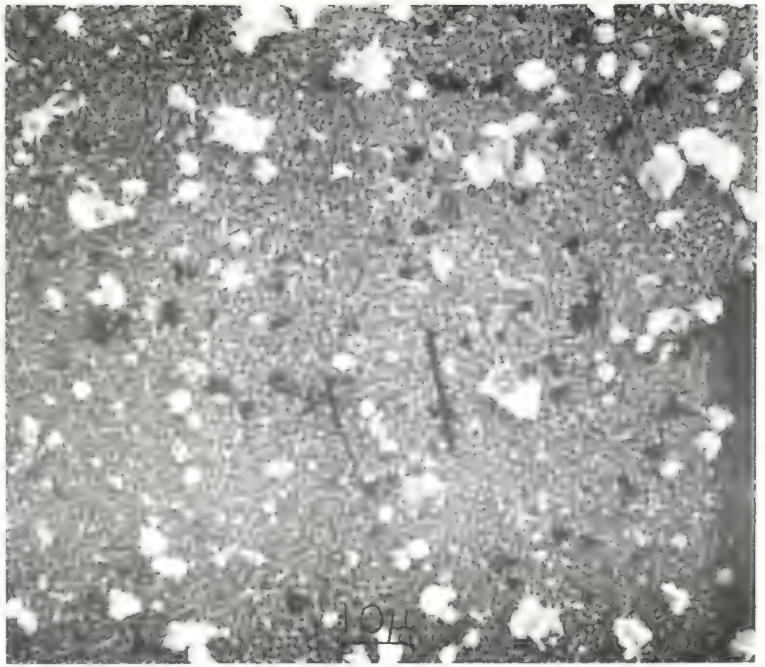

Figure 12. Duplex Film and Cement Grains on Glass (C6501G4)

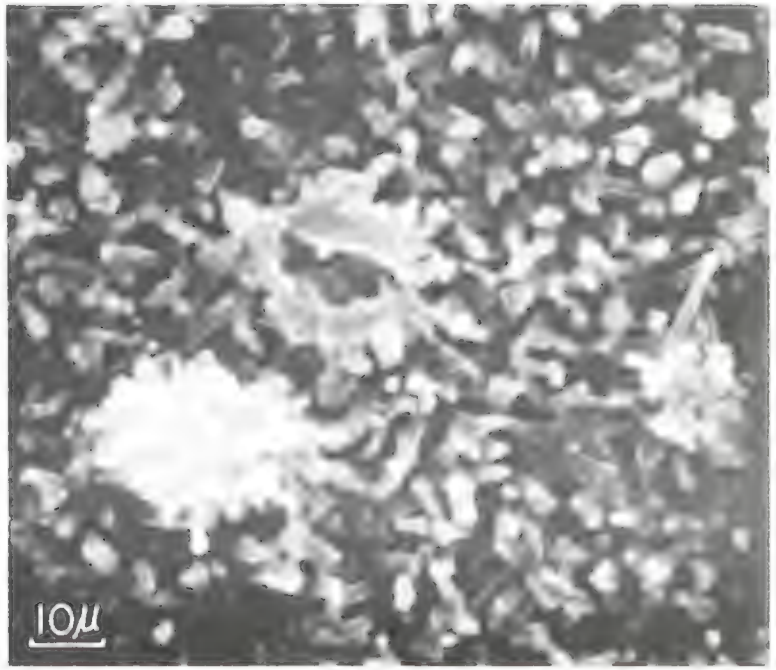

Figure 13. Residual Shell From an Approximately One Micrometer Diameter Cement Grain (C6501G5)

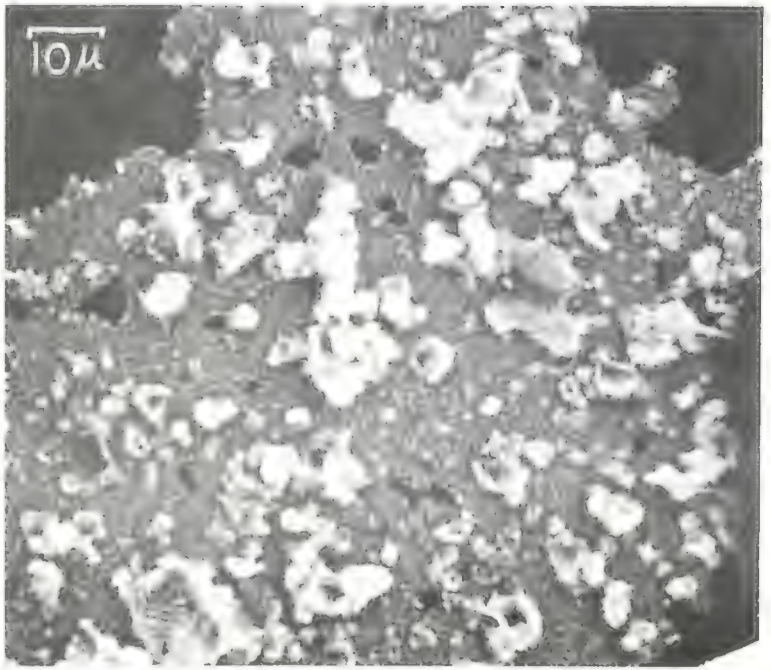

Figure 14. Small Hydrated Cement Grains Exhibiting Residual Grains and Interior Voids (D5001G1)

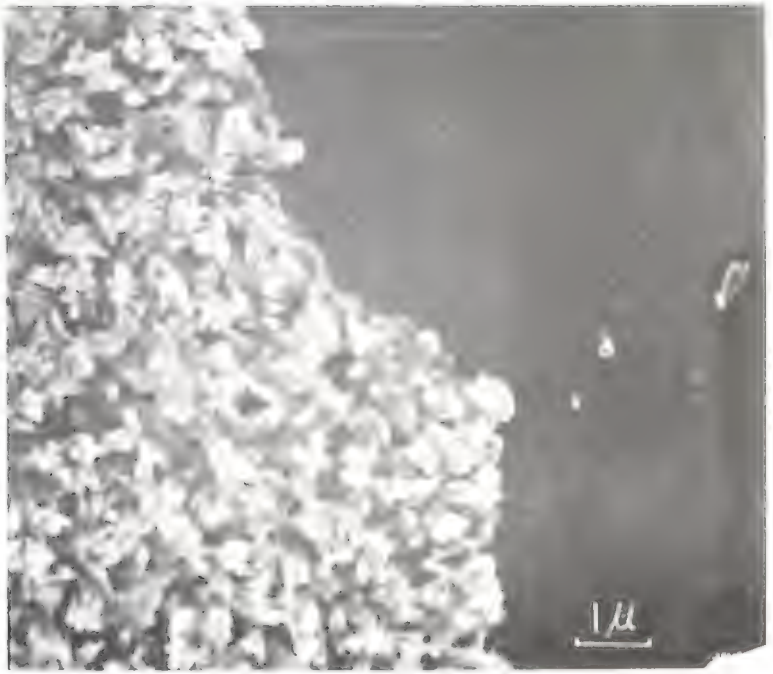

Figure 15. Sheaf-like C-S-H Gel Remaining on Glass (D5001G2)

Figure 16. Enlargement of C-S-H Gel with $Ca(OH)_2$ Layer Beneath (D5001G3)

No.	C/S	C/A	C/$\bar{S}$
1	0.25	174	176

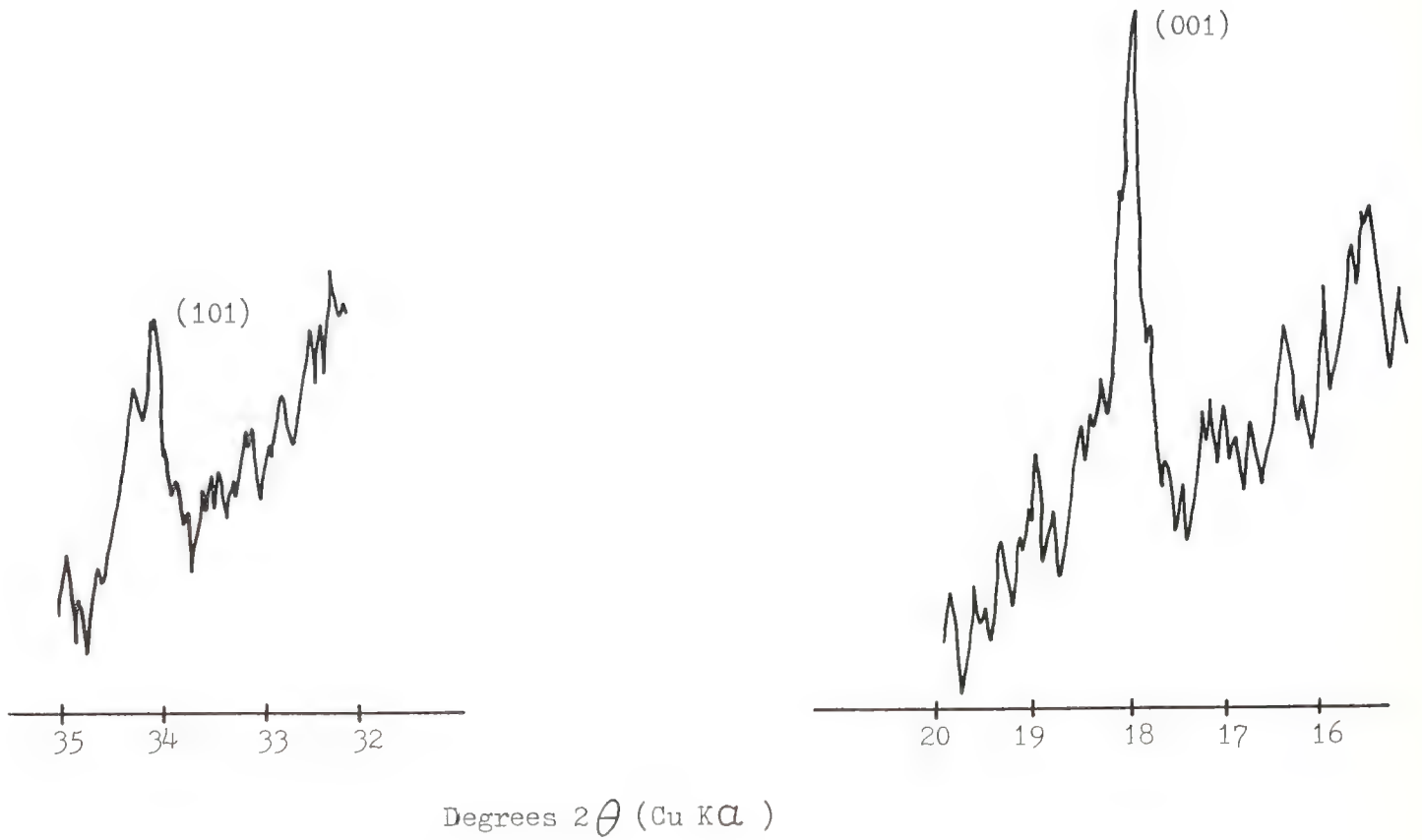

Figure 17. Typical X-Ray Diffraction Pattern for a One-Day-Old Specimen (A6501G)

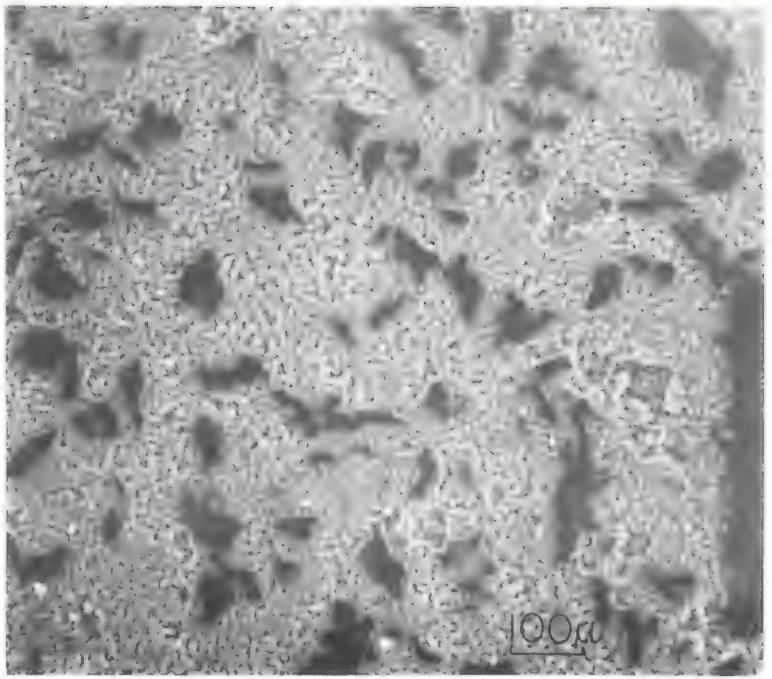

Figure 18. Low Magnification View of Cement Paste Interface (A5001P1)

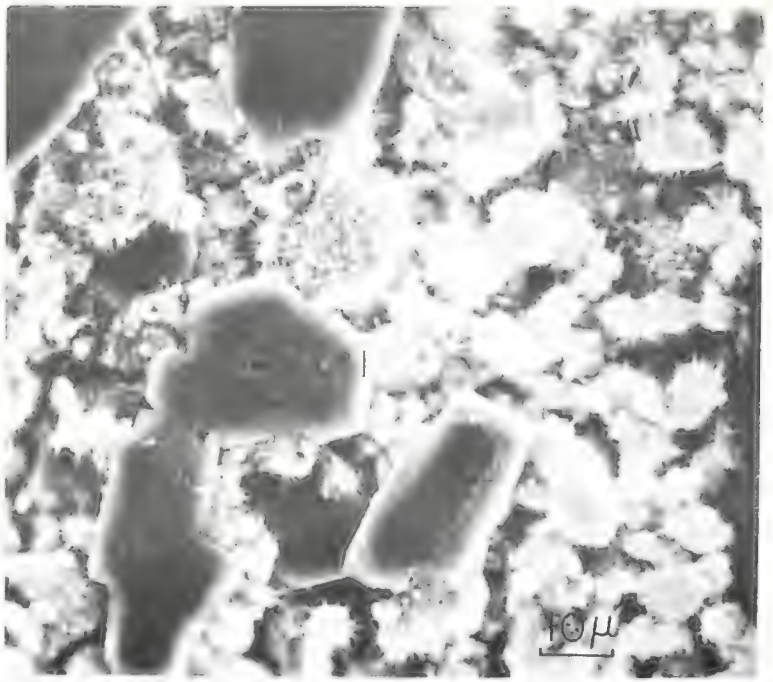

Figure 19. Close-up View of On-Edge $Ca(OH)_2$ Growing Into the Paste (A5001P5)

No.	C/S	C/A	C/$\bar{S}$
1	38.55	525.14	118.69
2	32.15	No A	No $\bar{S}$

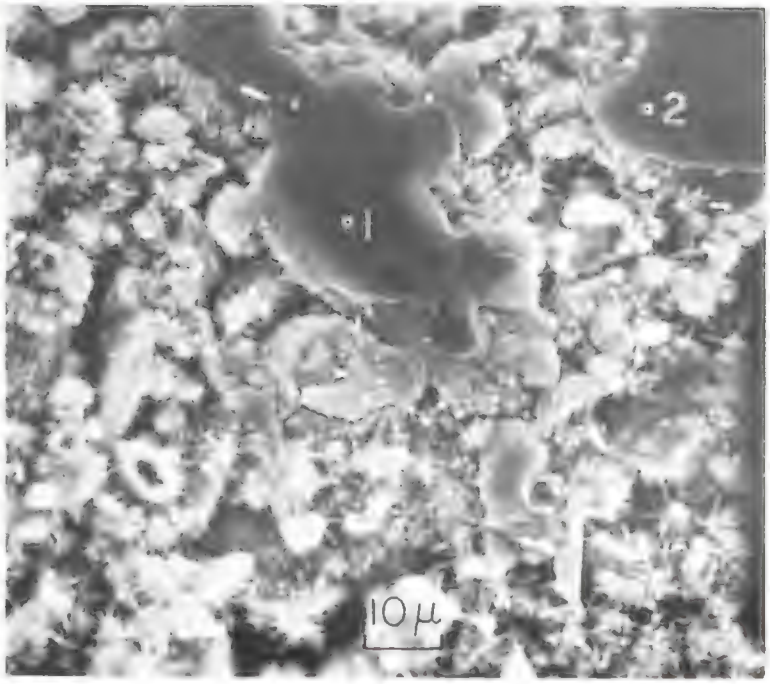

Figure 20. $Ca(OH)_2$ of the Duplex Film Adhering to the Paste (A5001P2)

No.	C/S	C/A	C/$\bar{S}$
1	32.59	1087	1037
2	12.36	1126	147

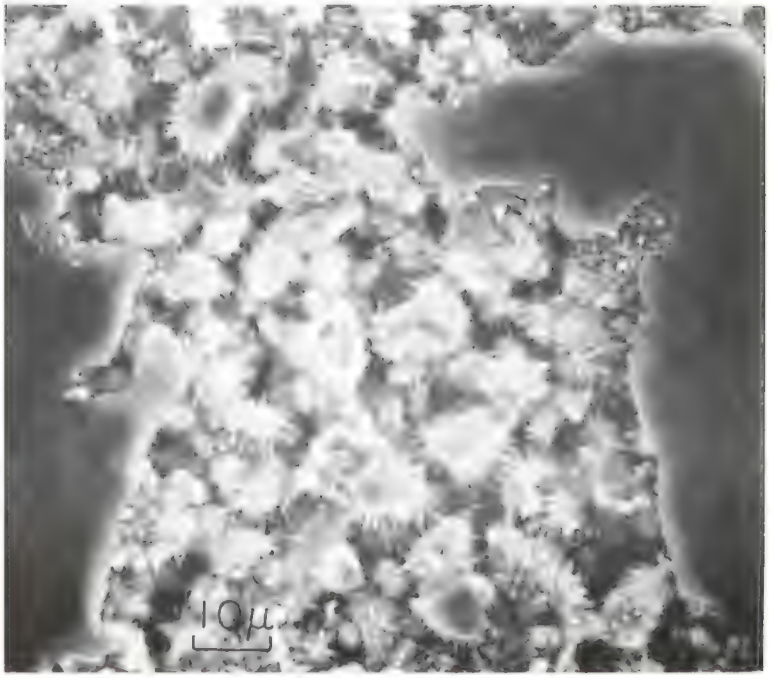

Figure 21. High Porosity Cement Paste with Duplex Film (B5001P1)

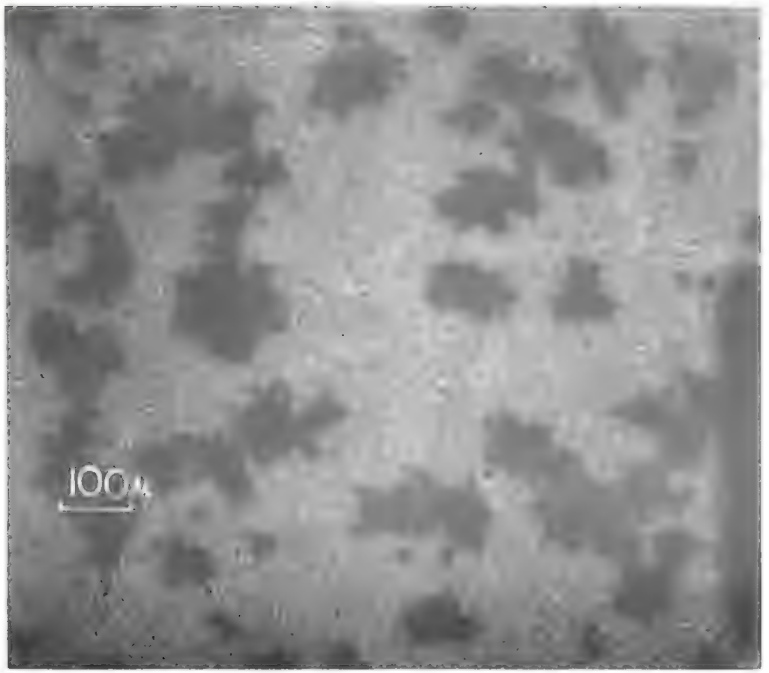

Figure 22. Large Planar Areas of Duplex Film Adhering to Paste (C5001P1)

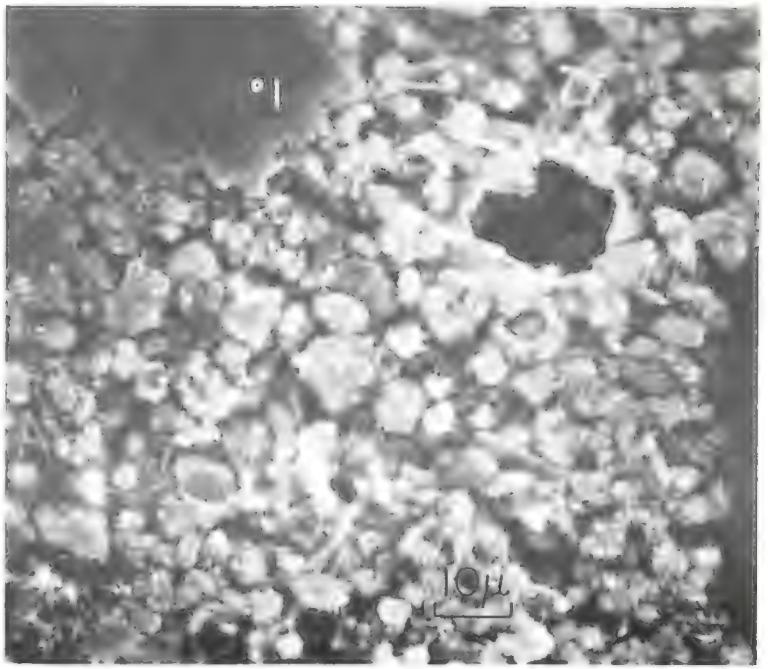

Figure 23. General View of Paste Showing Both Duplex Film and Residual Cement Grain (C6501P1)

No.	C/S	C/A	C/$\bar{S}$
1	46.96	No A	310.66

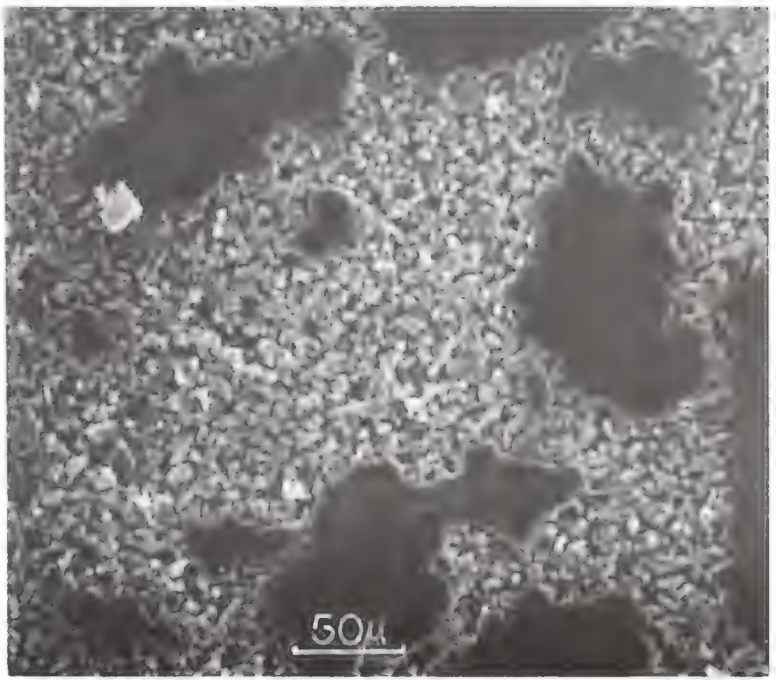

Figure 24. Duplex Film Adhering to High Porosity Cement Paste (D5001P1)

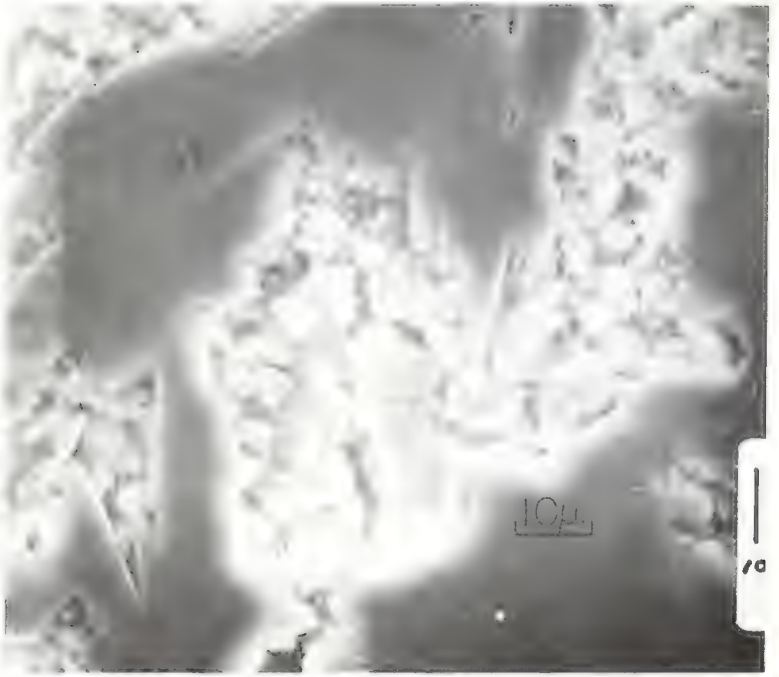

Figure 25. Duplex Film Underlain by Linear Features Extending into the Paste (One-day-old paste made from Hadley's Cement at a 0.50 w/c) (G1B)

No.	C/S	C/A	C/$\bar{S}$
1	66.15	12.89	No $\bar{S}$

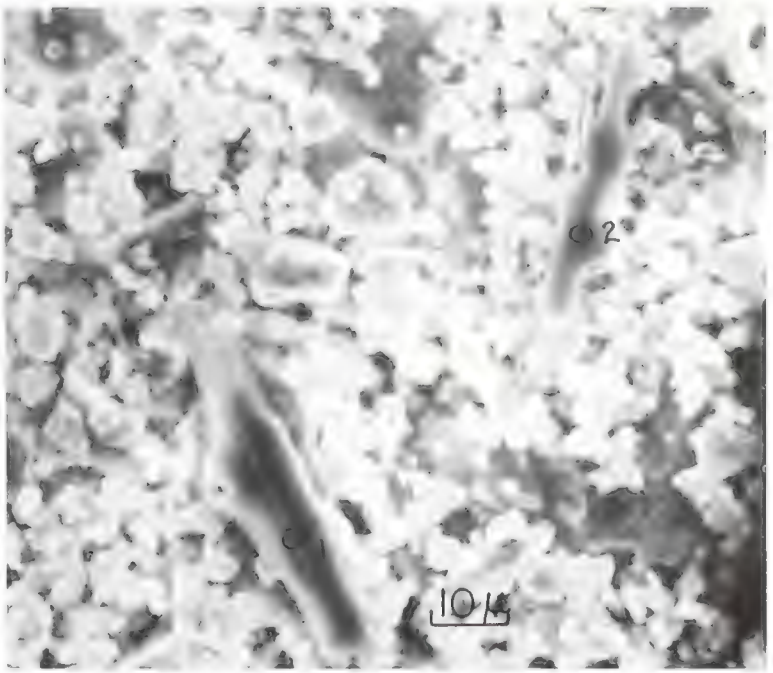

Figure 26. Early Hydration Micrograph Clearly Showing $Ca(OH)_2$ Platelets Growing in the Paste (^{2}four-hour-old paste made from Hadley's cement at a 0.50 w/c) (G 4/24 B)

No.	C/S	C/A	C/$\bar{S}$
1	96.99	185.16	269.79
2	18.75	143.98	123.30

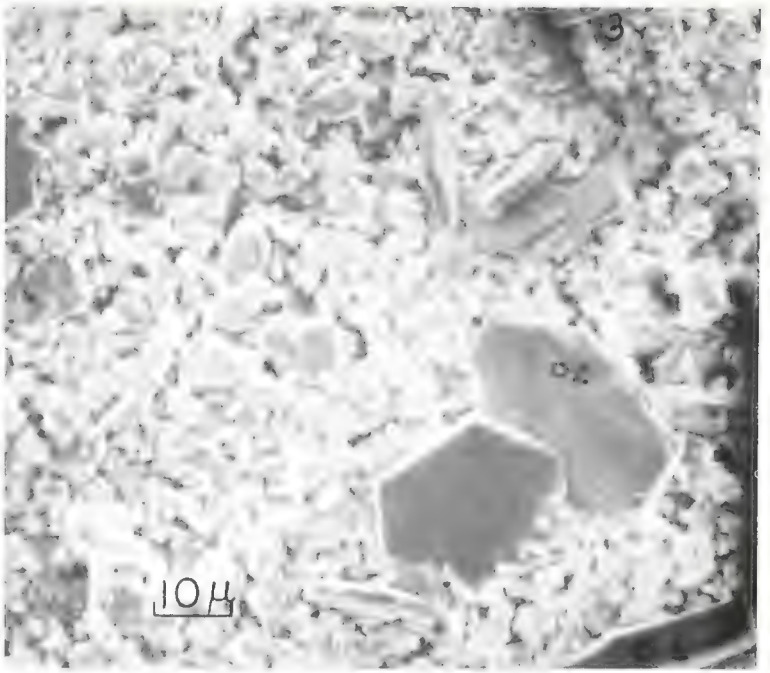

Figure 27. One-Day-Old Paste Hydrated Beneath a Glass Slide Showing Well Developed $Ca(OH)_2$ Crystals (Hadley's Cement; w/c $=^2$ 0.50) (G1C)

No.	C/S	C/A	C/$\bar{S}$
1	No S	10.08	No $\bar{S}$
2	No S	11.79	No $\bar{S}$
3	No S	11.17	No $\bar{S}$

Figure 28. Spherical Residual Cement Grain and Residual Shell (A5001G6)

No.	C/S	C/A	C/$\bar{S}$
1	1.65	108.81	91.30

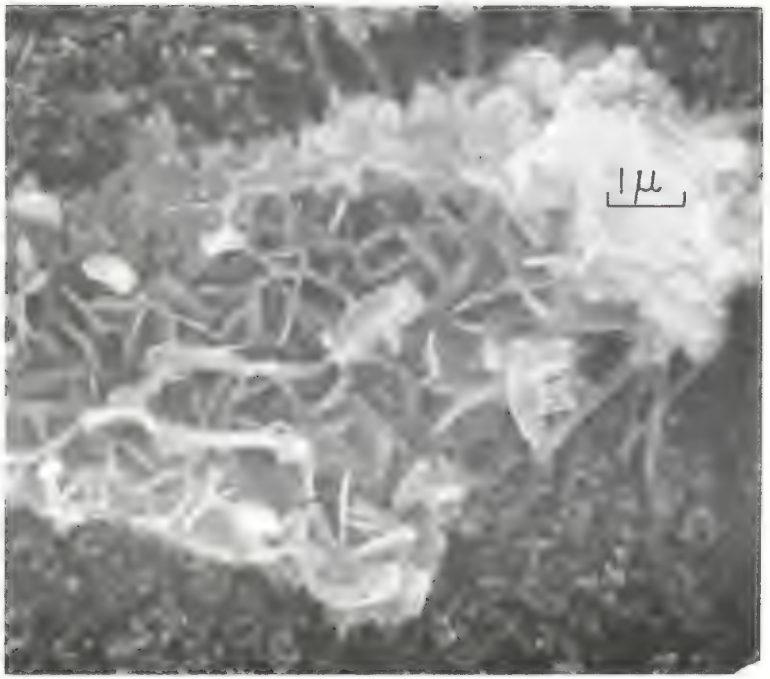

Figure 29. Interior of Residual Shell Adhering to Duplex Film (A5001G5)

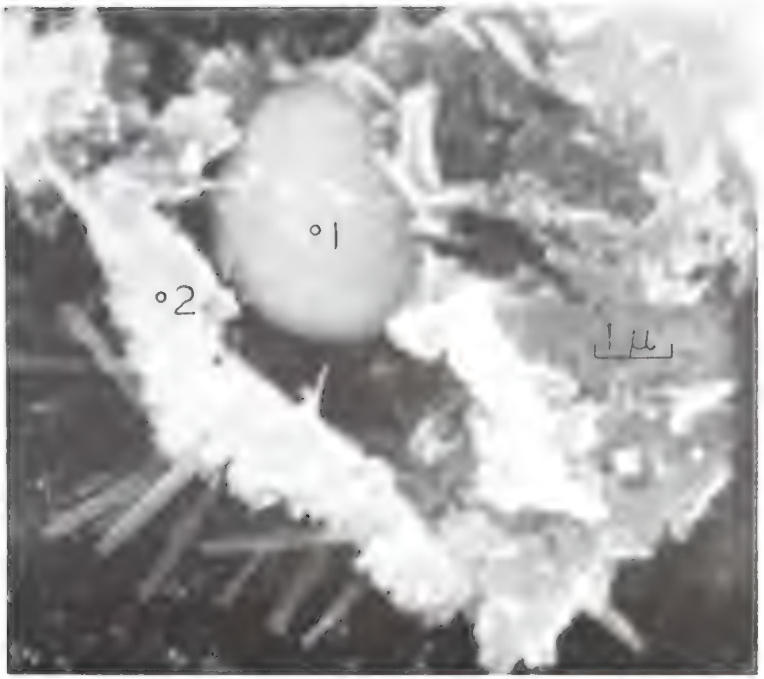

Figure 30. Spherical Residual Cement Grain and Residual Shell (B5001G2)

No.	C/S	C/A	C/$\bar{S}$
1	1.46	97.03	77.76
2	0.77	162.44	52.95

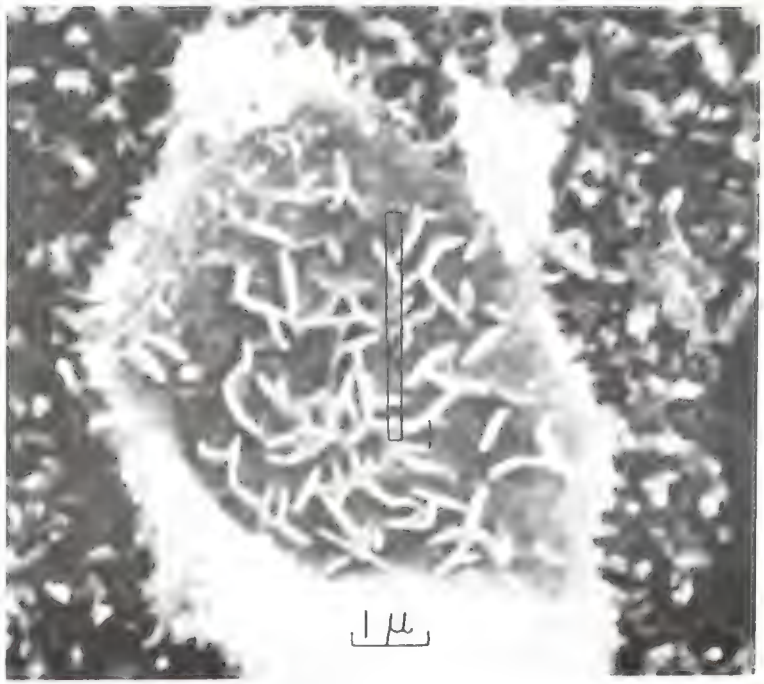

Figure 31. Interior of Residual Shell Adhering to Duplex Film (C5001G3)

No.	C/S	C/A	C/$\bar{S}$
1	0.18	2.08	22.33

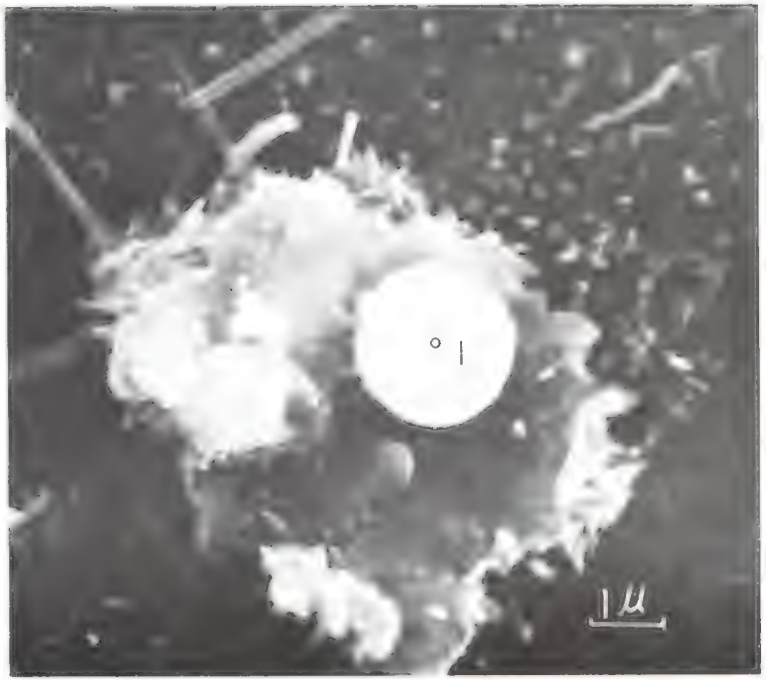

Figure 32. Spherical Residual Cement Grain with Residual Shell (C5001G4)

No.	C/S	C/A	C/$\bar{S}$
1	1.22	48.42	53.67

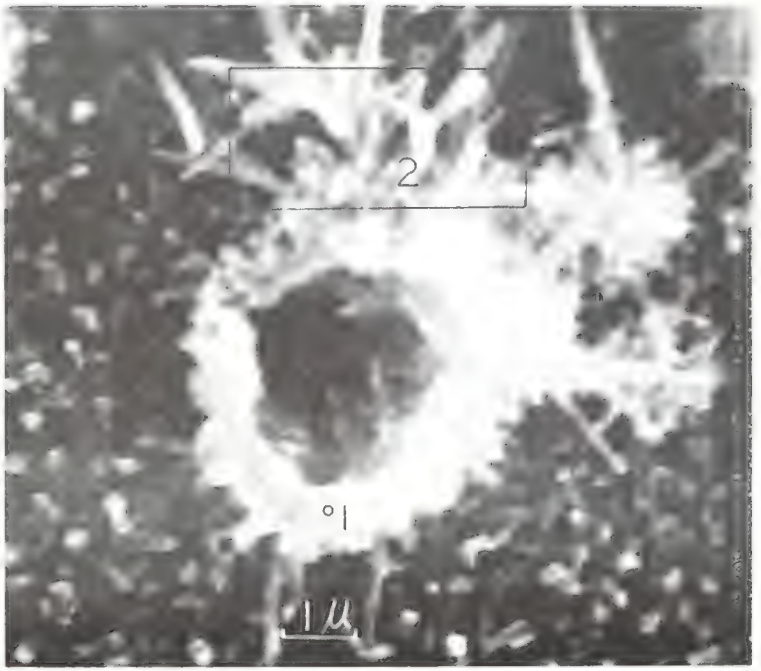

Figure 33. Empty Residual Hydration Shell Approximately Five Micrometers in Diameter (C6501G2)

No.	C/S	C/A	C/$\bar{S}$
1	0.24	3.86	17.23
2	0.26	4.76	14.67
3	0.22	4.48	61.04

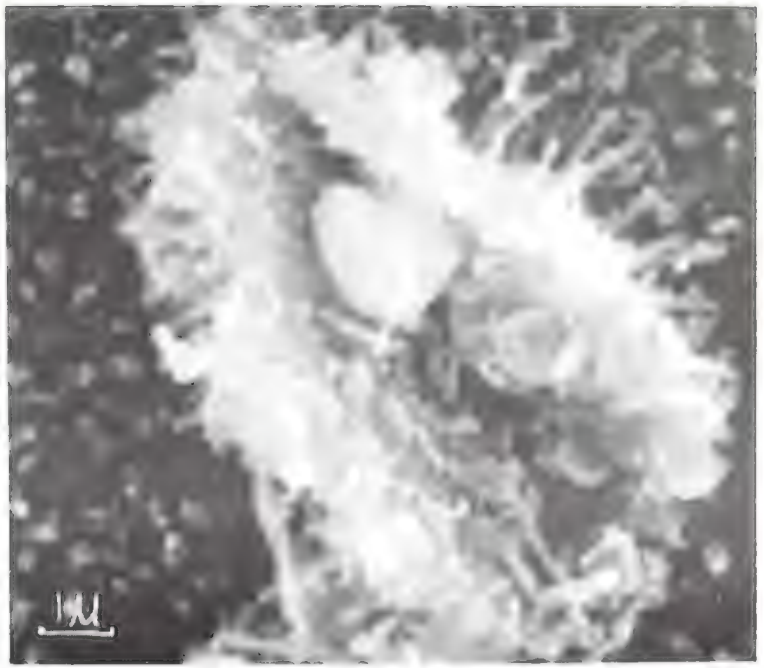

Figure 34. Residual Cement Grain Inside Residual Shell With Hexagonal Platelets (C6501G3)

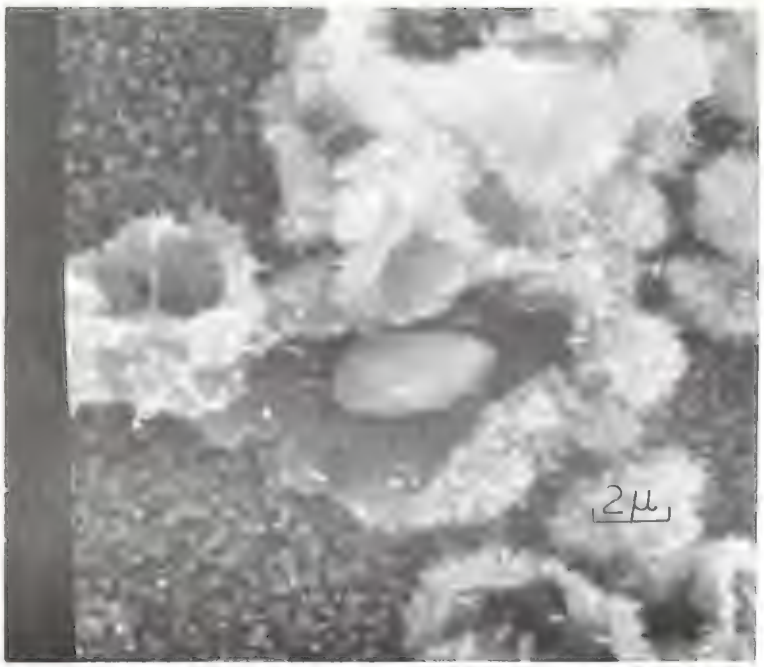

Figure 35. Residual Grain Showing Substantial Interior Void Space (D6501G4)

Figure 36. Hydrating Cement Grain Showing Residual Shell, Void Space, Residual Grain Morphology (A5001P4)

No.	C/S	C/A	C/$\bar{S}$
1	2.95	No A	No $\bar{S}$
2	2.50	111.21	40.20

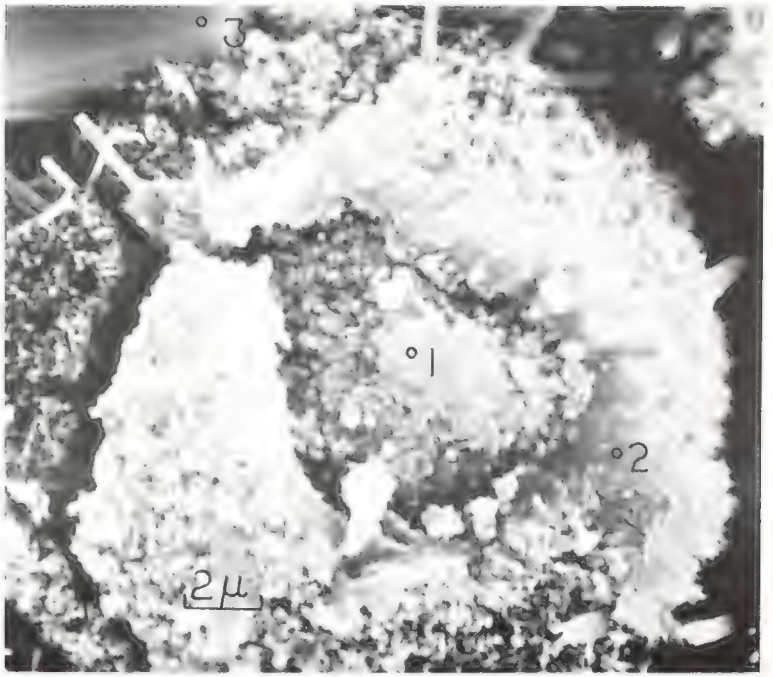

Figure 37. Rarely Observed Cement Grain Hydration Similar to Williamson's (60) Reports (A5001P3)

No.	C/S	C/A	C/$\bar{S}$
1	3.30	695.55	No $\bar{S}$
2	3.14	269.94	92.06
3	8.68	249.56	184.55

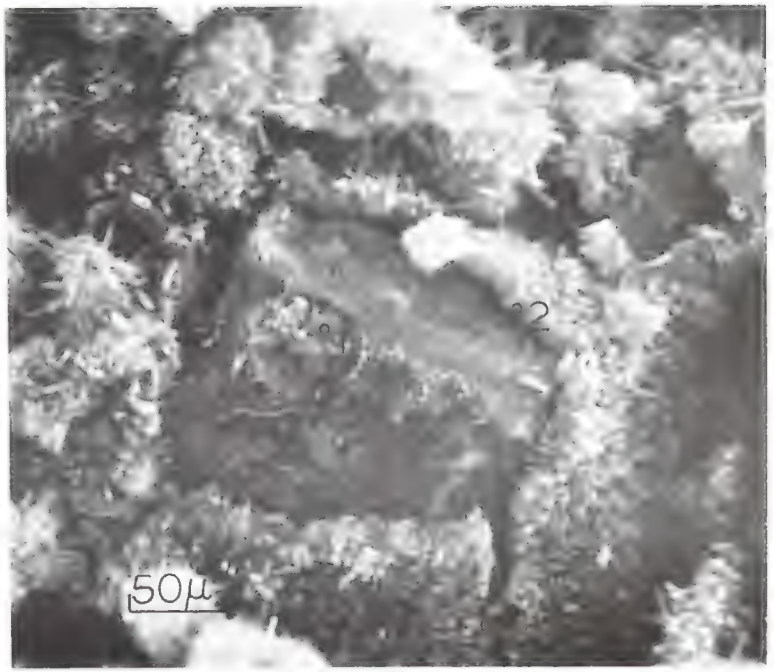

Figure 38. Hydration Similar to that Reported by Williamson (60) (A6501P7)

No.	C/S	C/A	C/$\bar{S}$
1	2.84	520.49	No $\bar{S}$
2	2.96	147.38	80.00

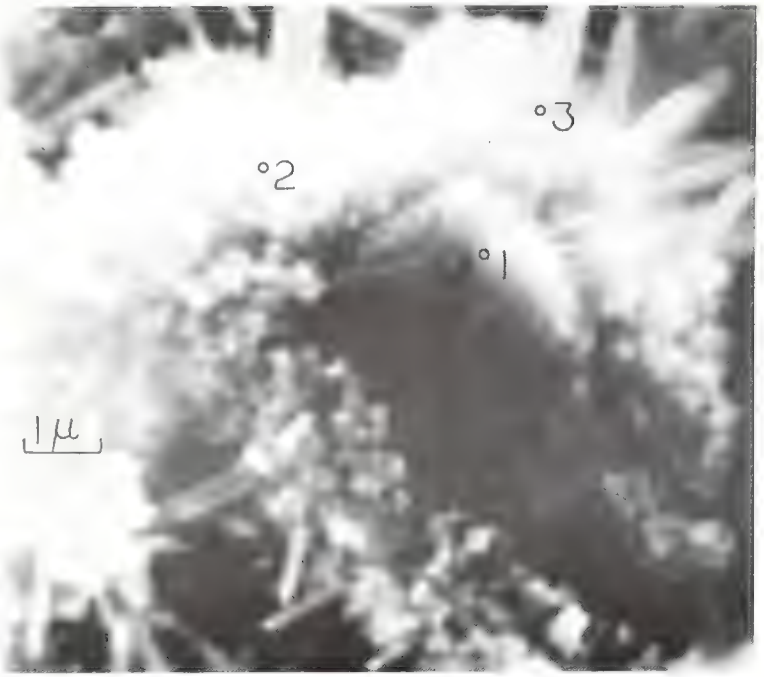

Figure 39. Apparent Inner and Outer Products of Hydration (A6501P2)

No.	C/S	C/A	C/$\bar{S}$
1	1.91	55.89	50.36
2	2.14	42.72	33.36
3	2.34	30.23	16.18

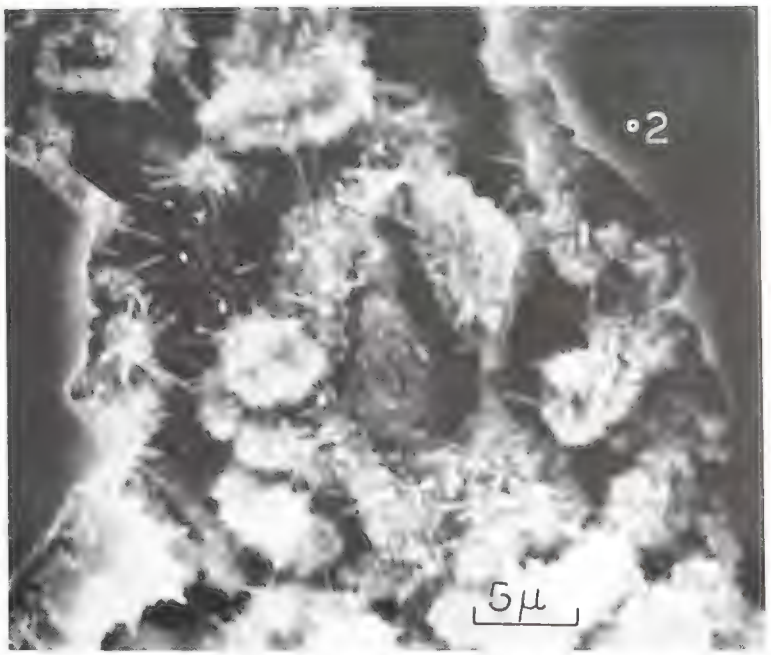

Figure 40. Apparently Solution Etched Cement Grain Showing Interior Void and Platelets (A6501P1)

No.	C/S	C/A	C/$\bar{S}$
1	3.76	335.17	No $\bar{S}$
2	14.31	No A	279.31

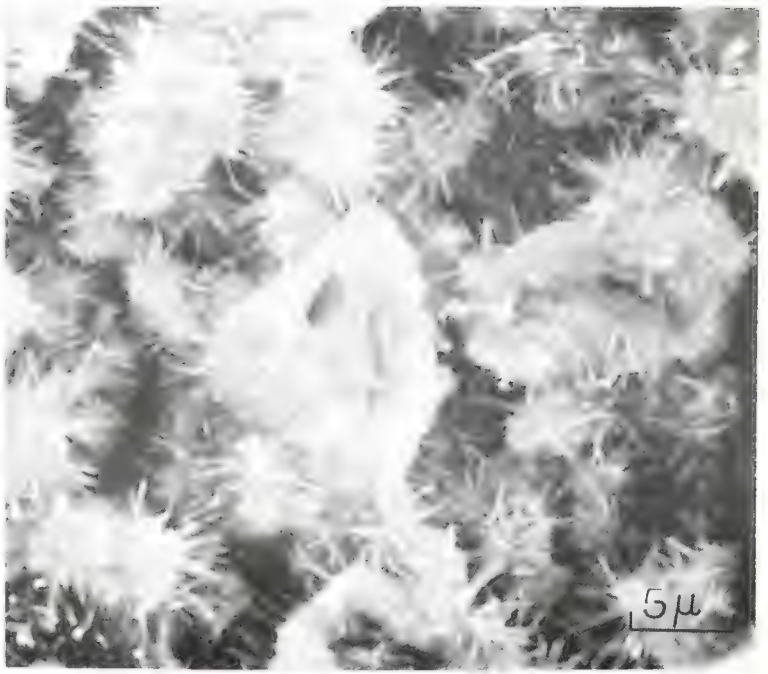

Figure 41. Residual Cement Grain Retaining Contact with Residual Shell (B5001P2)

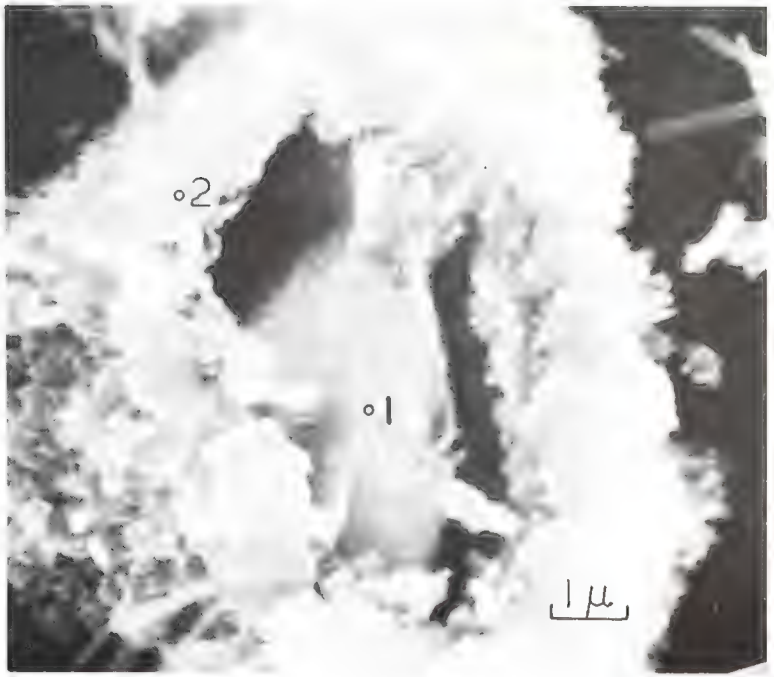

Figure 42. Enlargement of Cement Grain and Shell Shown in Figure 41 (B5001P3)

No.	C/S	C/A	C/$\bar{S}$
1	2.96	140.42	183.59
2	2.43	75.29	25.79

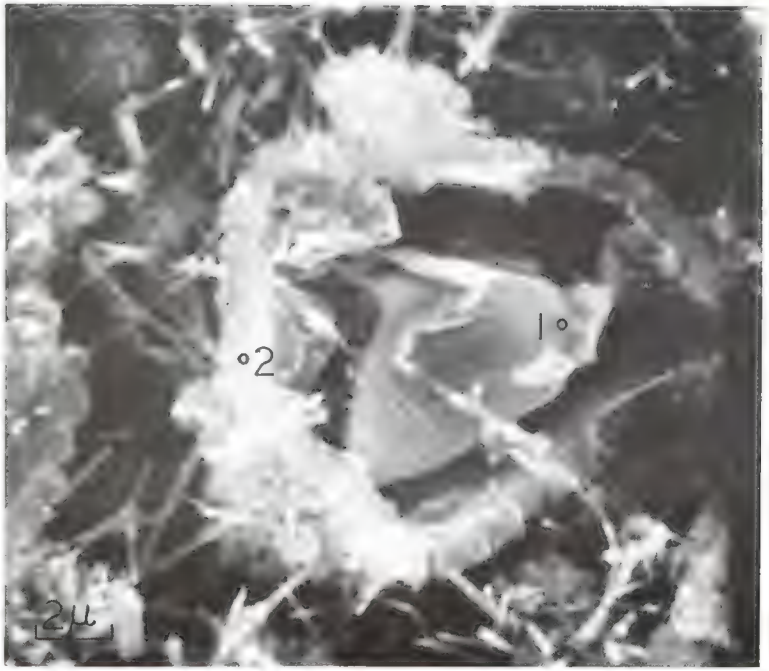

Figure 43. Relatively Smooth Residual Grain with Few Connections to Residual Shell (B6501P3)

No.	C/S	C/A	C/$\bar{S}$
1	2.88	122.30	66.63
2	4.36	41.42	22.22

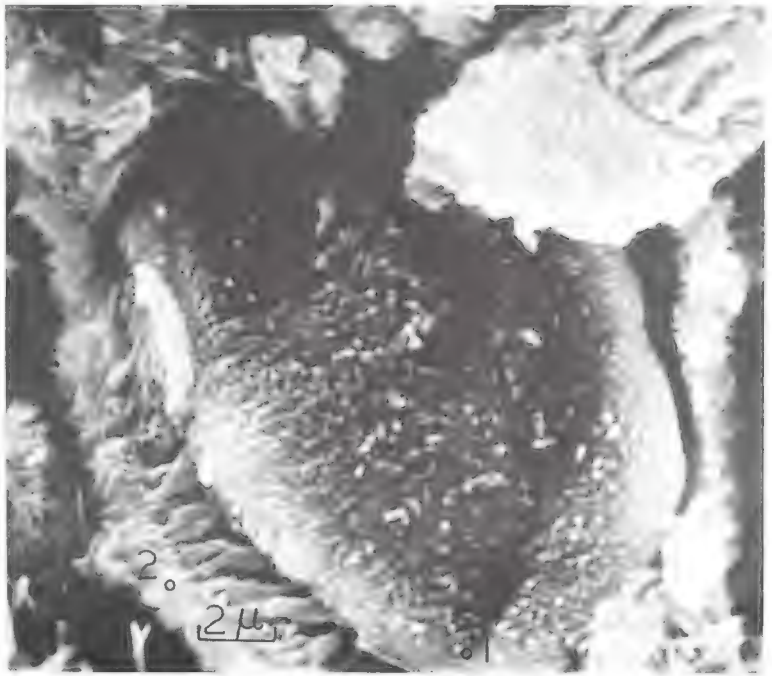

Figure 44. Etched Residual Grain with Many Planar Connections to the Residual Shell (B6501P2)

No.	C/S	C/A	C/S̄
1	3.43	160.73	118.86
2	2.72	61.30	26.59

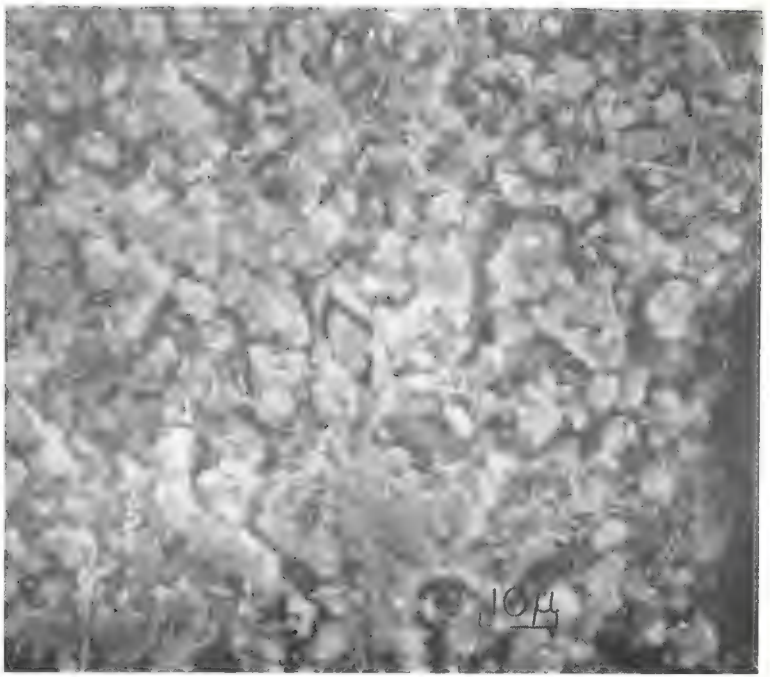

Figure 45. Typical View of Paste Interface at One Day (C5001P3)

Figure 46. Enlargement of Central Residual Cement Grain Shown in Figure 45 (C5001P4)

No.	C/S	C/A	C/$\bar{S}$
1	2.04	181.05	228.19

Figure 47. Residual Cement Grain Having Only a Few Visible Buttressing Crystals (C6501P2)

No.	C/S	C/A	C/$\bar{S}$
1	2.52	174.88	118.10
2	2.93	106.63	47.12

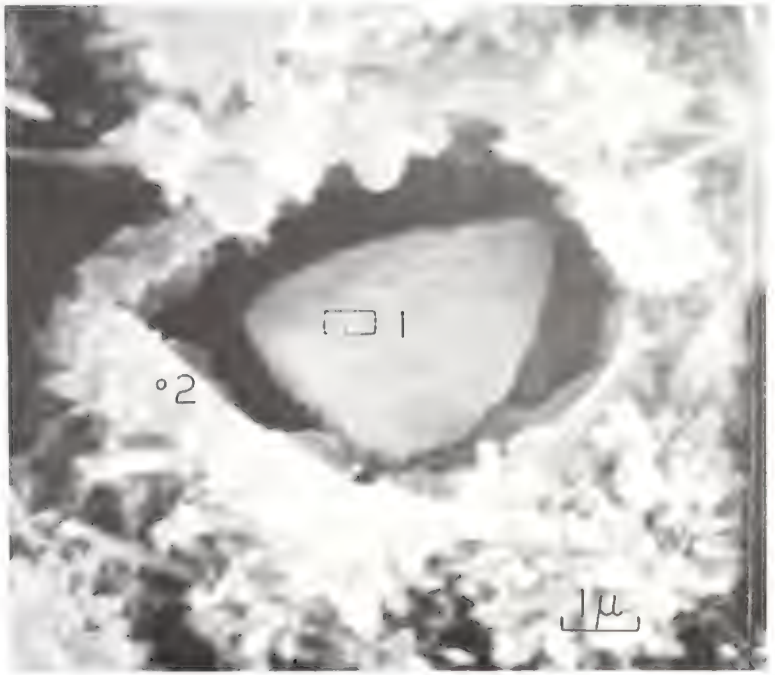

Figure 48. Residual Cement Grain Exhibiting a Large Interior Void (C6501P3)

No.	C/S	C/A	C/$\bar{S}$
1	3.20	181.47	54.01
2	2.35	78.06	24.21

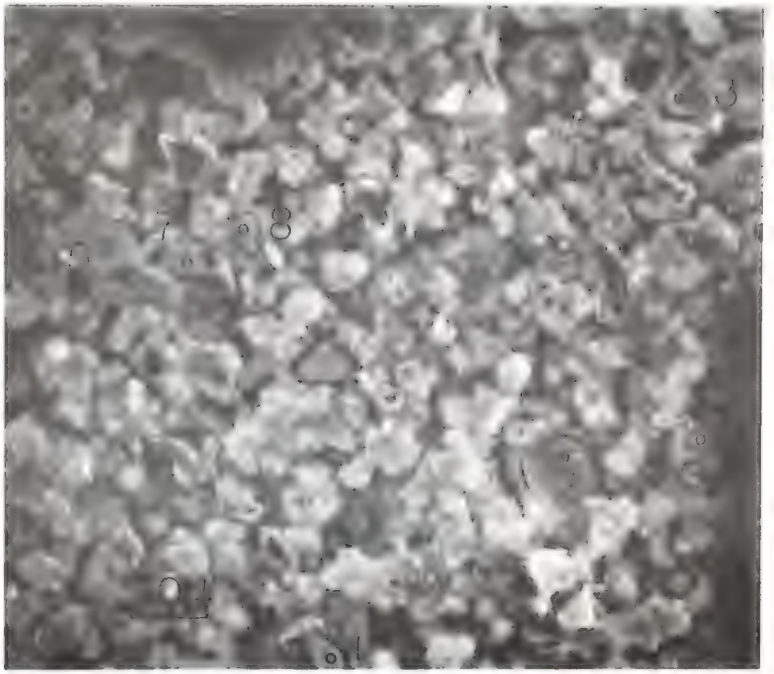

Figure 49. Typical View of the Paste Interface Showing an Absence of Hydrating Grains of the Type Described by Williamson (60) (D5001P2)

No.	C/S	C/A	C/$\bar{S}$
1	3.50	No A	339.06
2	3.29	No A	No $\bar{S}$
3	2.76	198.15	91.04
4	30.14	No A	229.70
5	3.14	No A	No $\bar{S}$
6	2.90	No A	84.25
7	2.95	597.76	236.19
8	2.63	385.01	91.93

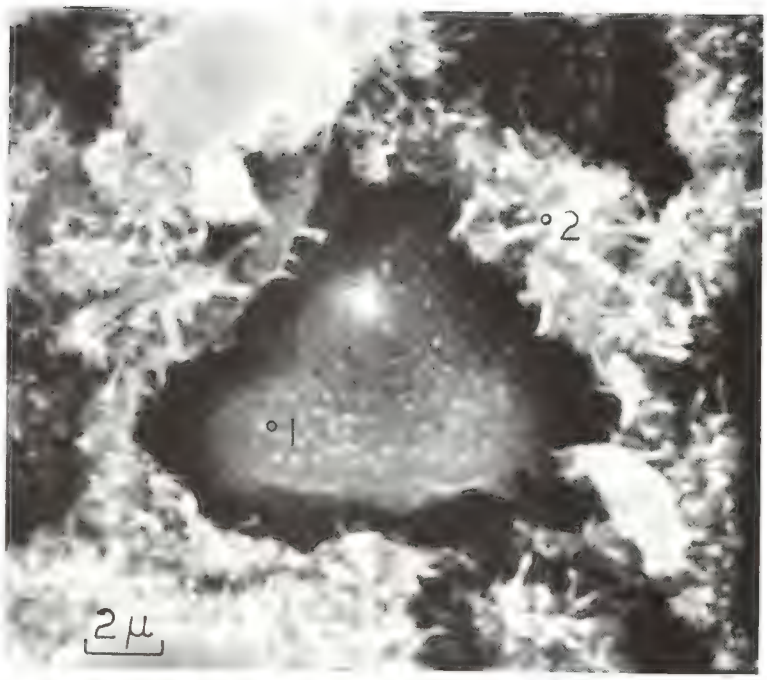

Figure 50. Enlargement of Central Cement Grain Shown in Figure 49 (D5001P3)

No.	C/S	C/A	C/$\bar{S}$
1	3.58	No A	1166.78
2	3.19	65.78	24.86

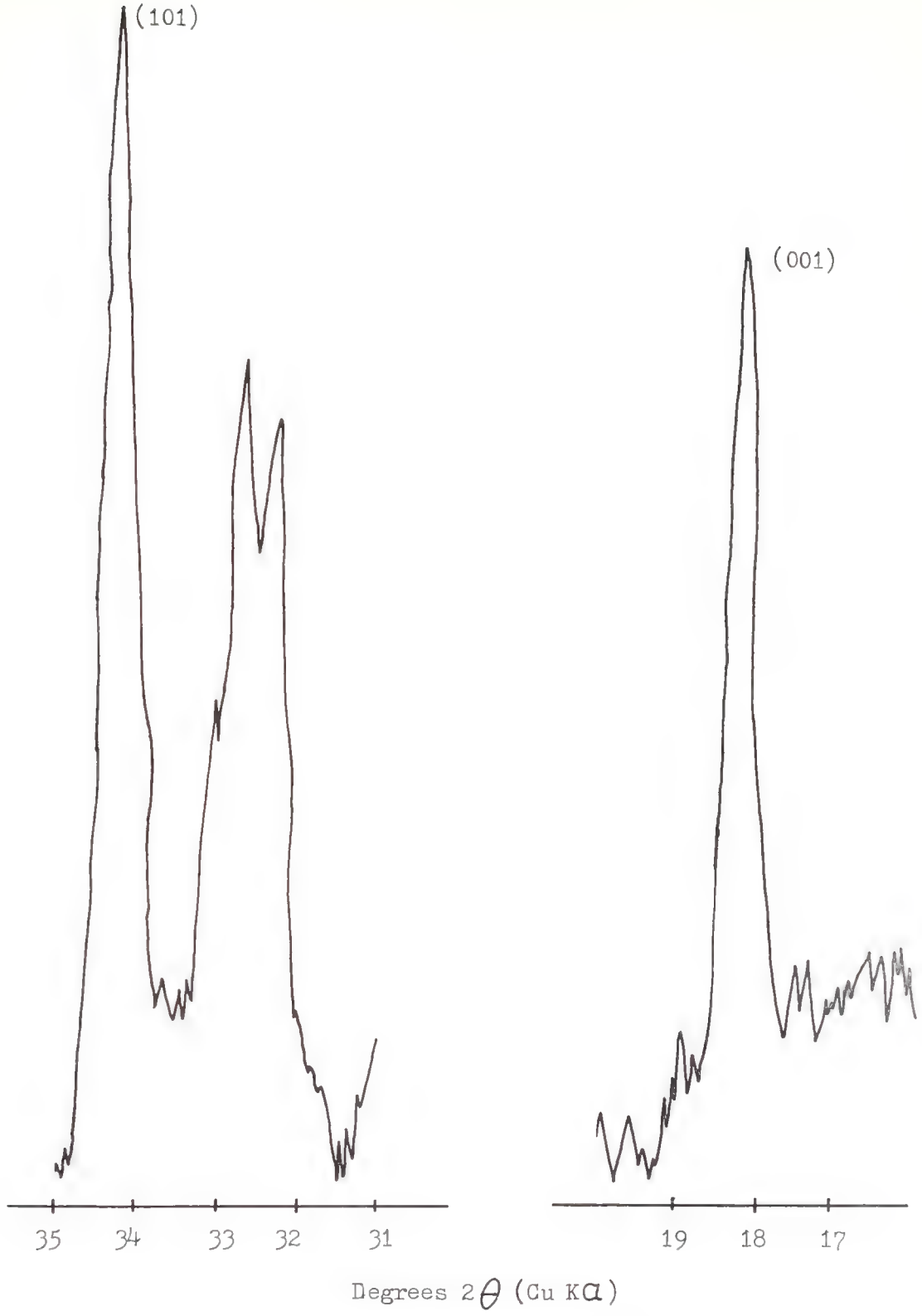

Figure 51. Typical X-Ray Diffraction Pattern for a Paste Having Little Retained Duplex Film (A6501P)

Figure 52. Photo-Mosaic of Paste Interface for Cement A (A5003M0

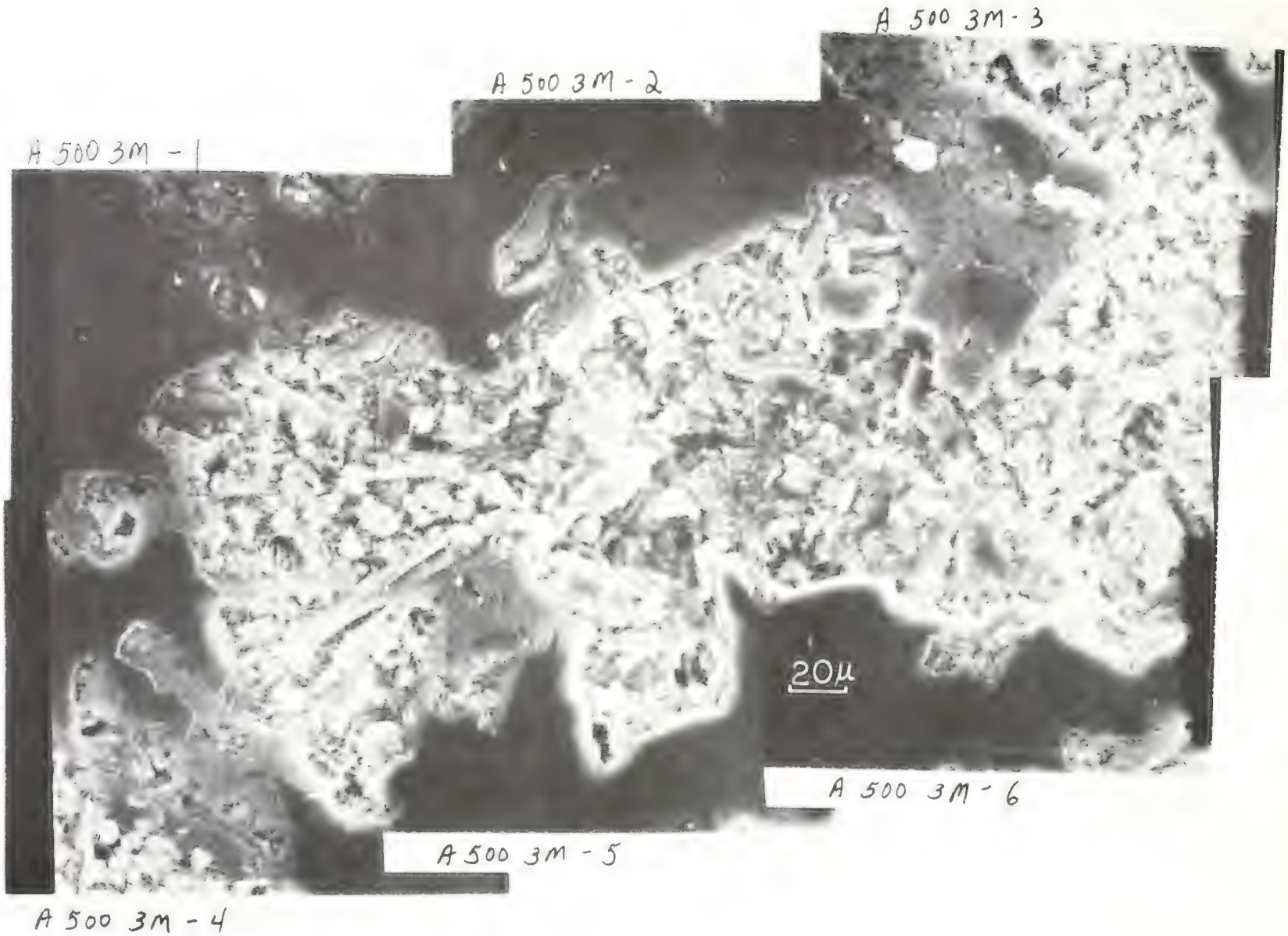
A 500 3M - 3
A 500 3M - 2
A 500 3M - 1
20μ
A 500 3M - 6
A 500 3M - 5
A 500 3M - 4

Figure 53. Photo-Mosaic of Paste Interface for Cement B (B5003M)

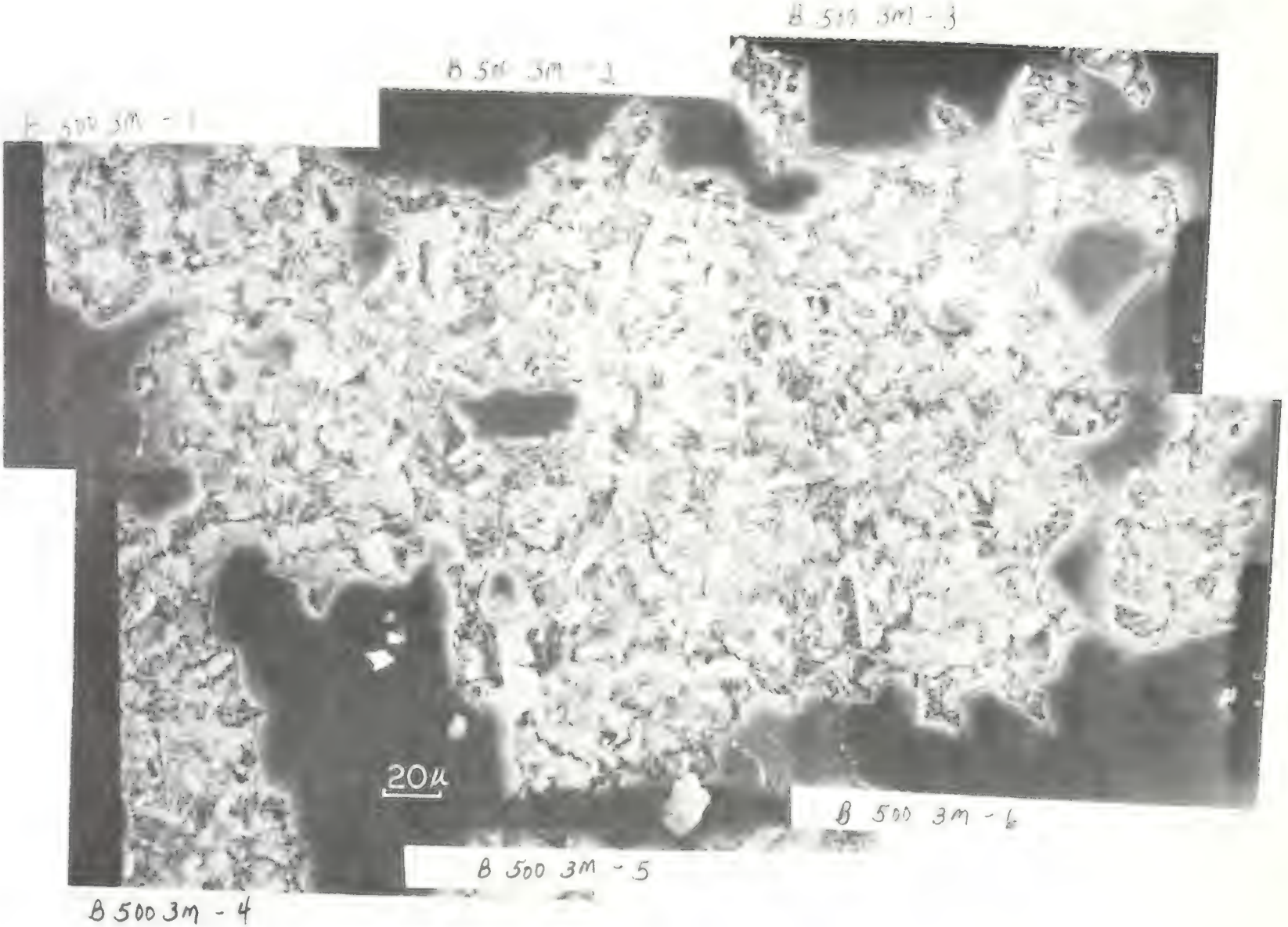
B 500 3M - 3
B 500 3M - 2
B 500 3M - 1
20μ
B 500 3M - 6
B 500 3M - 5
B 500 3M - 4

Figure 54. Photo-Mosaic of Paste Interface for Cement C (C5003M)

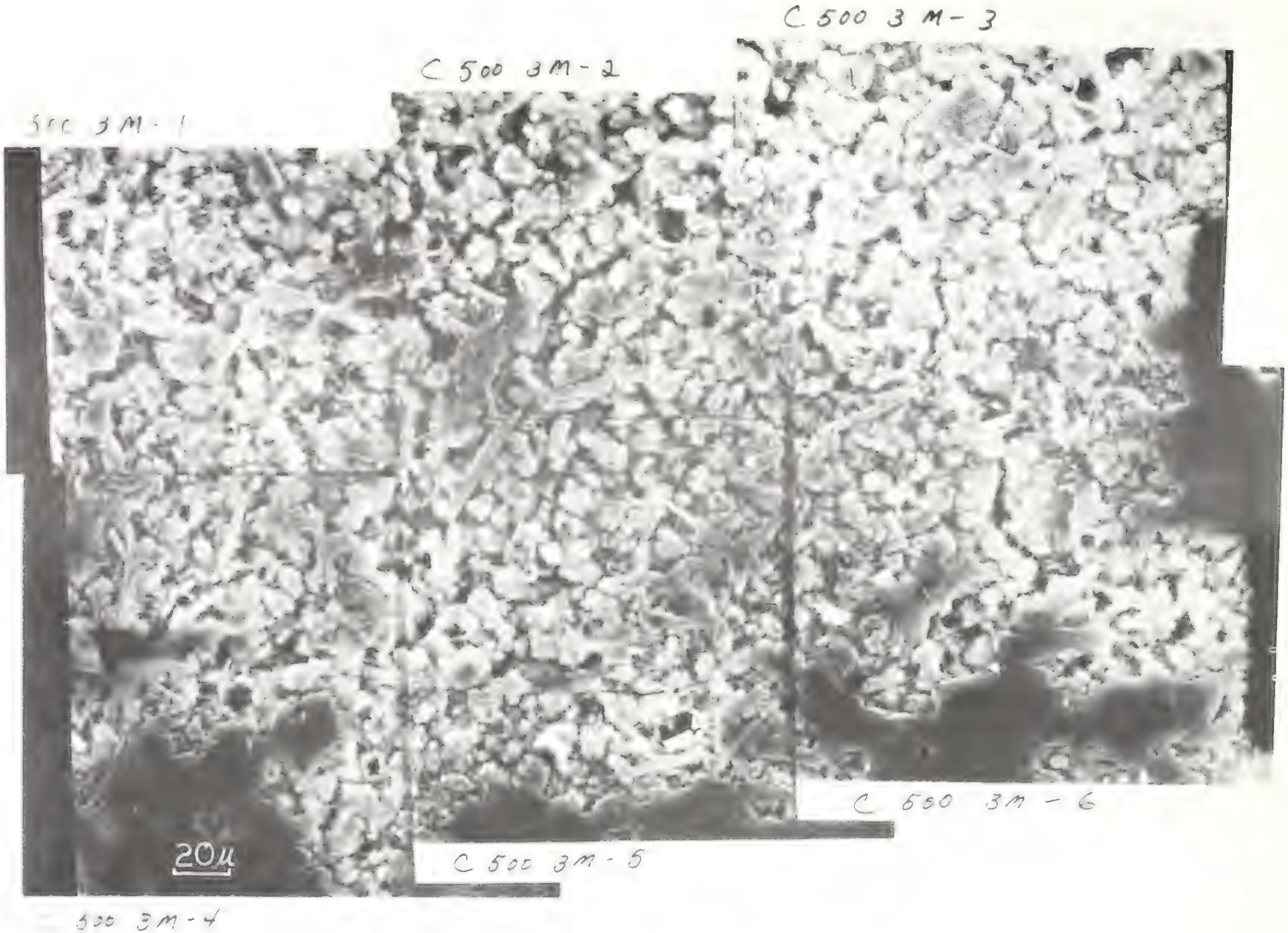
C 500 3M-3
C 500 3M-2
500 3M-1
20μ
C 500 3M-6
C 500 3M-5
500 3M-4

Figure 55. Photo-Mosaic of Paste Interface for Cement D (D5003M)

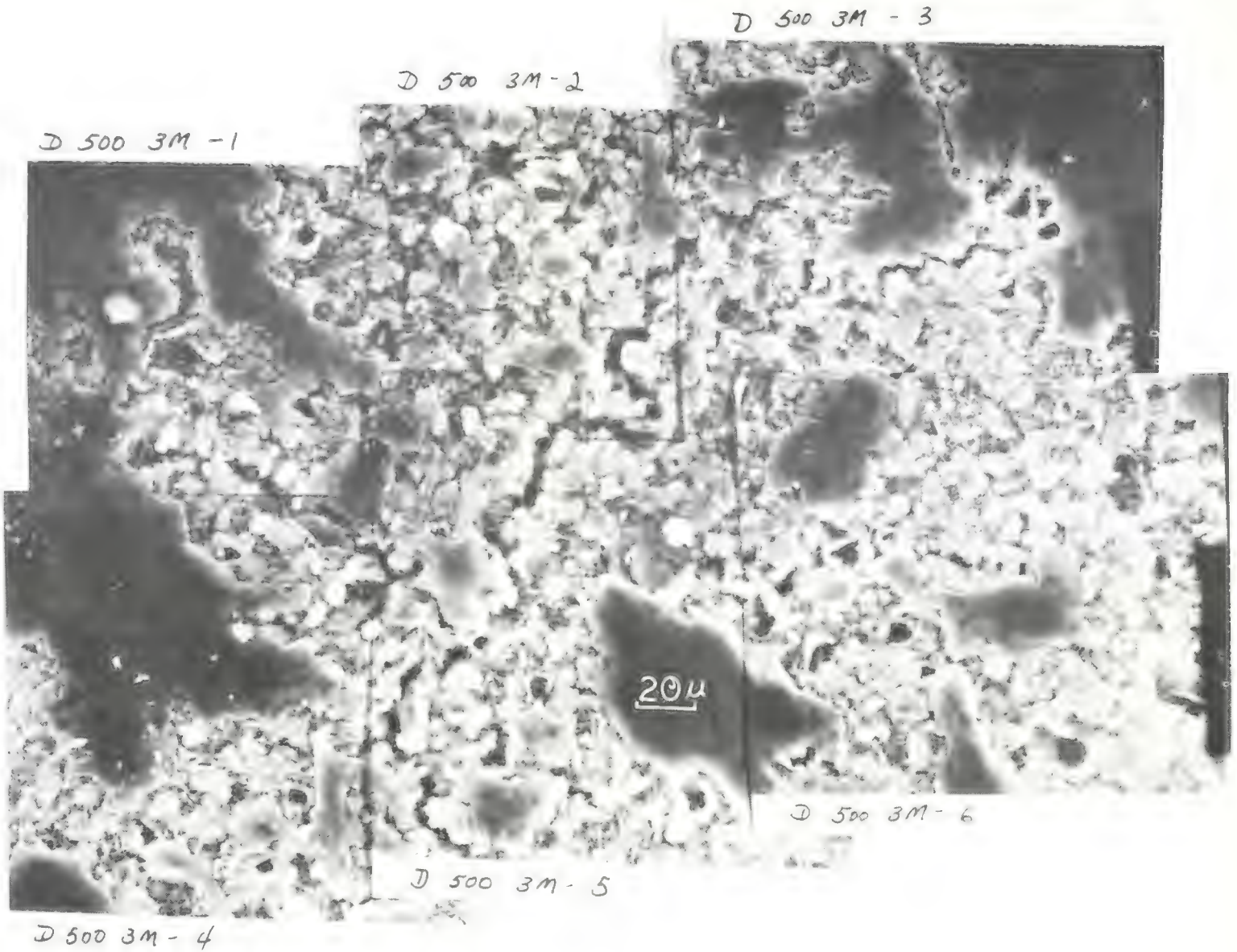
D 500 3M - 3
D 500 3M - 2
D 500 3M - 1
20μ
D 500 3M - 6
D 500 3M - 5
D 500 3M - 4

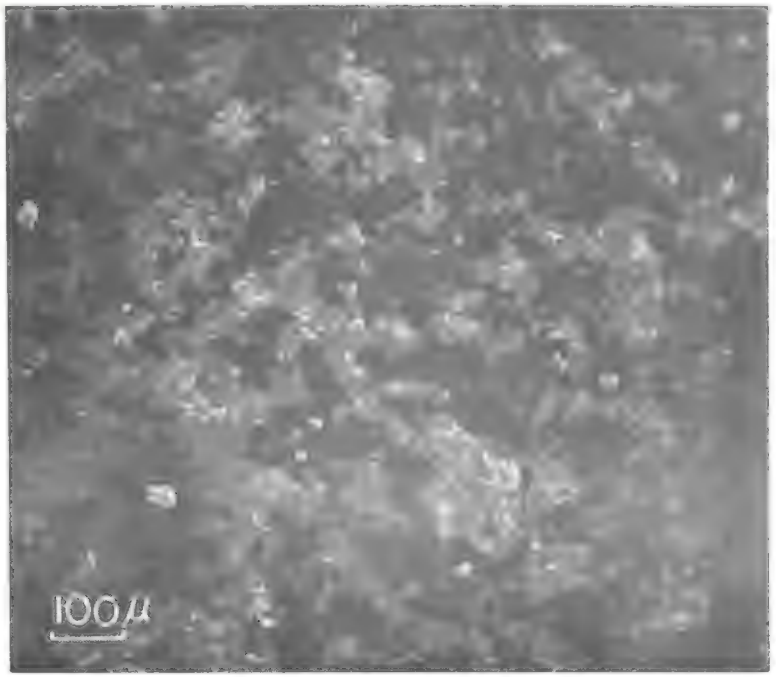

Figure 56. Low Magnification View of Hydration Products Adhering to the Glass Substrate at Three Days (A5003G4)

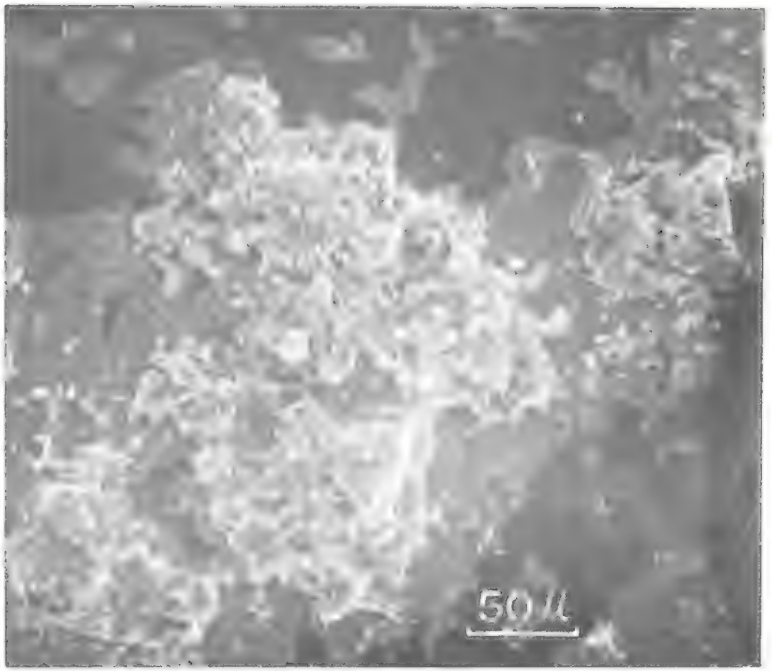

Figure 57. Typical Aggregation of Cement Grains Adhering to the Duplex Film (A5003G1)

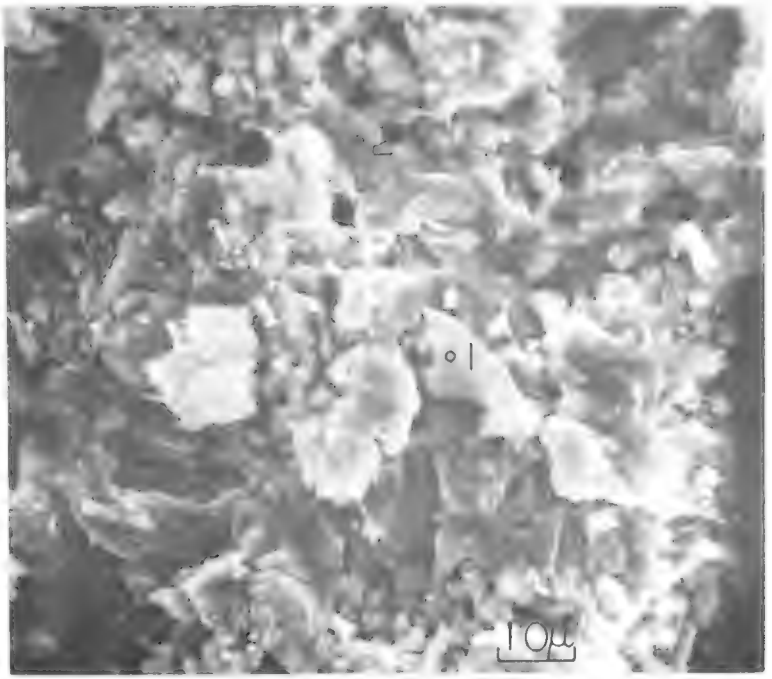

Figure 58. Enlargement of the Aggregation Shown in Figure 57 Showing Encapsulating Lime (A5003G2)

No.	C/S	C/A	C/$\bar{S}$
1	24.78	No A	No $\bar{S}$
2	25.20	No A	No $\bar{S}$

Figure 59. Aggregation of Cement Grains Encapsulated by $Ca(OH)_2$ Crystals (Hadley's Cement, three days curing, w/c = 0.50)

Figure 61. Close-up View of Encapsulating $Ca(OH)_2$

Figure 60. Enlargement of Figure 59

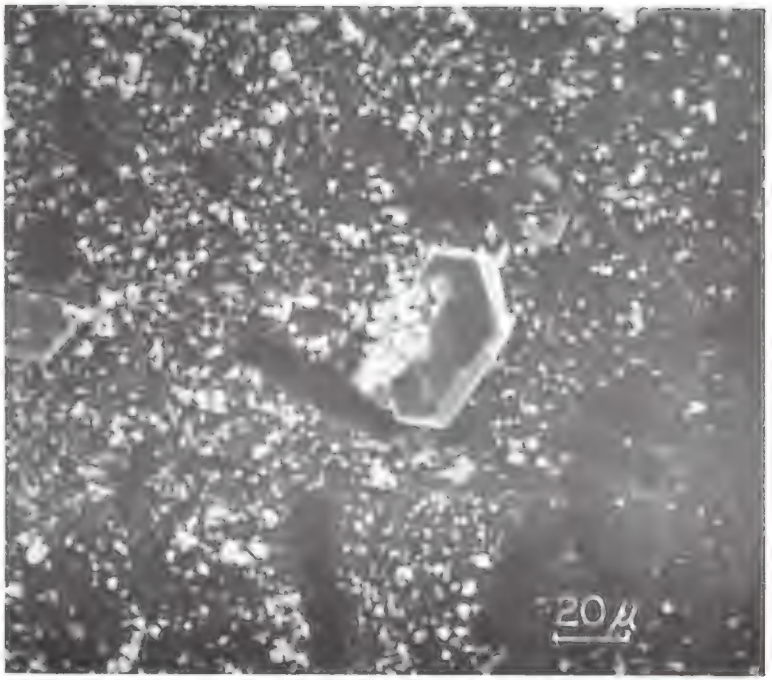

Figure 62. $Ca(OH)_2$ Crystal Attached to Duplex Film Formed on a Glass Slide Placed on Top of a 0.50 w/c Ratio Paste Cured for One Day

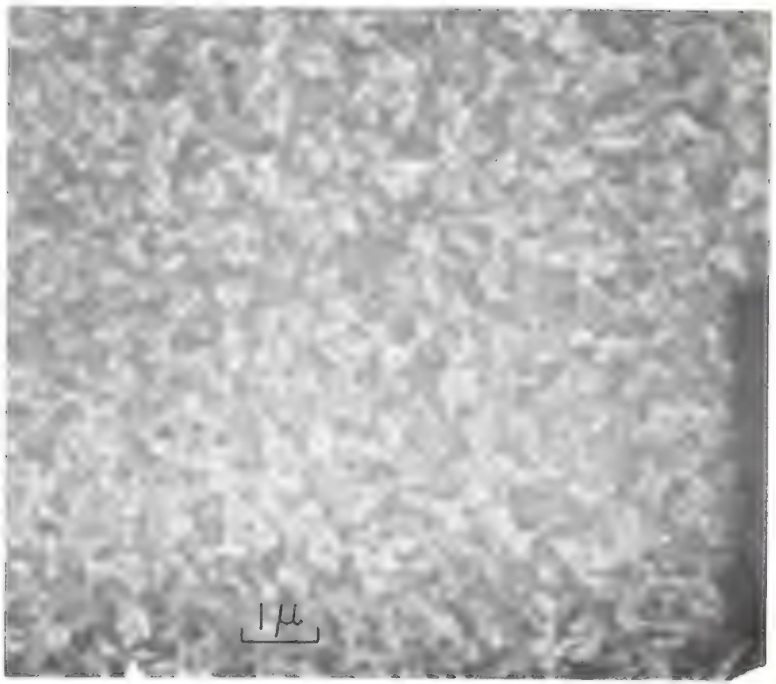

Figure 63. Close-up of Developing Duplex Film After Three Days Hydration (A500365)

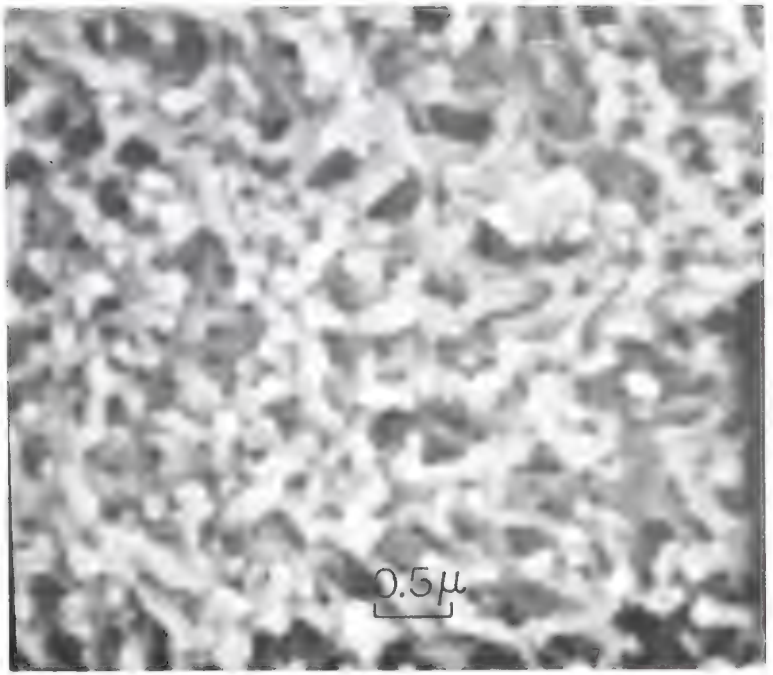

Figure 64. Enlargement of a Region Similar to Figure 63 Showing the Changing Morphology of the C-S-H Gel (A6503G4)

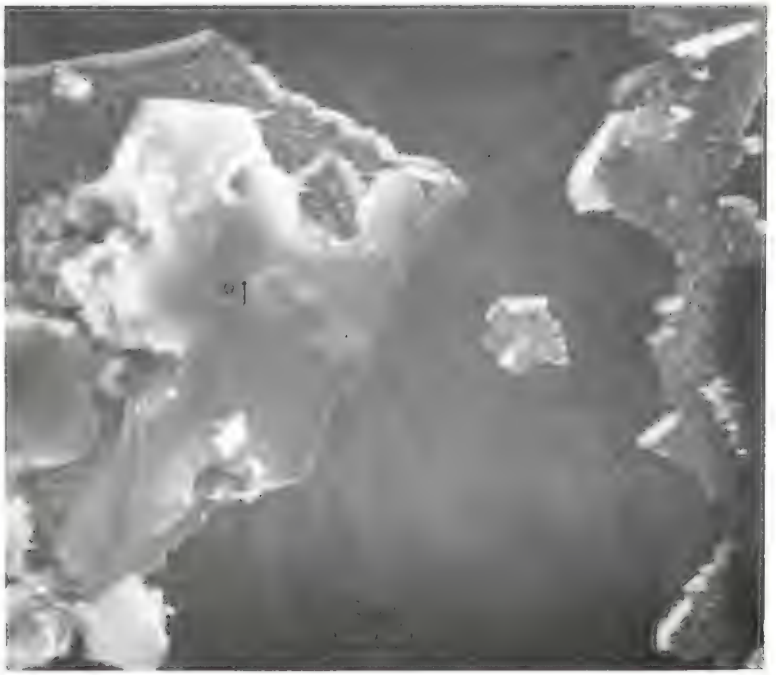

Figure 65. Folded Over Duplex Film Probably Occurring During the Separation Process (A6503G1)

No.	C/S	C/A	C/$\bar{S}$
1	18.44	88.95	193.77

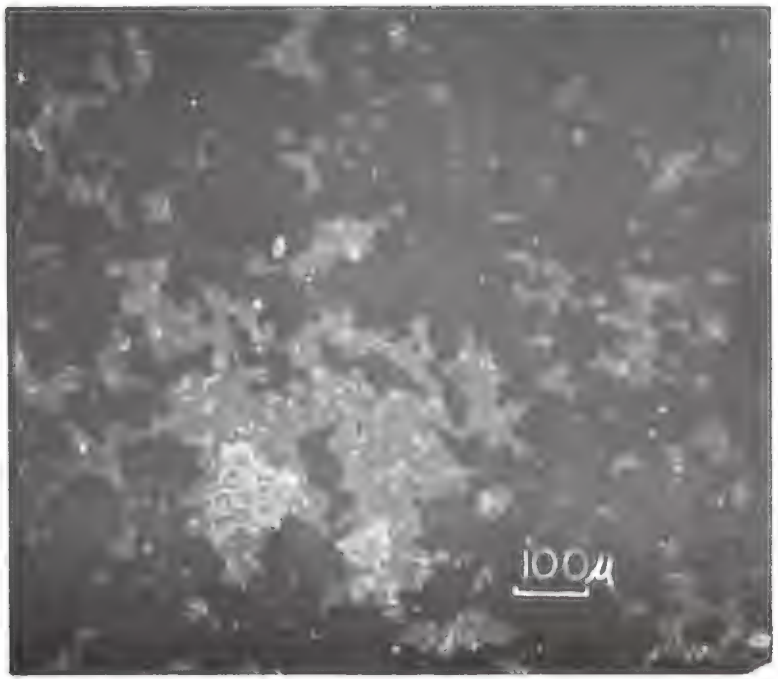

Figure 66. Low Magnification View of the Glass Substrate Showing Increased Removal of the Duplex Film (B5003G1)

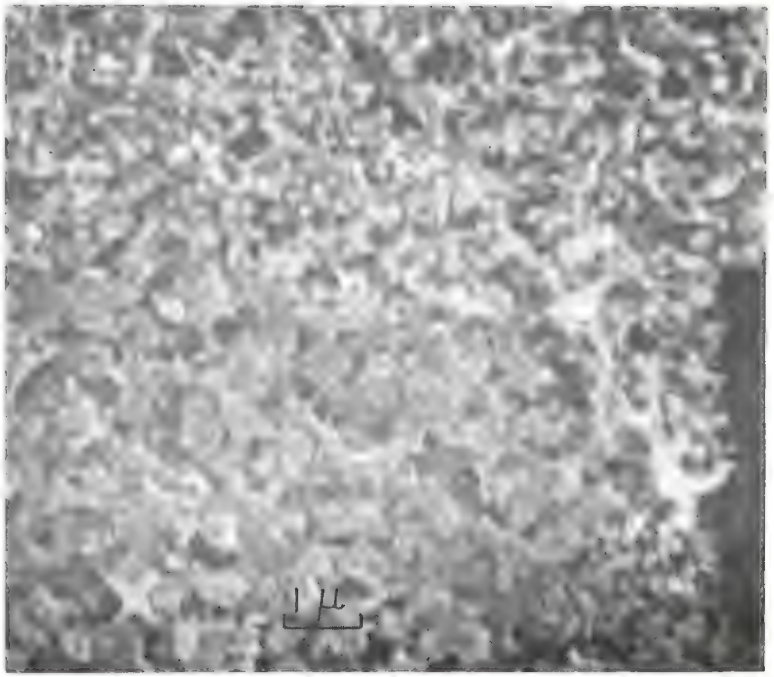

Figure 67. Duplex Film Against Glass Showing Two C-S-H Gel Morphologies (B6503G5)

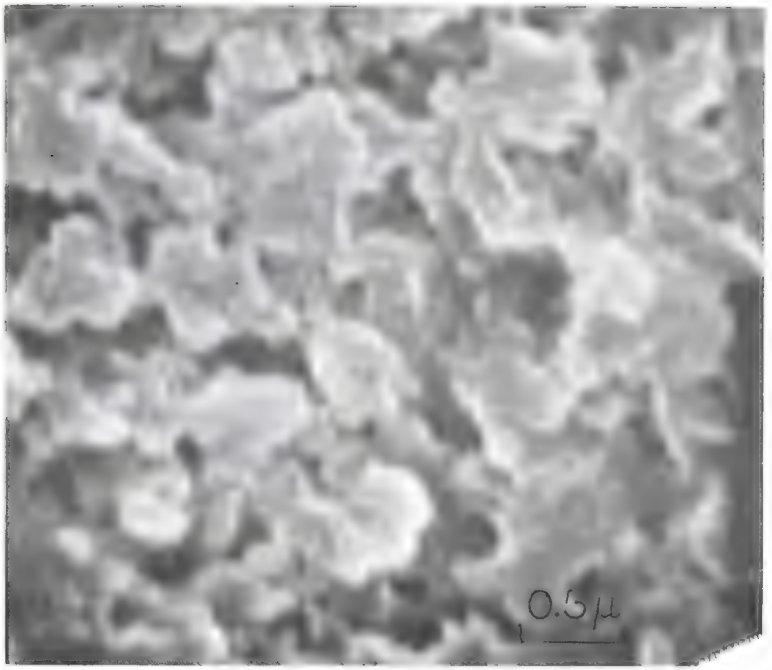

Figure 68. Enlarged View of Foreshortened C-S-H Appearing in Figure 67 (B6503G7)

No.	C/S	C/A	C/$\bar{S}$
1	0.31	No A	No $\bar{S}$

Figure 69. Enlarged View of Rod-Like C-S-H Appearing in Figure 67 (B6503G6)

No.	C/S	C/A	C/$\bar{S}$
1	0.30	No A	No $\bar{S}$

Figure 70. Low Magnification View of Glass Interface (C5003G1)

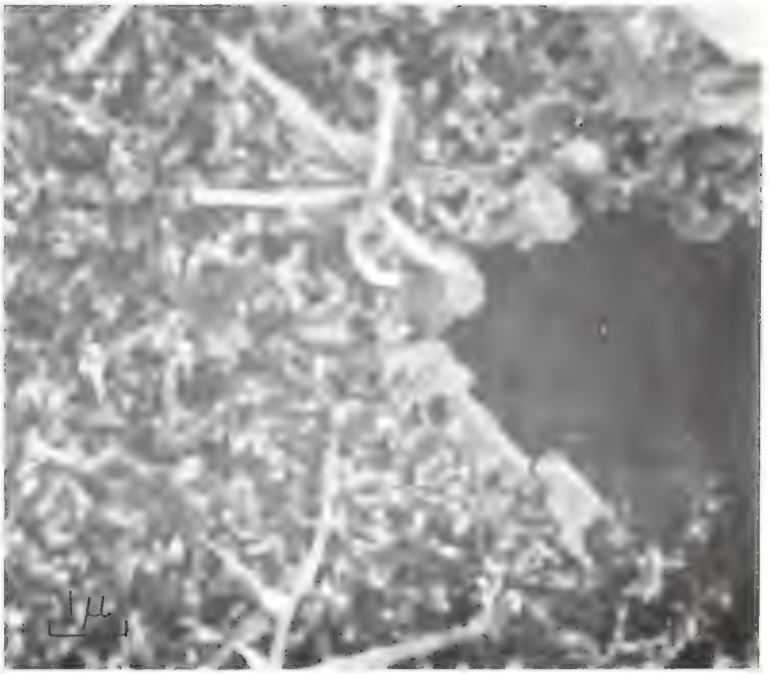

Figure 71. Enlargement of Duplex Film Appearing in Figure 70 (C5003G3)

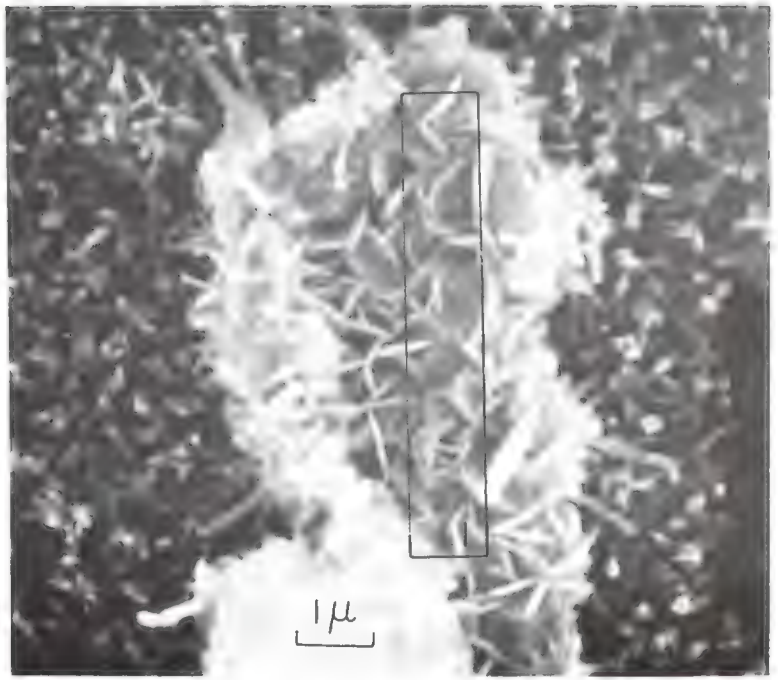

Figure 72. Residual Hydration Shell with Interior Platelets Adhering to Duplex Film (C6503G1)

No.	C/S	C/A	C/$\bar{S}$
1	0.25	No A	No $\bar{S}$

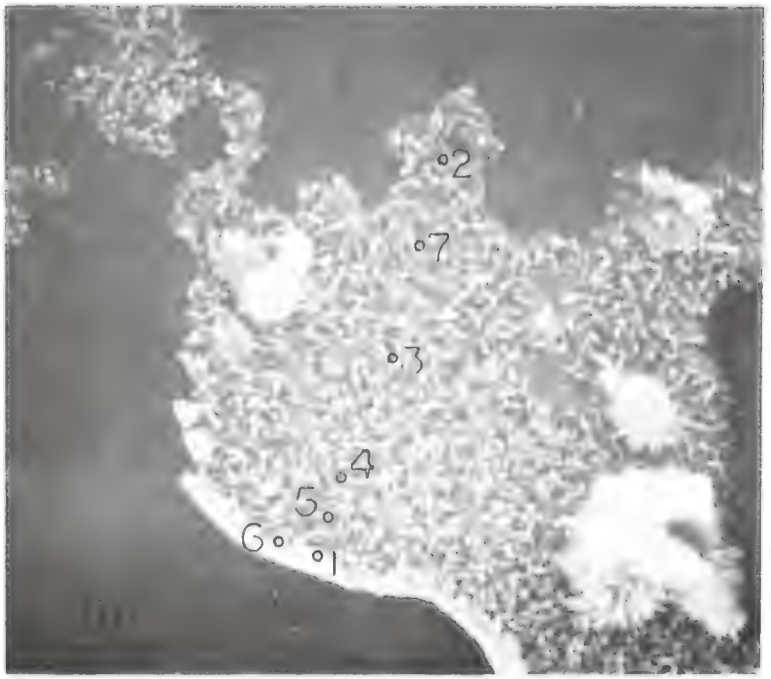

Figure 73. EDXA Analysis Appears to Indicate a Varying Thickness $Ca(OH)_2$ Layer (C6503G2)

No.	C/S	C/A	C/$\bar{S}$
1	0.36	No A	135.50
2	0.21	No A	No $\bar{S}$
3	0.22	No A	No $\bar{S}$
4	0.20	No A	No $\bar{S}$
5	0.26	No A	No $\bar{S}$
6	0.34	No A	No $\bar{S}$
7	0.22	No A	No $\bar{S}$

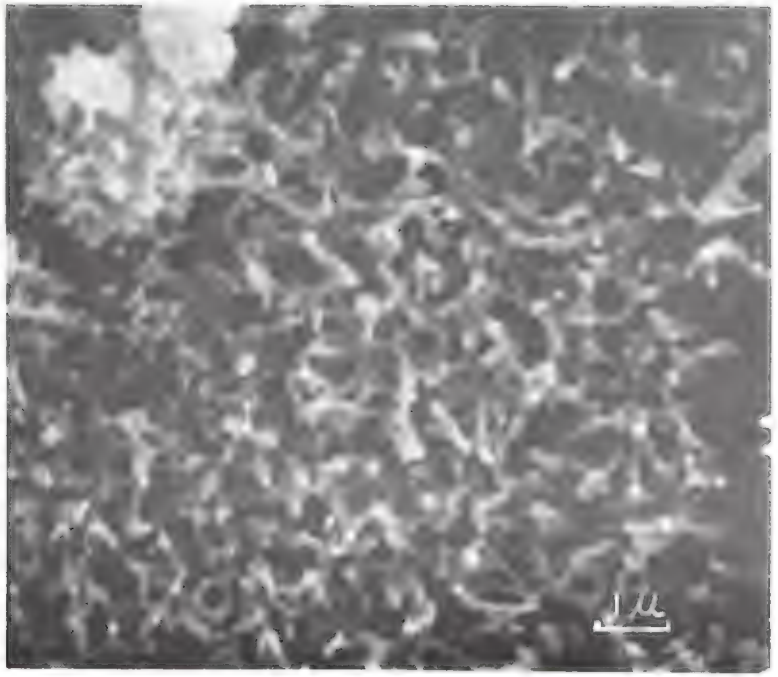

Figure 74. C-S-H Gel Forming a Reticulated Network (C6503G3)

Figure 75. Low Magnification View of Hydration Products Adhering to Glass (D5003G1)

Figure 76. Additional Photograph of Hydration Products Adhering to Glass Substrate (D6503G1)

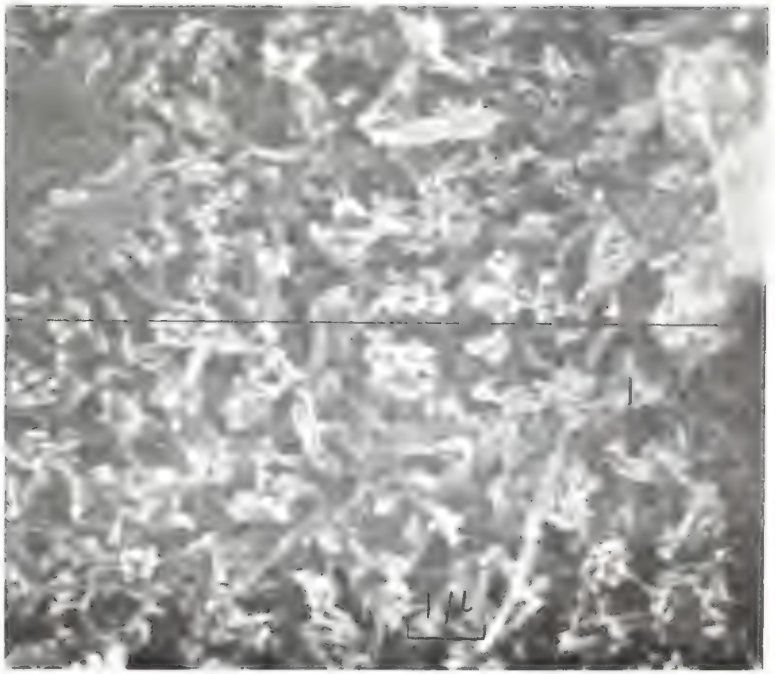

Figure 77. Reticulated Network C-S-H Gel Forming (D6503G3)

No.	C/S	C/A	C/$\bar{S}$
1	0.29	No A	No $\bar{S}$

Figure 78. Secondary Lime Layer Forming Between the Duplex Film and Cement Paste (A5003P1)

No.	C/S	C/A	C/$\bar{S}$
1	67.60	No A	No $\bar{S}$
2	7.53	No A	447.69
3	16.90	No A	294.49
4	9.41	8.93	8.23
5	6.50	11.03	9.68

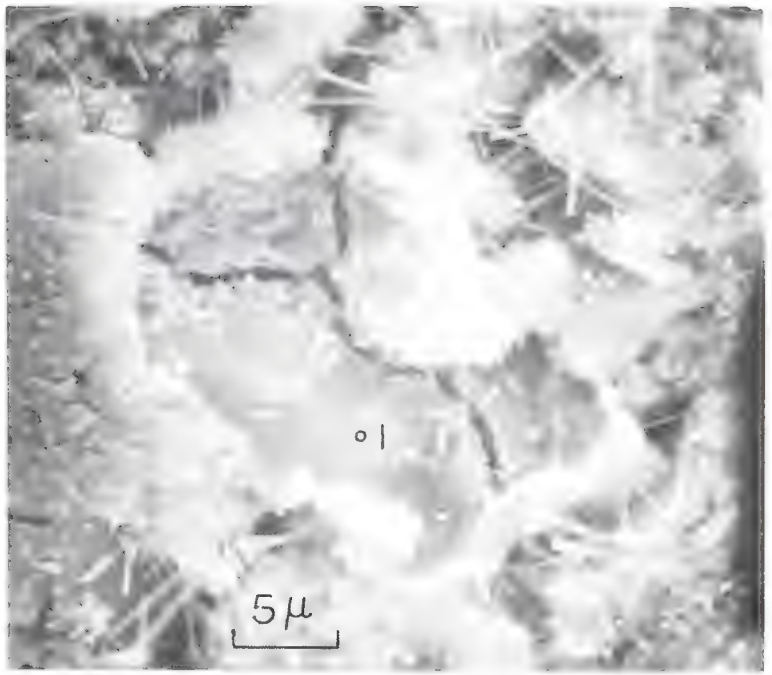

Figure 79. Stereomicrograph Showing Secondary Lime and Hollow Hydration Shell (A5003P2)

No.	C/S	C/A	C/$\bar{S}$
1	3.36	68.92	27.74

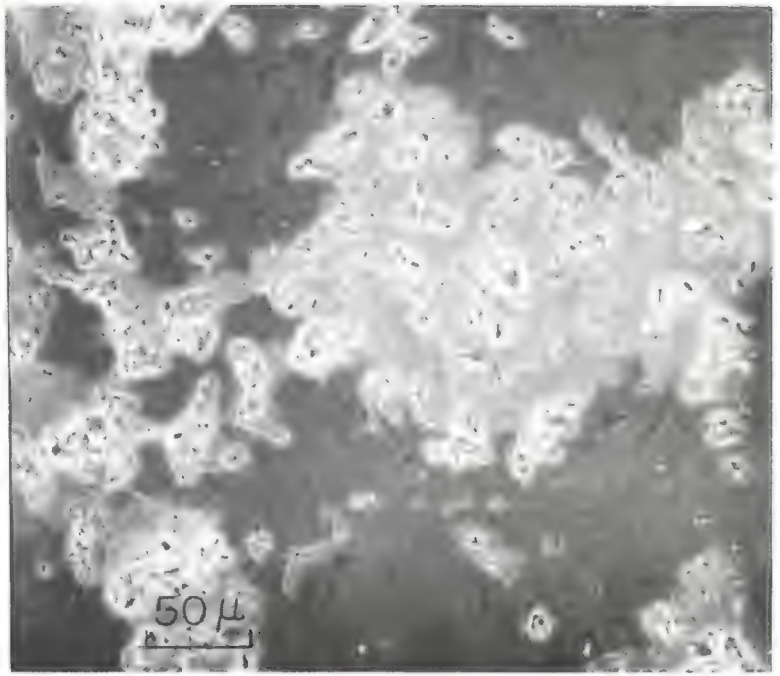

Figure 80. Extensive Development of Secondary Lime on Cement Paste (B6503P1)

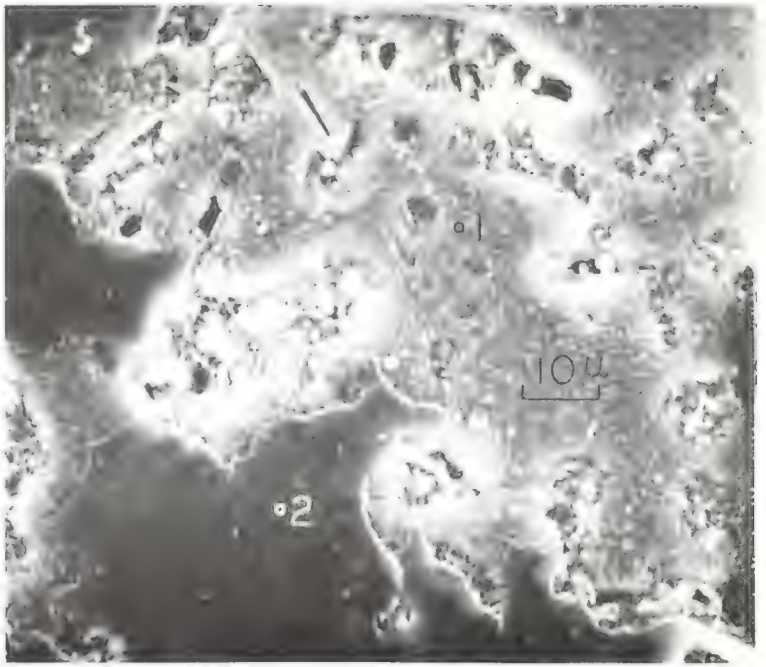

Figure 81. Comparison of C/S Ratio in Duplex Film and Secondary Lime (B6503P2)

No.	C/S	C/A	C/$\bar{S}$
1	240.74	No A	342.49
2	22.16	1306.31	No $\bar{S}$

Figure 82. Variation of C/S Ratio in Duplex Film and Secondary Lime (C6503P6)

No.	C/S	C/A	C/$\bar{S}$
1	59.63	No A	No $\bar{S}$
2	32.45	No A	477.03
3	4.08	349.56	70.18
4	5.32	91.64	39.21

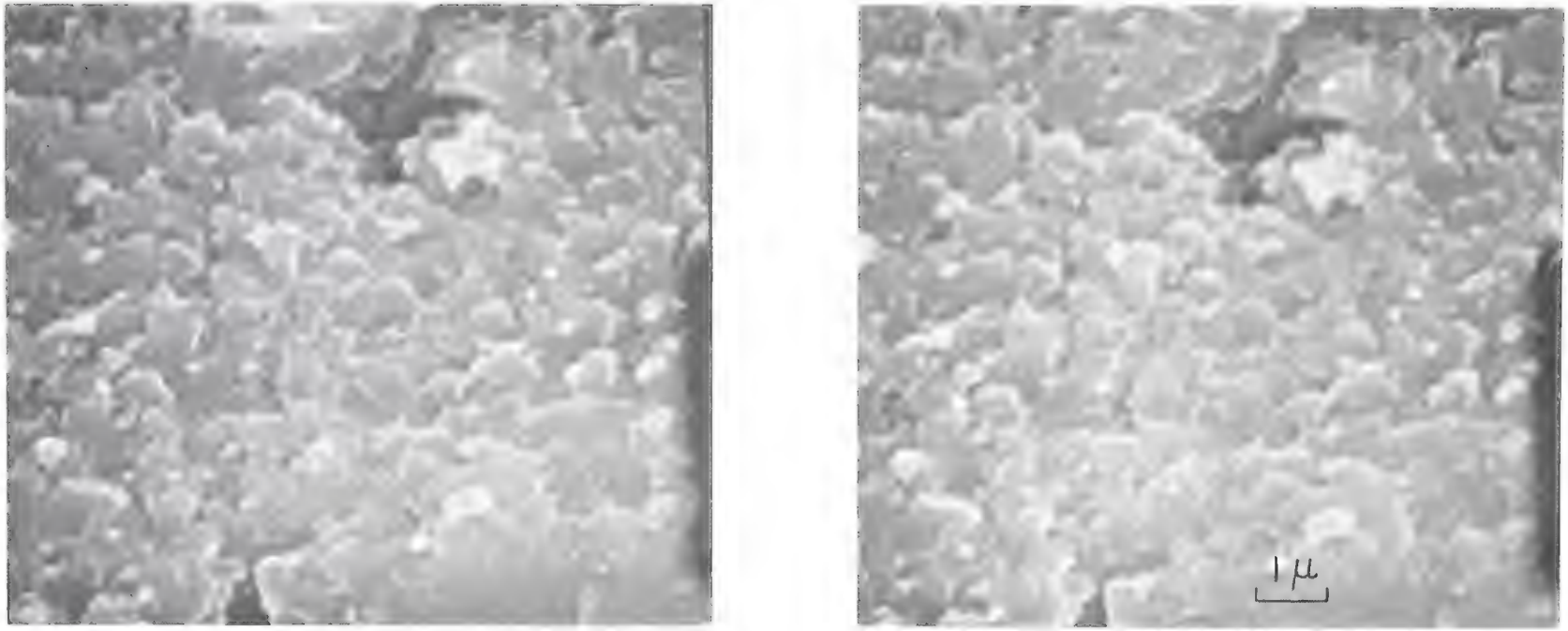

Figure 83. High Magnification Stereomicrograph of Secondary Lime (C6503P7)

Figure 84. Hadley Grain With Residual Grain Adhering to Only One Side of the Residual Shell (C6503P8)

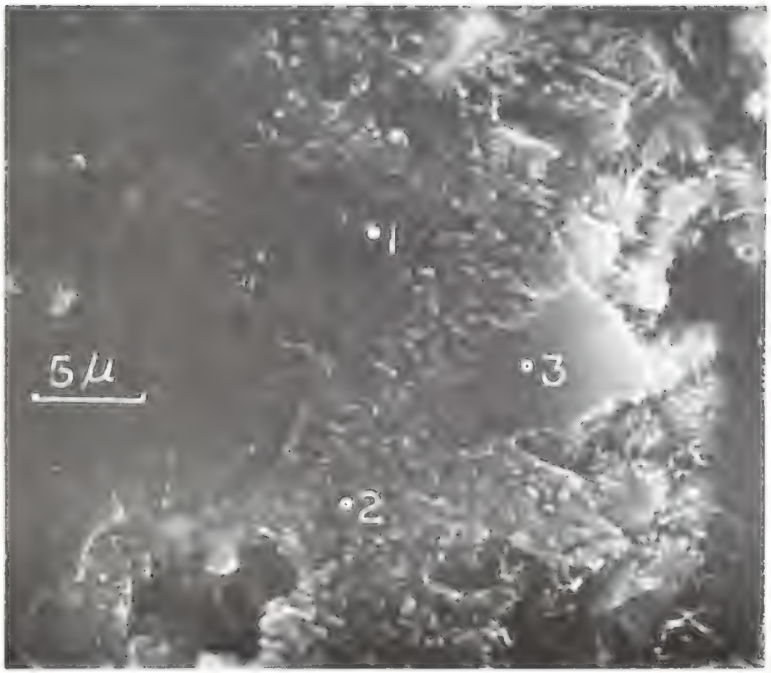

Figure 85. Duplex Film, Secondary Lime, Cement Paste Layered Structure (D6503P4)

No.	C/S	C/A	C/$\bar{S}$
1	344.94	No A	237.89
2	40.39	No A	444.55
3	8.43	No A	No $\bar{S}$

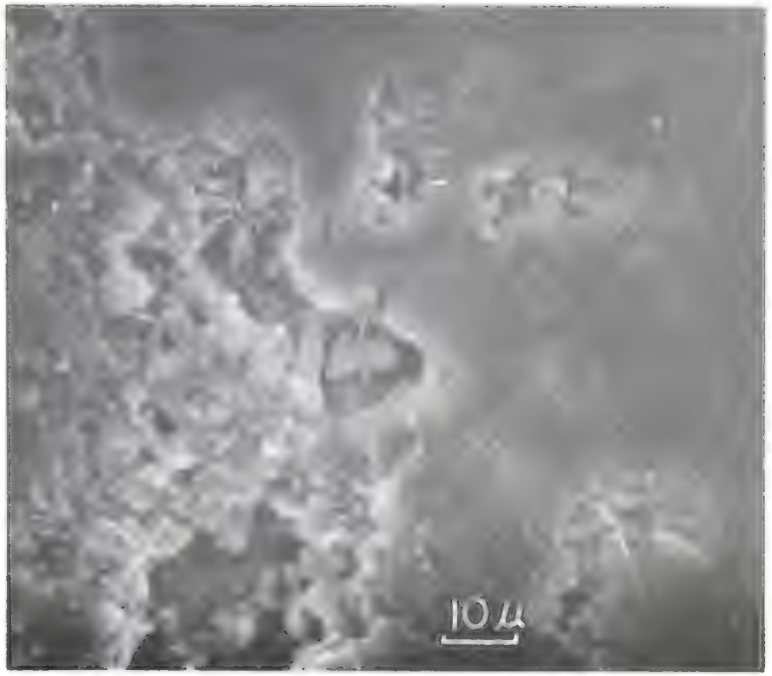

Figure 86. Large Hadley Grain at Low Magnification (D6503P6)

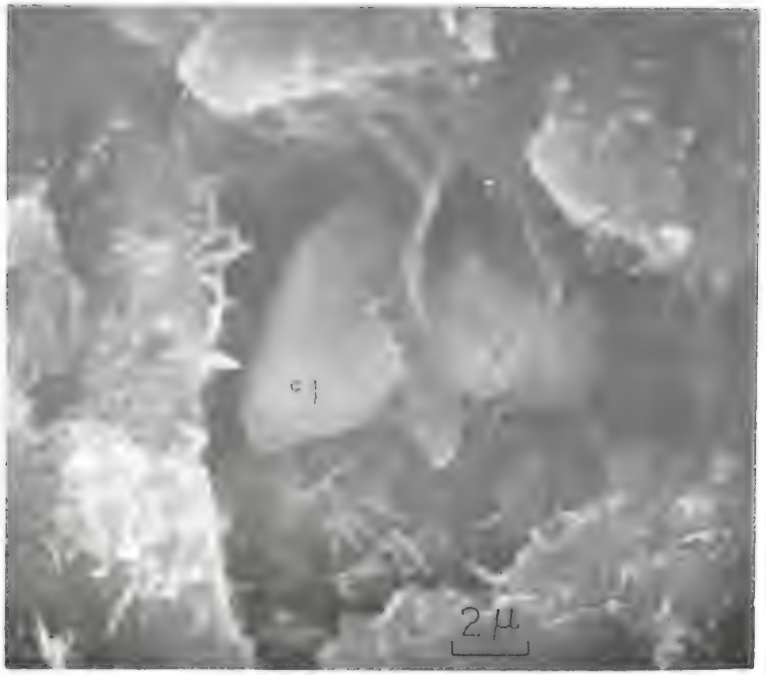

Figure 87. Enlargement of Hadley Grain Shown in Figure 86 (D6503P7)

No.	C/S	C/A	C/$\bar{S}$
1	3.24	No A	201.90

Figure 88. Low Magnification View of Hydration Products Remaining on Glass Substrate at Seven Days (A5007G1)

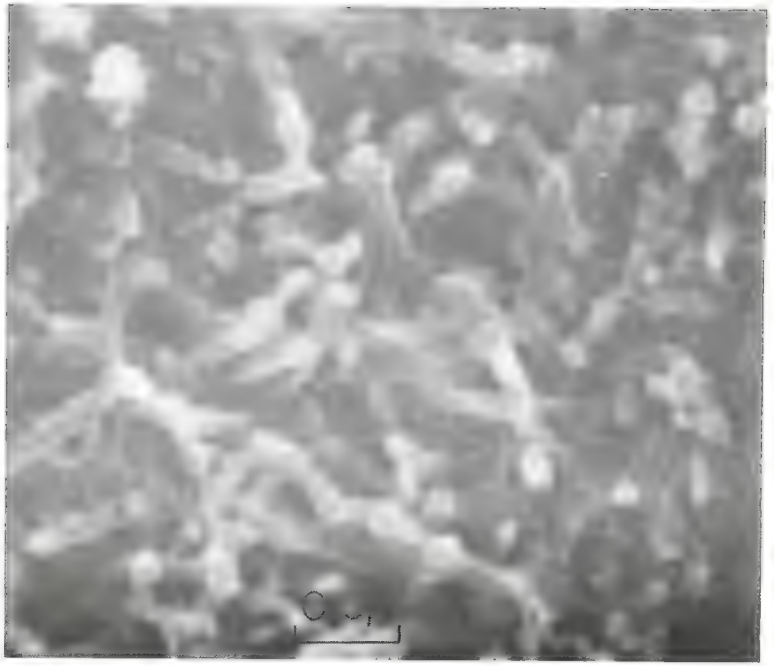

Figure 89. Enlargement of Duplex Film Shown in Figure 88 Showing Developing Reticulated Network Structure (A5007G5)

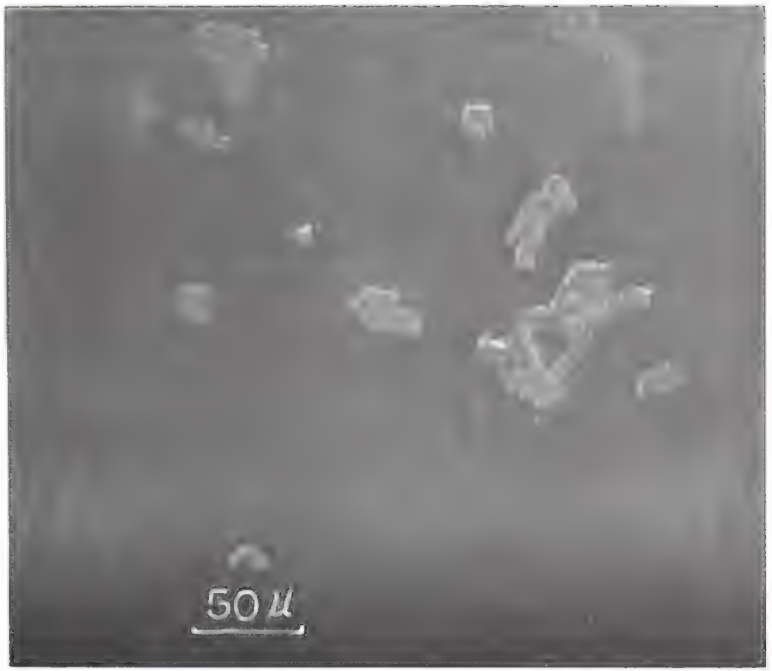

Figure 90. Duplex Film on Glass Substrate at Fourteen Days

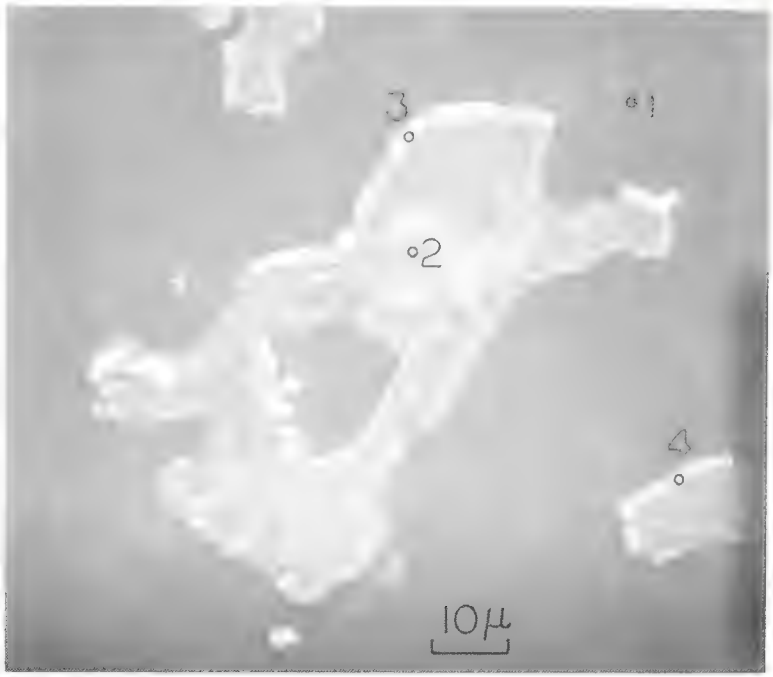

Figure 91. Close-up of Duplex Film Region Shown in Figure 90 (A5014G2)

No.	C/S	C/A	C/$\bar{S}$
1	0.20	No A	No $\bar{S}$
2	0.99	88.74	43.19
3	0.42	No A	72.64
4	0.37	No A	No $\bar{S}$

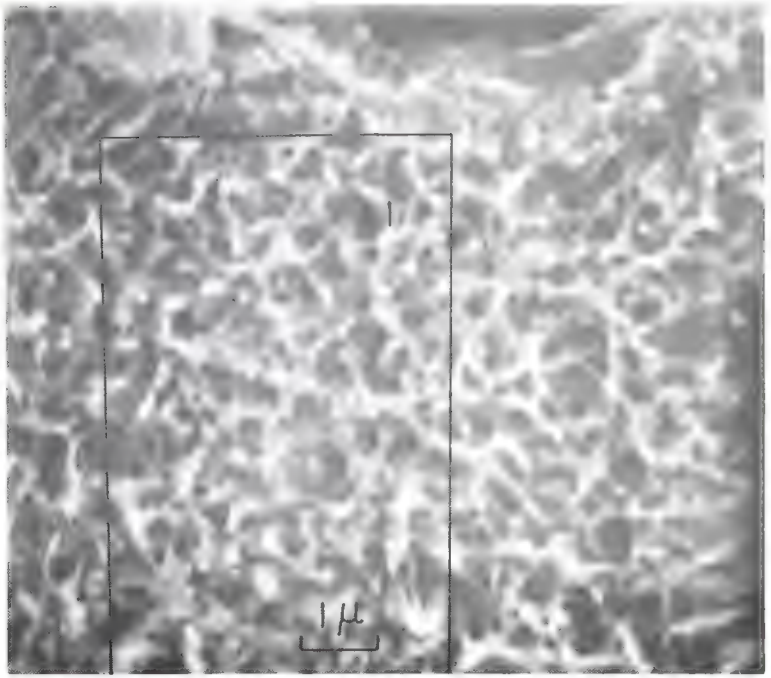

Figure 92. Enlargement of Duplex Film Shown in Figure 91 (A5014G1)

No.	C/S	C/A	C/$\bar{S}$
1	0.38	No A	No $\bar{S}$

Figure 93. Glass Substrate Seemingly Devoid of Any Hydration Product by Fourteen Days (A5014G4)

Figure 94. Dimpled Appearance of Glass Substrate Shown in Figure 93 at Higher Magnification (A5014G5)

No.	C/S	C/A	C/$\bar{S}$
1	0.21	No A	No $\bar{S}$

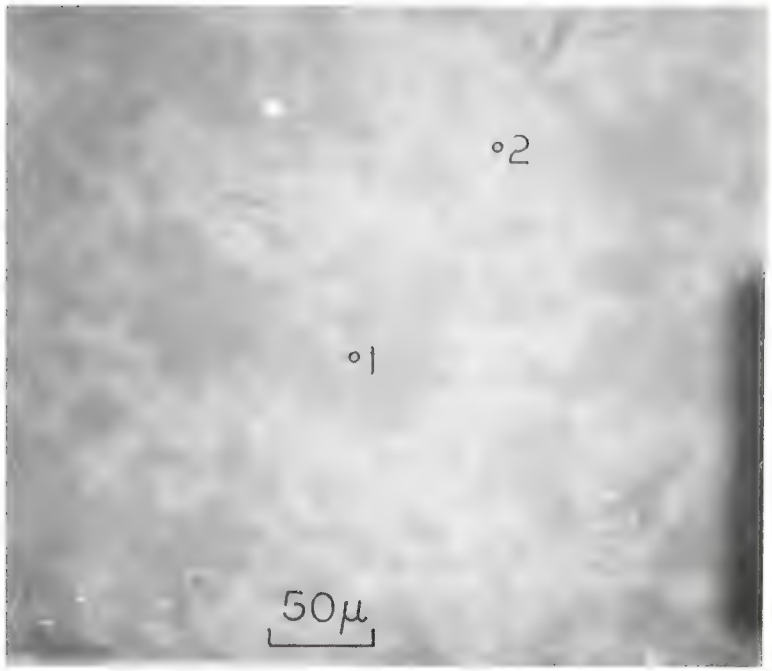

Figure 95. Alternating Light And Dark Zones Appearing on Glass Substrate at Twenty-Eight Days (A5028G1)

No.	C/S	C/A	C/$\bar{S}$
1	0.19	No A	No $\bar{S}$
2	0.20	No A	No $\bar{S}$

Figure 96. Dimpled Structure Retained on Twenty-Eight Day Glass Substrate (A5028G2)

No.	C/S	C/A	C/$\bar{S}$
1	0.20	No A	No $\bar{S}$

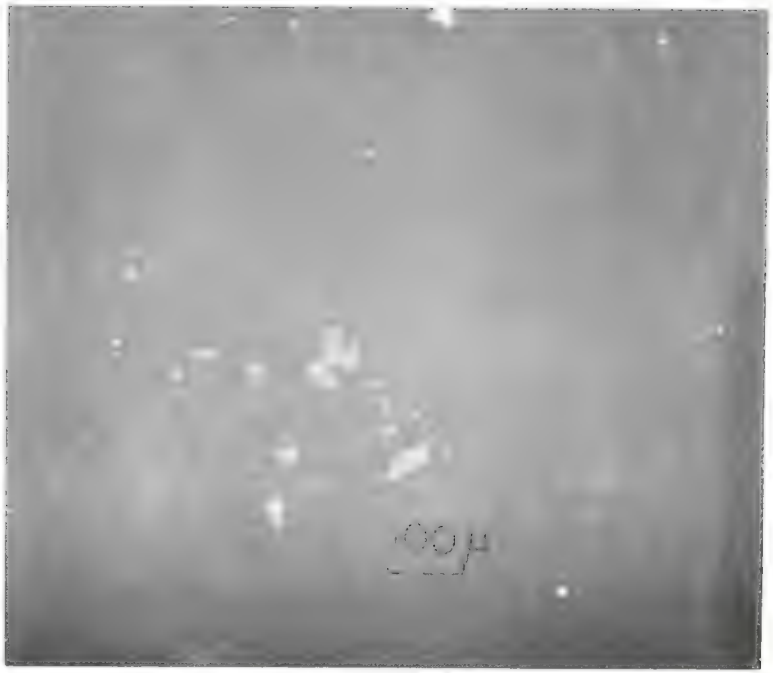

Figure 97. One of the Few Areas Having Retained Hydration Products on the Glass Substrate (B5007G1)

Figure 98. Retained Duplex Film and Hydration Shells on Glass (B5007G2)

No.	C/S	C/A	C/$\bar{S}$
1	0.281	No A	No $\bar{S}$

Figure 99. Enlargement of C-S-H Shown in Figure 98 Showing a Rod-Like and a Foreshortened Morphology (B5007G3)

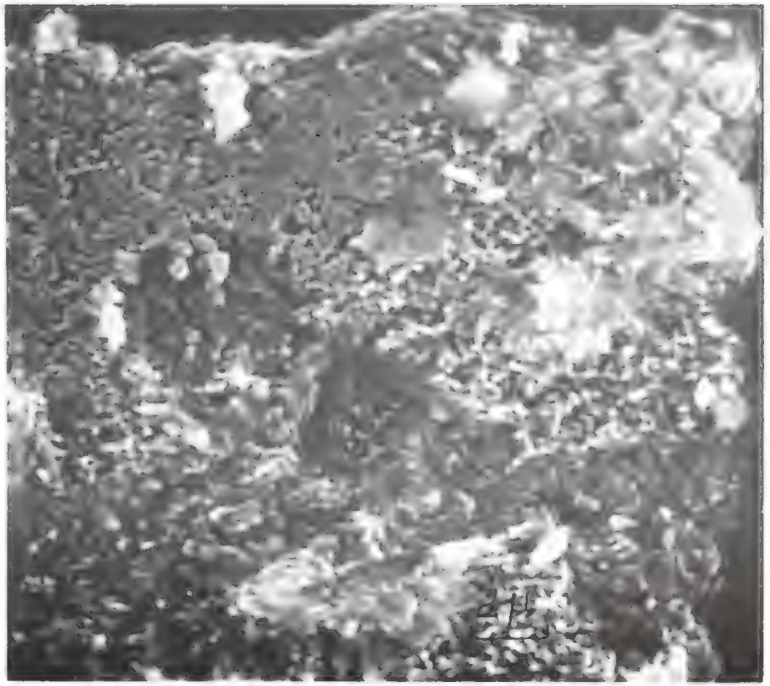

Figure 100. Additional Micrograph of Foreshortened and Rod-Like C-S-H Gel (B5007G5)

No.	C/S	C/A	C/$\bar{S}$
1	0.299	No A	No $\bar{S}$

Figure 101. Extensive Development of Dimpled Structure at Fourteen Days (B5014G1)

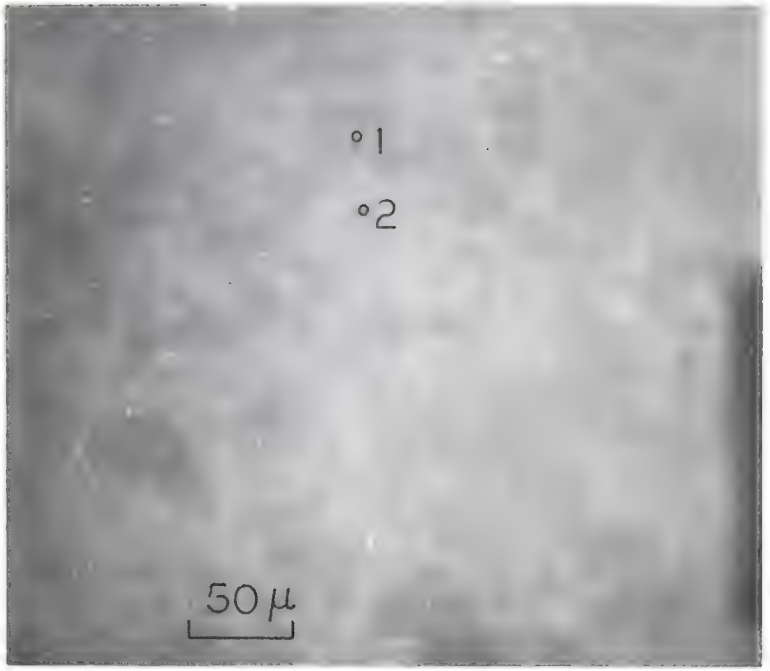

Figure 102. Low Magnification of Dimpled Substrate (B5028G1)

No.	C/S	C/A	C/$\bar{S}$
1	0.20	No A	No $\bar{S}$
2	0.20	No A	173.65

Figure 103. Enlargement of Figure 102 (B5028G2)

No.	C/S	C/A	C/$\bar{S}$
1	0.20	No A	No $\bar{S}$

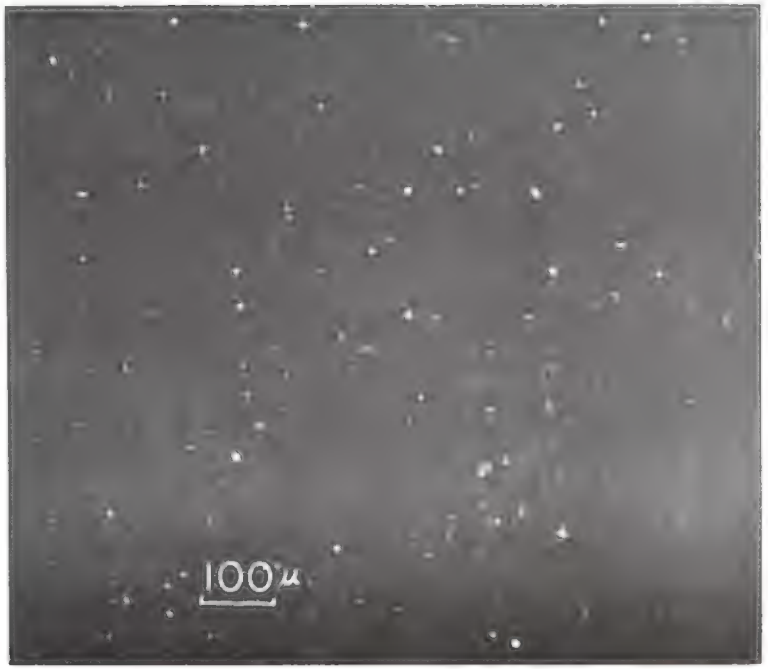

Figure 104. Hydration Products Remaining on Substrate at Seven Days (C5007G4)

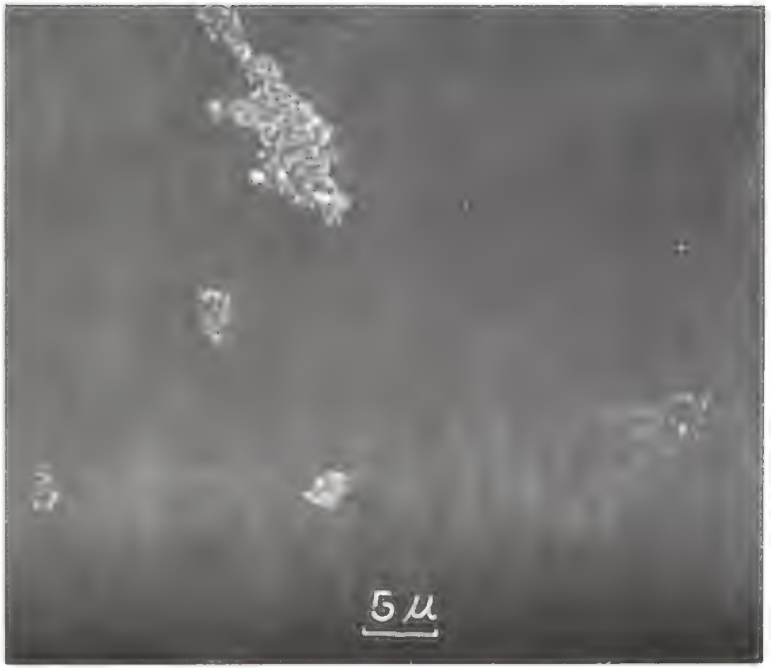

Figure 105. Seven-Day-Old Duplex Film (C5007G3)

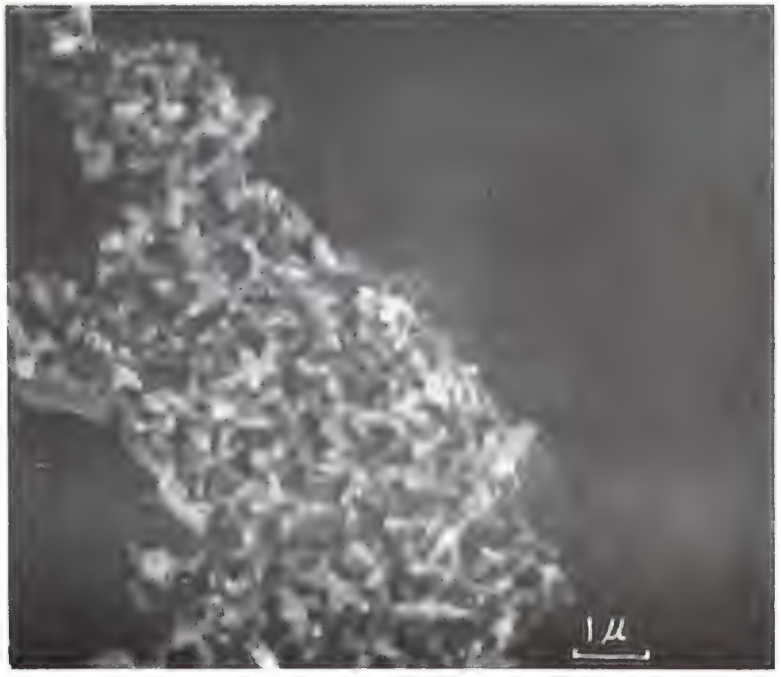

Figure 106. General Morphology of Seven-Day-Old Duplex Film C-S-H (C5007G2)

Figure 107. High Magnification of Seven-Day-Old Rod-Like C-S-H Gel of the Duplex Film (C5007G1)

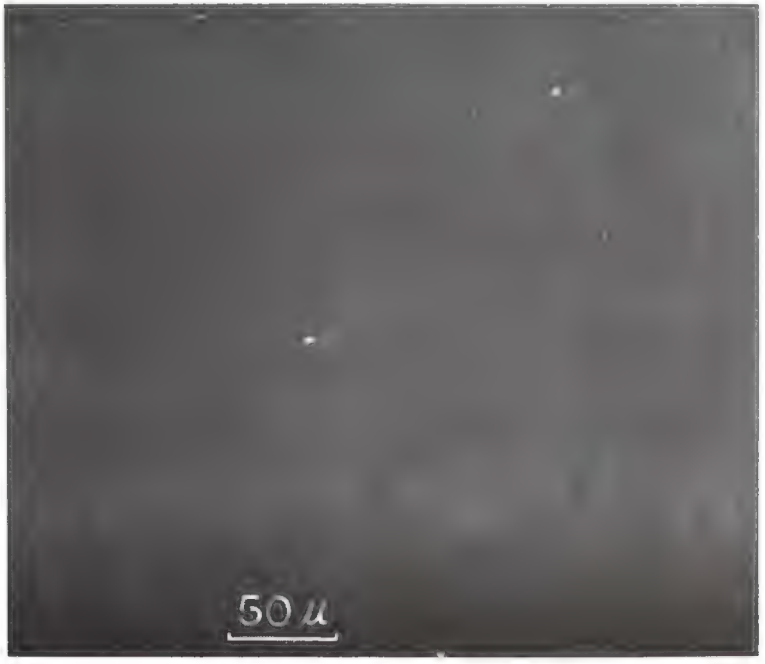

Figure 108. Substrate Almost Devoid of Hydration Products at Fourteen Days (C5014G3)

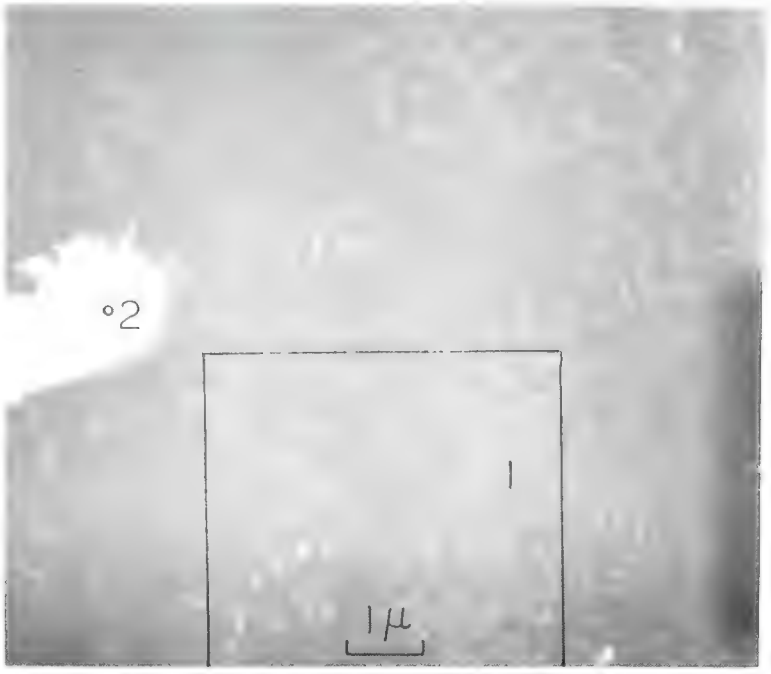

Figure 109. Peculiar Etch or Precipitation Pattern Found with Cement C at Fourteen Days (C5014G2)

No.	C/S	C/A	C/$\bar{S}$
1	0.20	No A	No $\bar{S}$
2	0.19	No A	No $\bar{S}$

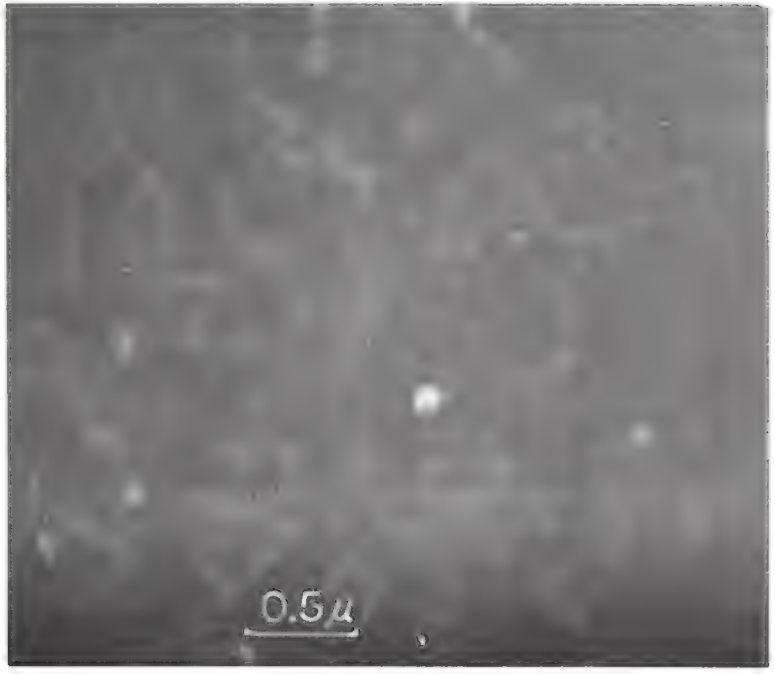

Figure 110. High Magnification View of Figure 109 (C5014G1)

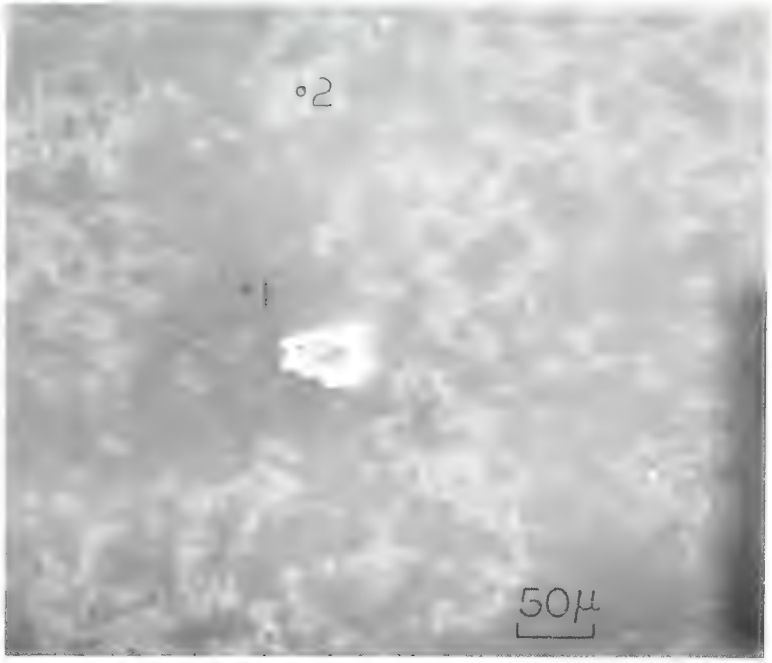

Figure 111. Blotchy Pattern Apparent on Substrate at Twenty-Eight Days (C5028G1)

No.	C/S	C/A	C/$\bar{S}$
1	0.20	No A	No $\bar{S}$
2	0.20	No A	No $\bar{S}$

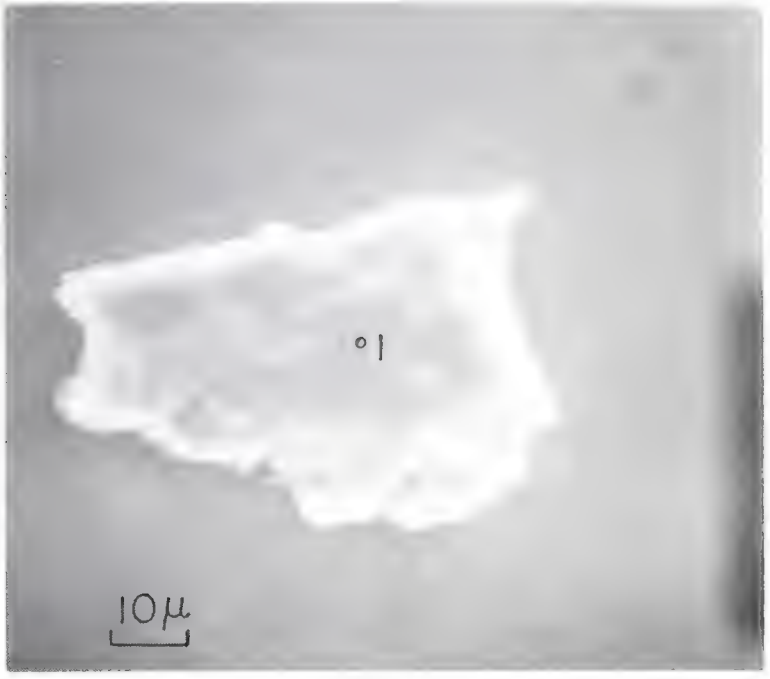

Figure 112. Unidentified Particle Shown in the Center of Figure 111 (C5028G2)

No.	C/S	C/A	C/$\bar{S}$
1	0.21	No A	No $\bar{S}$

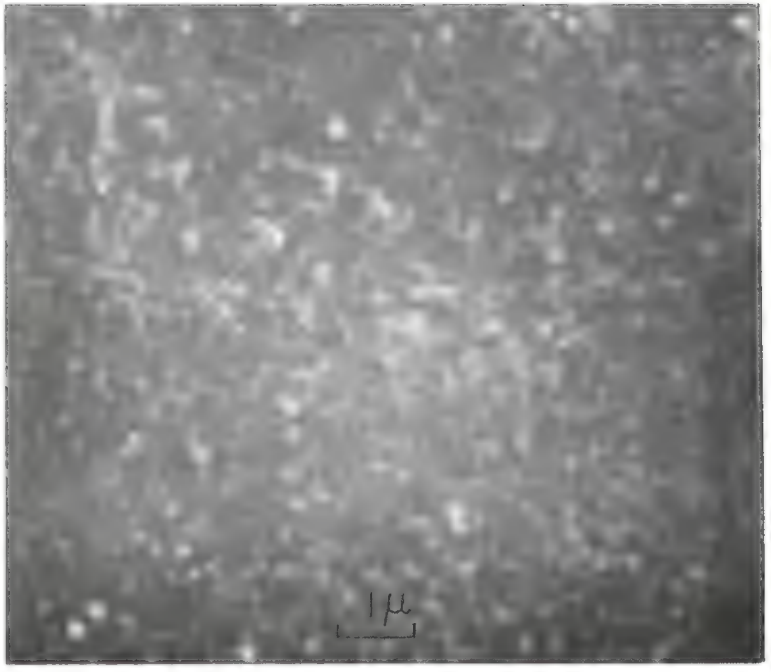

Figure 113. High Magnification of Dimpled Substrate (C5028G3)

No.	C/S	C/A	C/$\bar{S}$
1	0.20	No A	No $\bar{S}$

Figure 114. Scattered Hydration Products on Substrate (D5007G3)

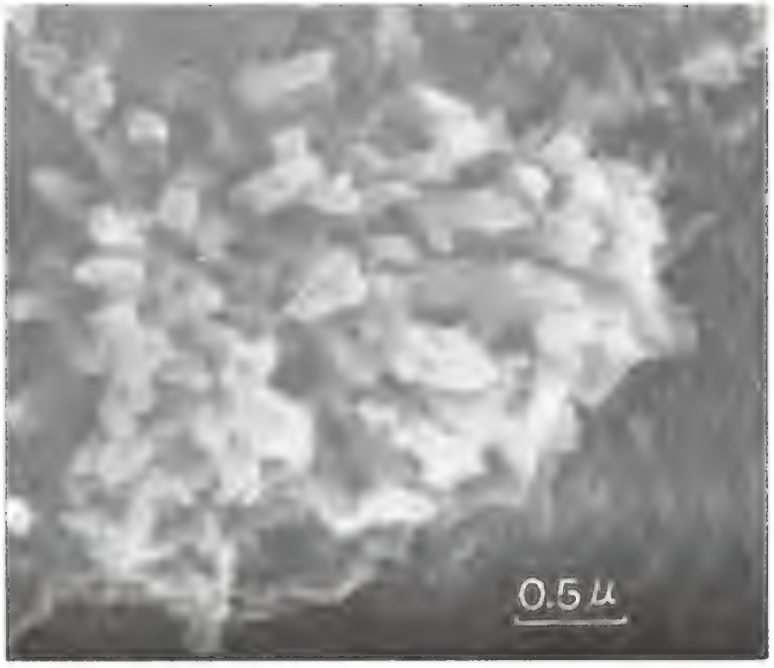

Figure 115. C-S-H Gel Developed on Small Particle Remaining on Substrate (D5007G1)

Figure 116. Blotchy Grey Pattern on Substrate at Fourteen Days (D5014G3)

Figure 117. Hydration Products on Glass Substrate at Twenty-Eight Days (D5028G1)

No.	C/S	C/A	C/$\bar{S}$
1	0.20	No A	No $\bar{S}$
2	0.20	No A	No $\bar{S}$

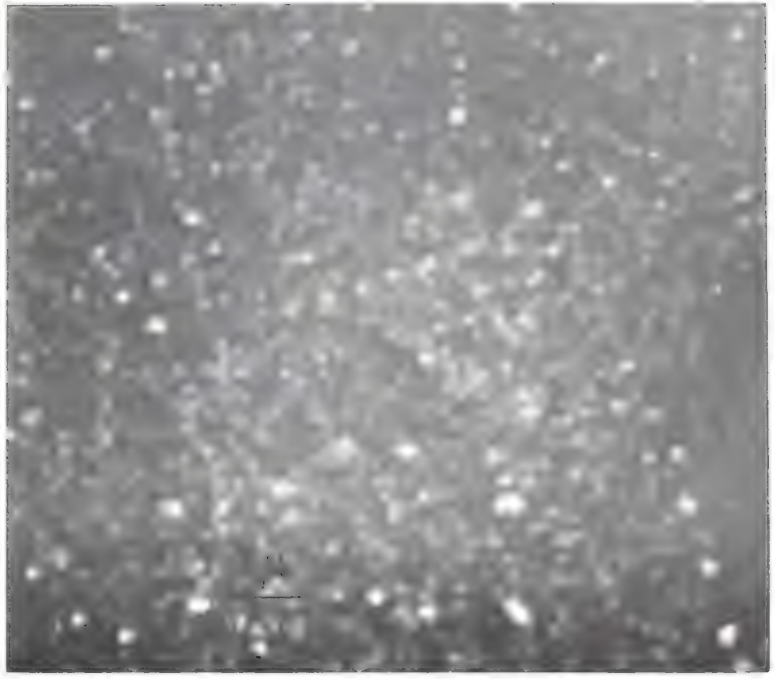

Figure 118. Close-up View of Dimpled Structure Developed with Cement D (D5028G2)

No.	C/S	C/A	C/$\bar{S}$
1	0.20	No A	No $\bar{S}$

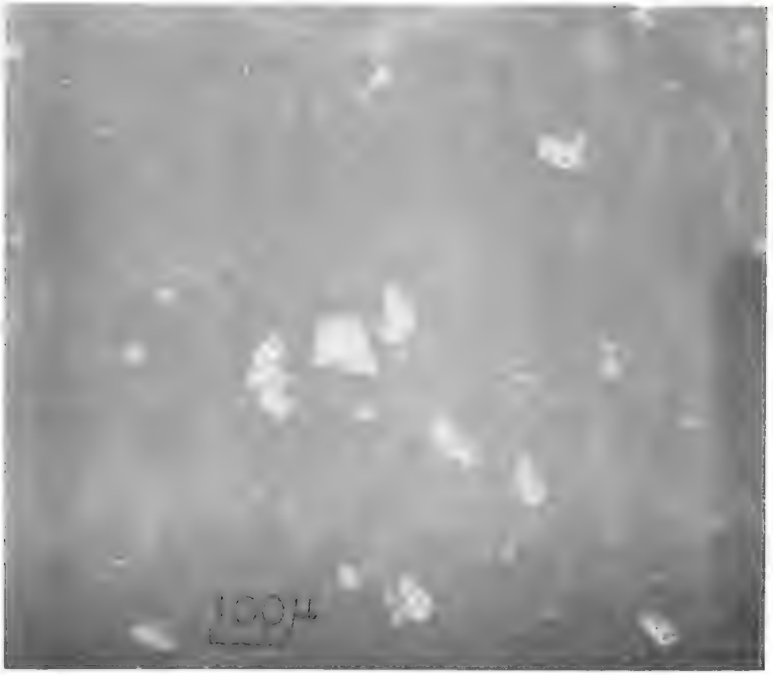

Figure 119. Low Magnification of Cement Paste Interface Exhibiting Several "Windows" (A5007P1)

Figure 120. Hydration Products Overlain by Duplex Film (A5007P2)

Figure 121. Low Contrast View Through a Duplex Film Window (A5007P10)

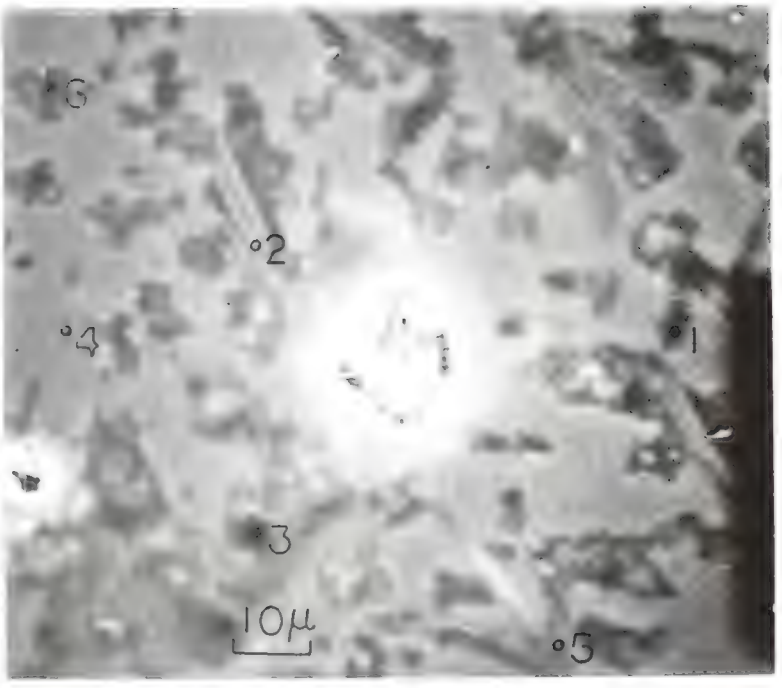

Figure 122. High Contrast View of Figure 121 (A5007P9)

No.	C/S	C/A	C/$\bar{S}$
1	10.05	No A	1025.15
2	11.95	15.62	9.17
3	4.22	314.55	71.20
4	30.83	No A	No $\bar{S}$
5	22.12	16.20	10.51
6	6.98	60.49	23.08

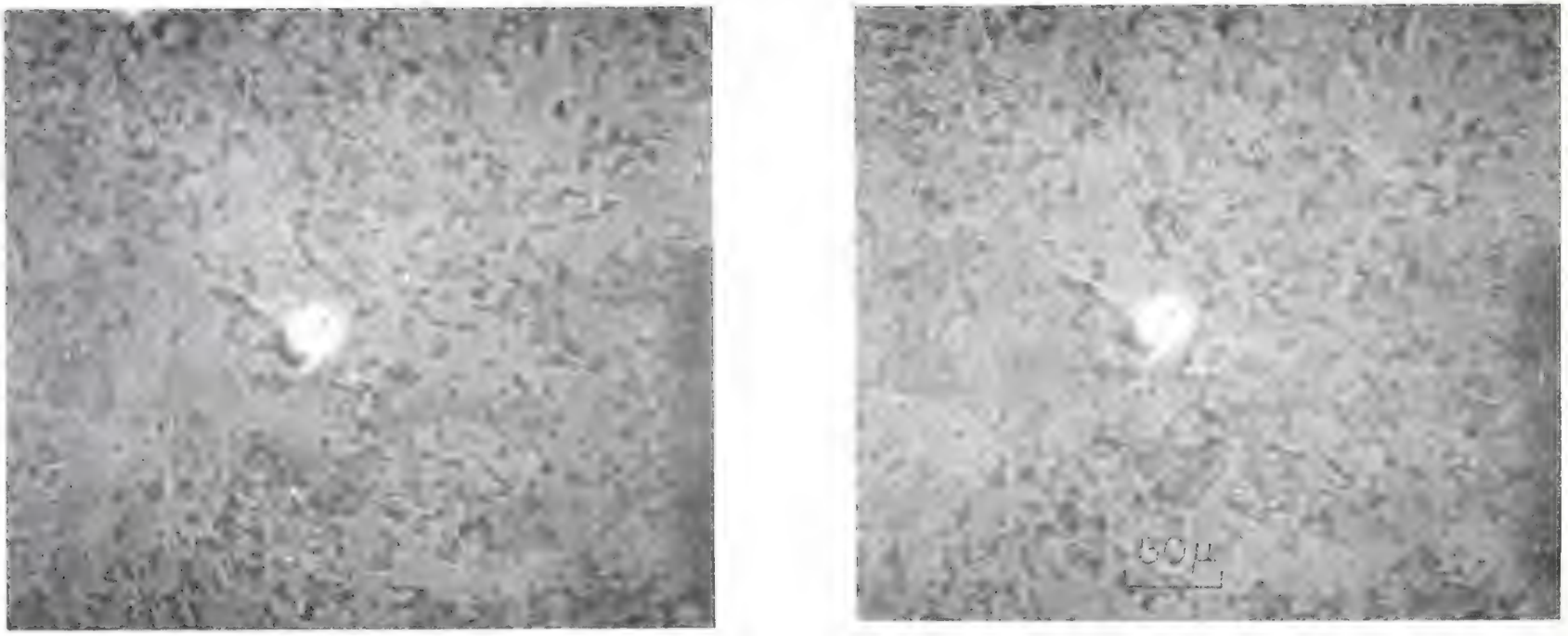

Figure 123. High Contrast Stereomicrograph of Fourteen-Day-Old Paste Interface (A5014P1)

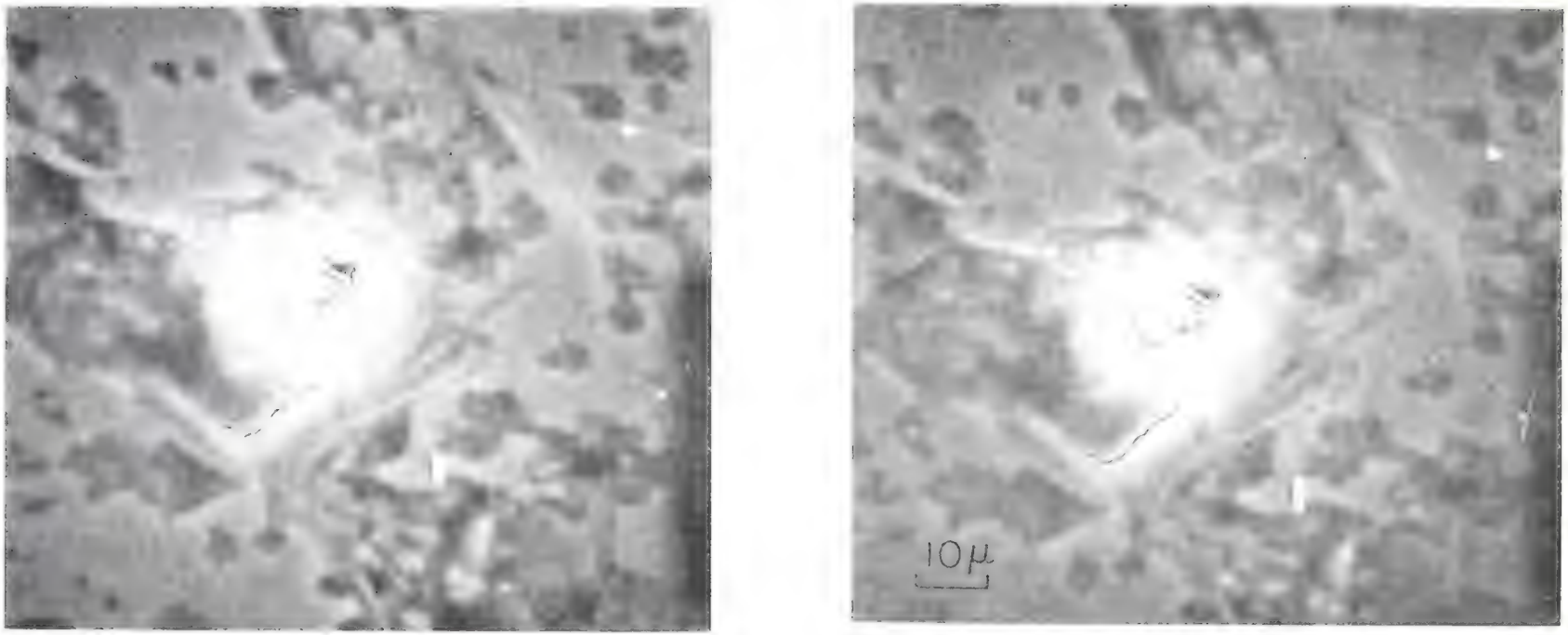

Figure 124. High Contrast Enlargement of Figure 123 (A5014P2)

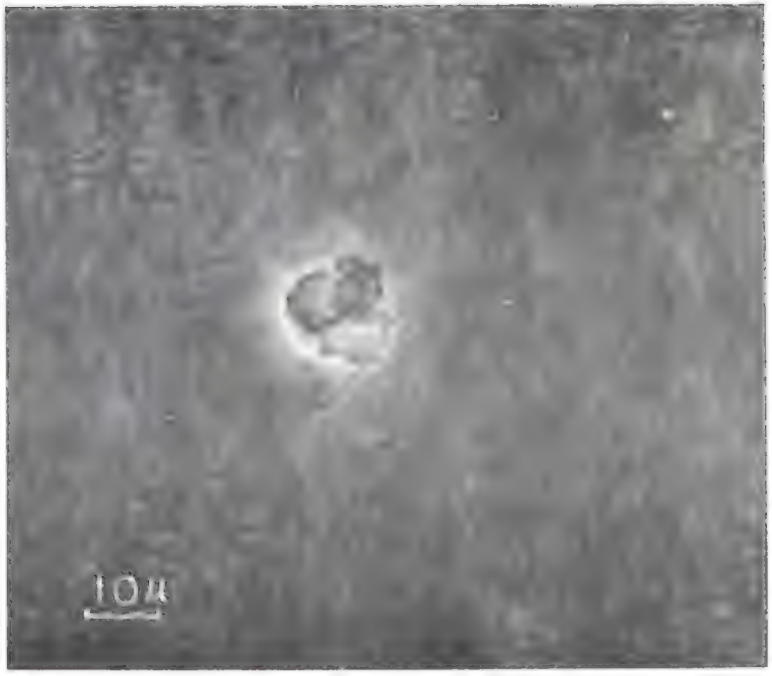

Figure 125. Normal Contrast Well-Focused View of Figure 124 (A5014P2)

Figure 126. High Contrast Photomicrograph of Blotchy Paste (A5028P3)

No.	C/S	C/A	C/$\bar{S}$
1	3.81	75.18	57.10
2	16.66	No A	No $\bar{S}$

Figure 127. Cement Grains and $Ca(OH)_2$ (?) Crystal Under Duplex Film (A5028P1)

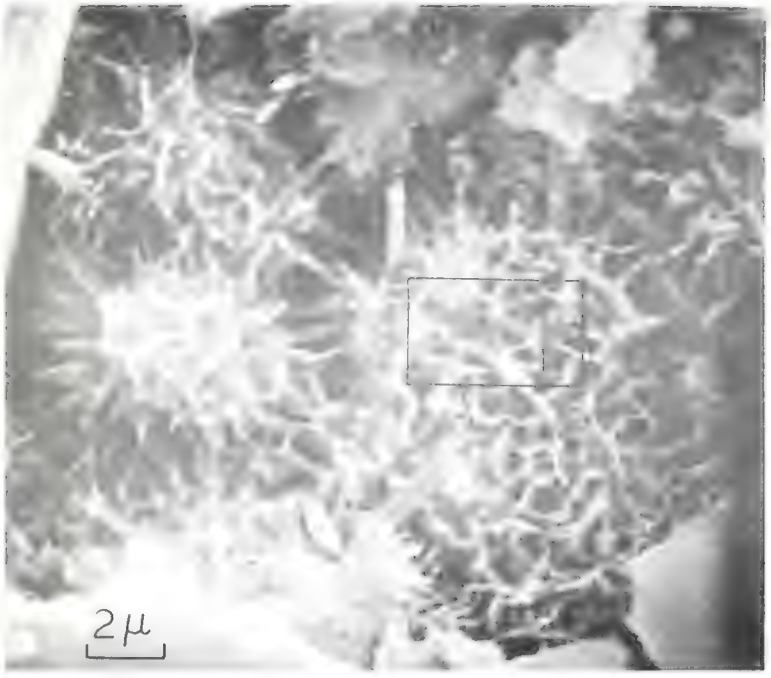

Figure 128. Reticulated Network Morphology of C-S-H on Cement Grains (A5028P2)

No.	C/S	C/A	C/$\bar{S}$
1	3.67	77.24	43.11

Figure 129. Large "Window" Appearing on Seven-Day Paste (B5007P1)

Figure 130. Close-up of Figure 129 Window (B5007P2)

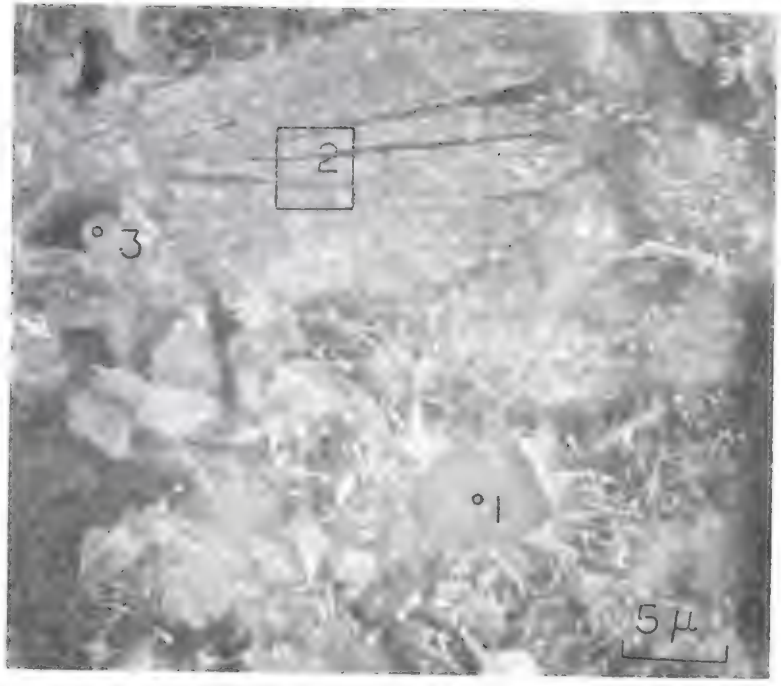

Figure 131. Enlargement of Fan Shaped $Ca(OH)_2$ and Hydrating Cement Grains (B5007P3)

No.	C/S	C/A	C/$\bar{S}$
1	2.08	108.86	94.39
2	29.96	5.92	5.12
3	2.43	81.54	58.49

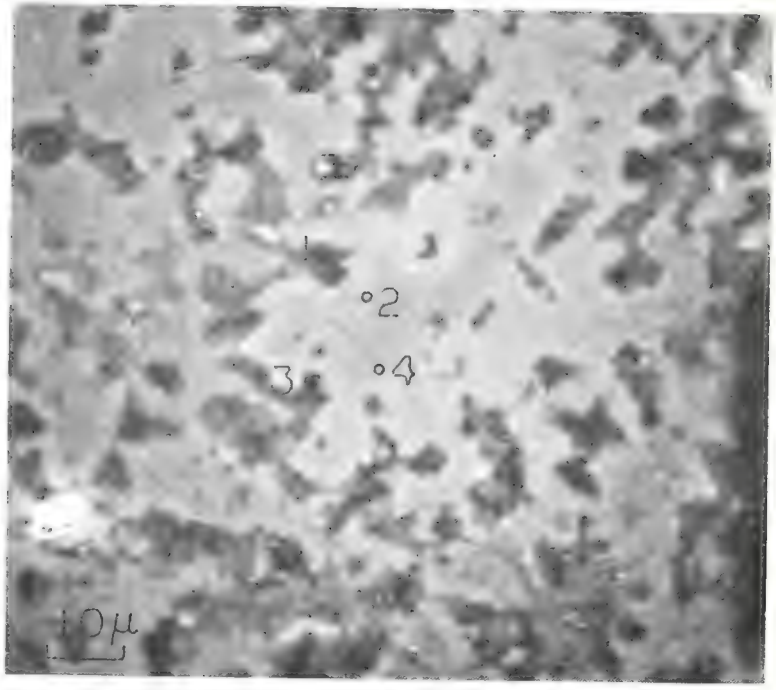

Figure 132. Composition of Blotchy Pastes Varies from the Dark to Light Areas (B5007P4)

No.	C/S	C/A	C/$\bar{S}$
1	5.63	294.09	65.07
2	55.94	No A	1193.60
3	8.97	No A	89.95
4	80.62	No A	356.16

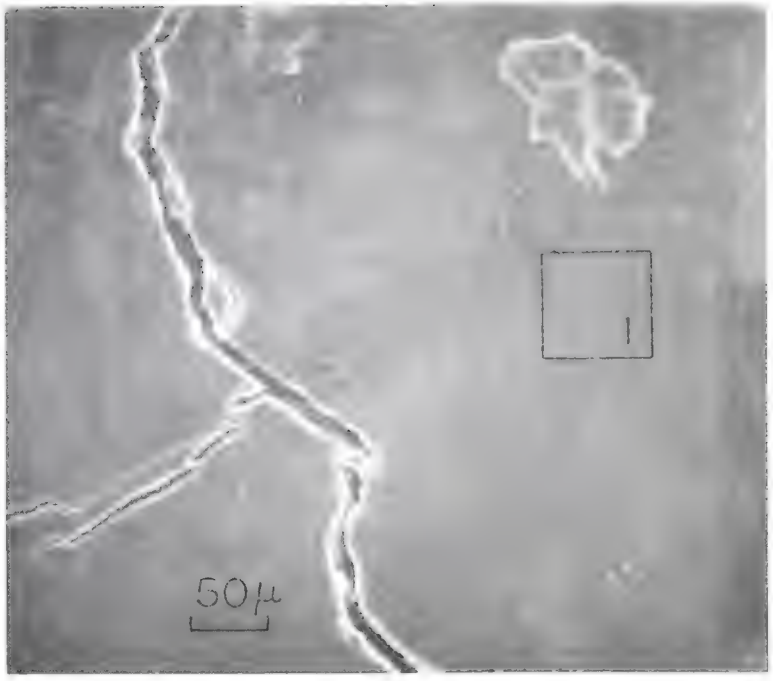

Figure 133. Shrinkage Crack in Fourteen-Day-Old Paste Interface (B5014P2)

No.	C/S	C/A	C/$\bar{S}$
1	8.24	No A	123.60

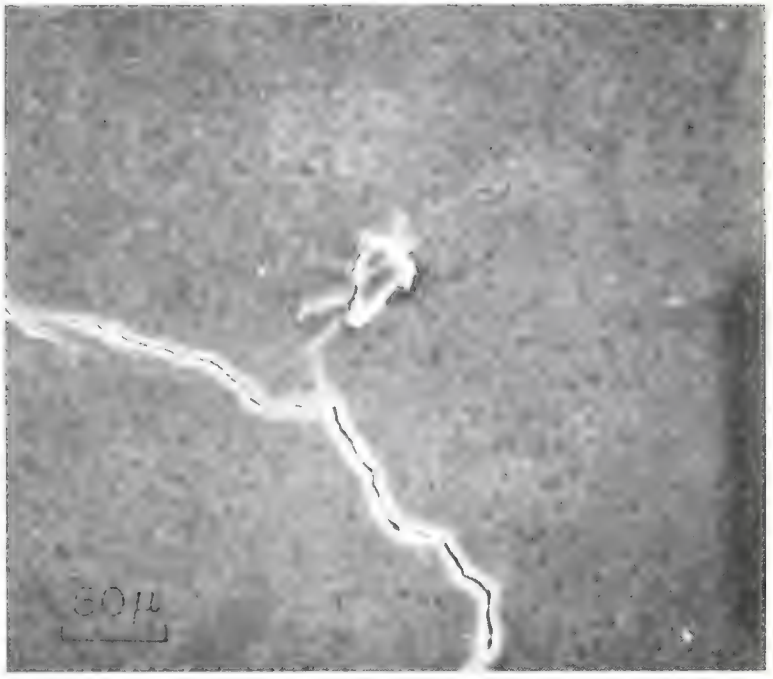

Figure 134. Shrinkage and Blotchy Pattern Noted on Twenty-Eight-Day-Old Paste (B5028P1)

Figure 135. Numerous Small Windows on Cement C Interface (C5007P1)

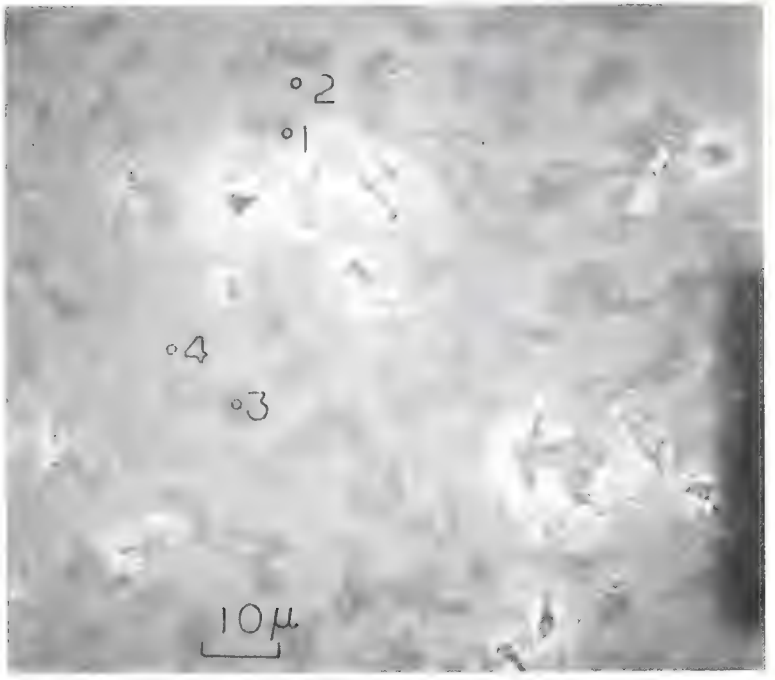

Figure 136. Windows in Duplex Film (C5007P2)

No.	C/S	C/A	C/$\bar{S}$
1	6.51	No A	126.22
2	37.73	No A	No $\bar{S}$
3	8.49	No A	283.35
4	72.48	No A	No $\bar{S}$

Figure 137. Rod-Like C-S-H on Cement Grains as Seen Through Duplex Window (C5007P3)

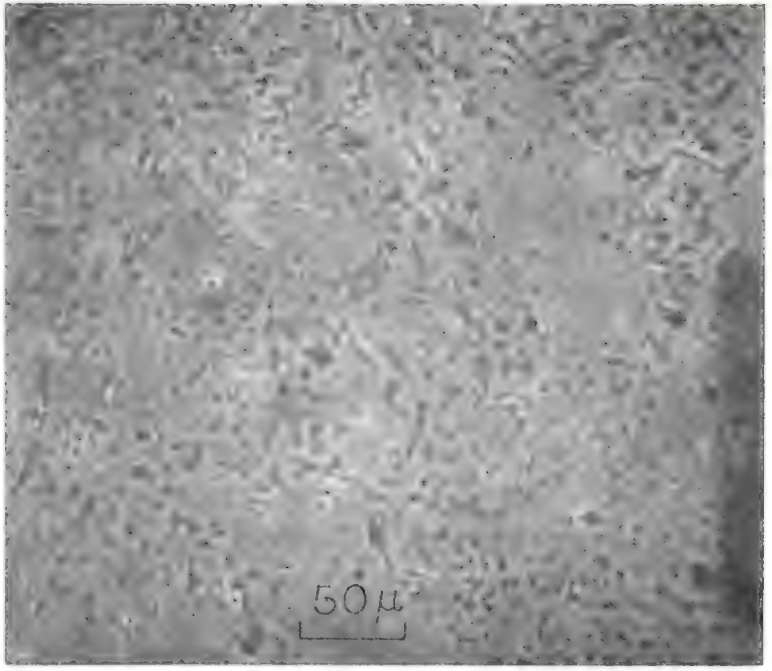

Figure 138. Fourteen-Day-Old Cement Paste with No Breaks in Duplex Film (C5014P1)

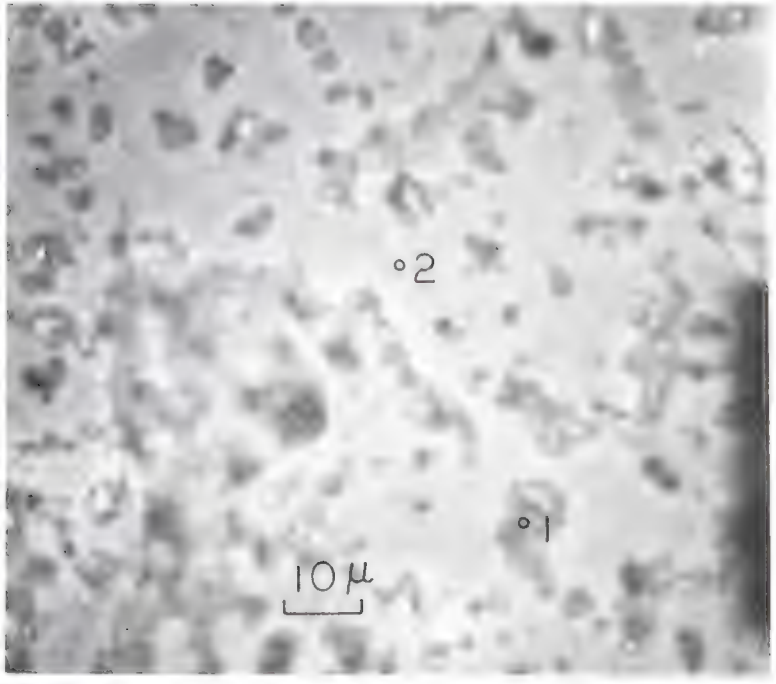

Figure 139. Enlarged View of Blotchy Paste Interface Shown in Figure 138 (C5014P2)

No.	C/S	C/A	C/$\bar{S}$
1	4.21	16.03	50.00
2	29.41	No A	No $\bar{S}$

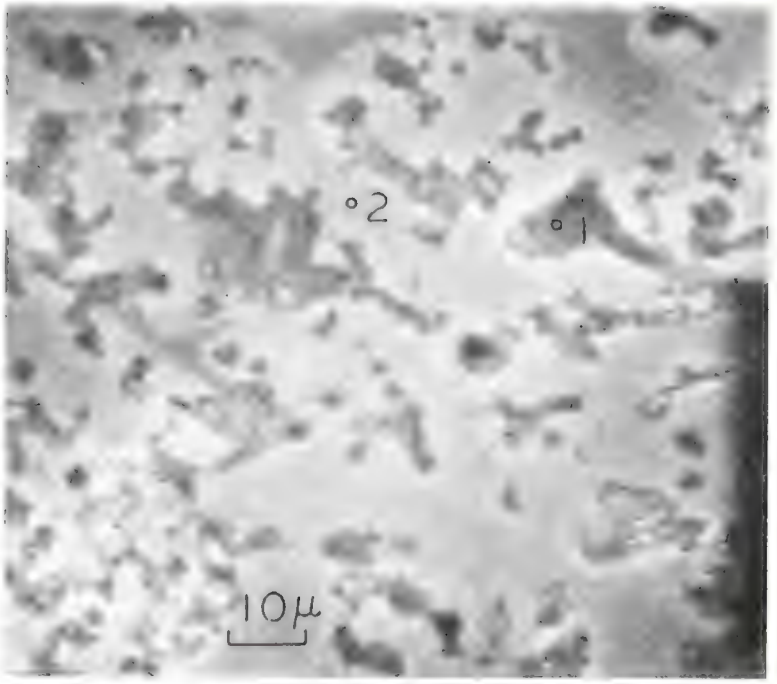

Figure 140. Twenty-Eight-Day-Old Paste Interface (C5028P1)

No.	C/S	C/A	C/$\bar{S}$
1	7.27	933.58	67.47
2	29.79	No A	299.85

Figure 141. Few Small Windows in Seven-Day Paste Made from Cement D (D5007P1)

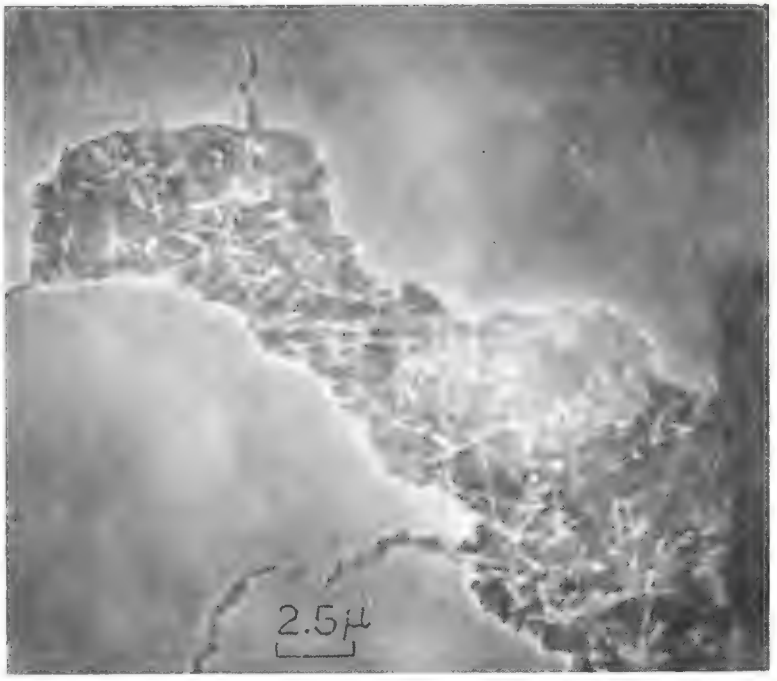

Figure 142. Probable Ettringite Needles Immediately Underneath Duplex Film (D5007P2)

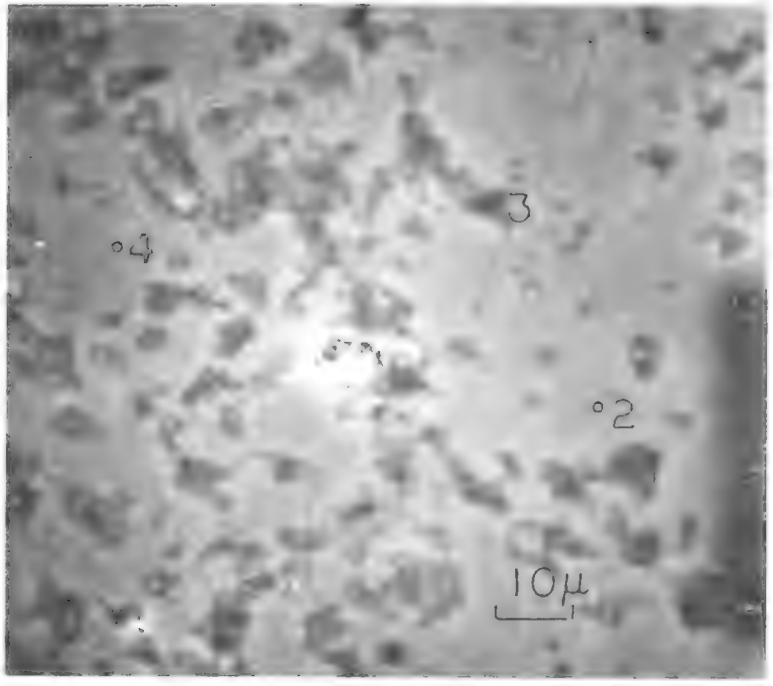

Figure 143. Compositional Analysis of Cement D Paste Interface (D5007P6)

No.	C/S	C/A	C/$\bar{S}$
1	9.12	No A	76.53
2	34.75	No A	No $\bar{S}$
3	7.75	No A	56.85
4	34.27	No A	No $\bar{S}$

Figure 144. Blotchy Fourteen-Day-Old Paste with Shrinkage Cracks Through Duplex Film (D5014P1)

No.	C/S	C/A	C/$\bar{S}$
1	9.05	No A	85.82
2	44.44	No A	529.15

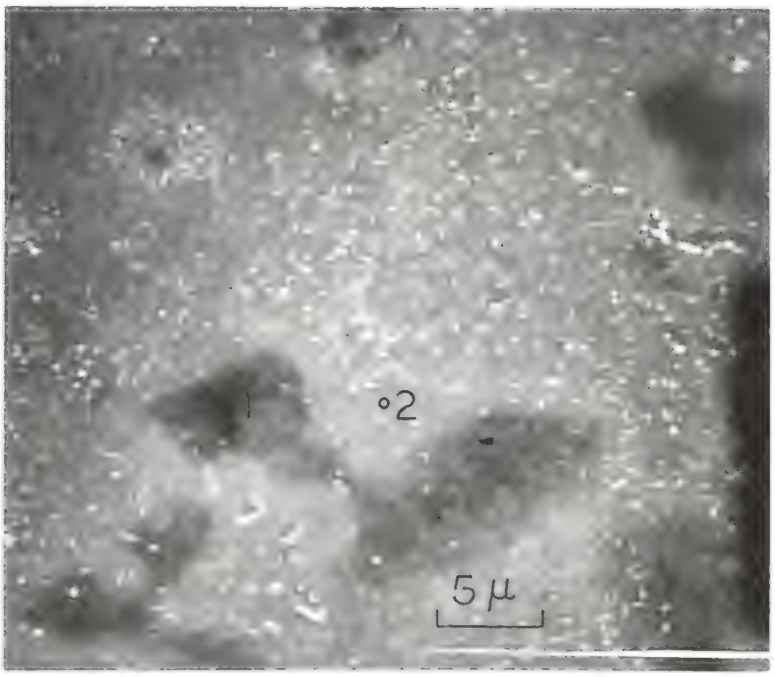

Figure 145. Dimpled Duplex Film on Twenty-Eight-Day Paste (D5028P1)

No.	C/S	C/A	C/$\bar{S}$
1	7.25	987.17	98.50
2	12.52	No A	415.23

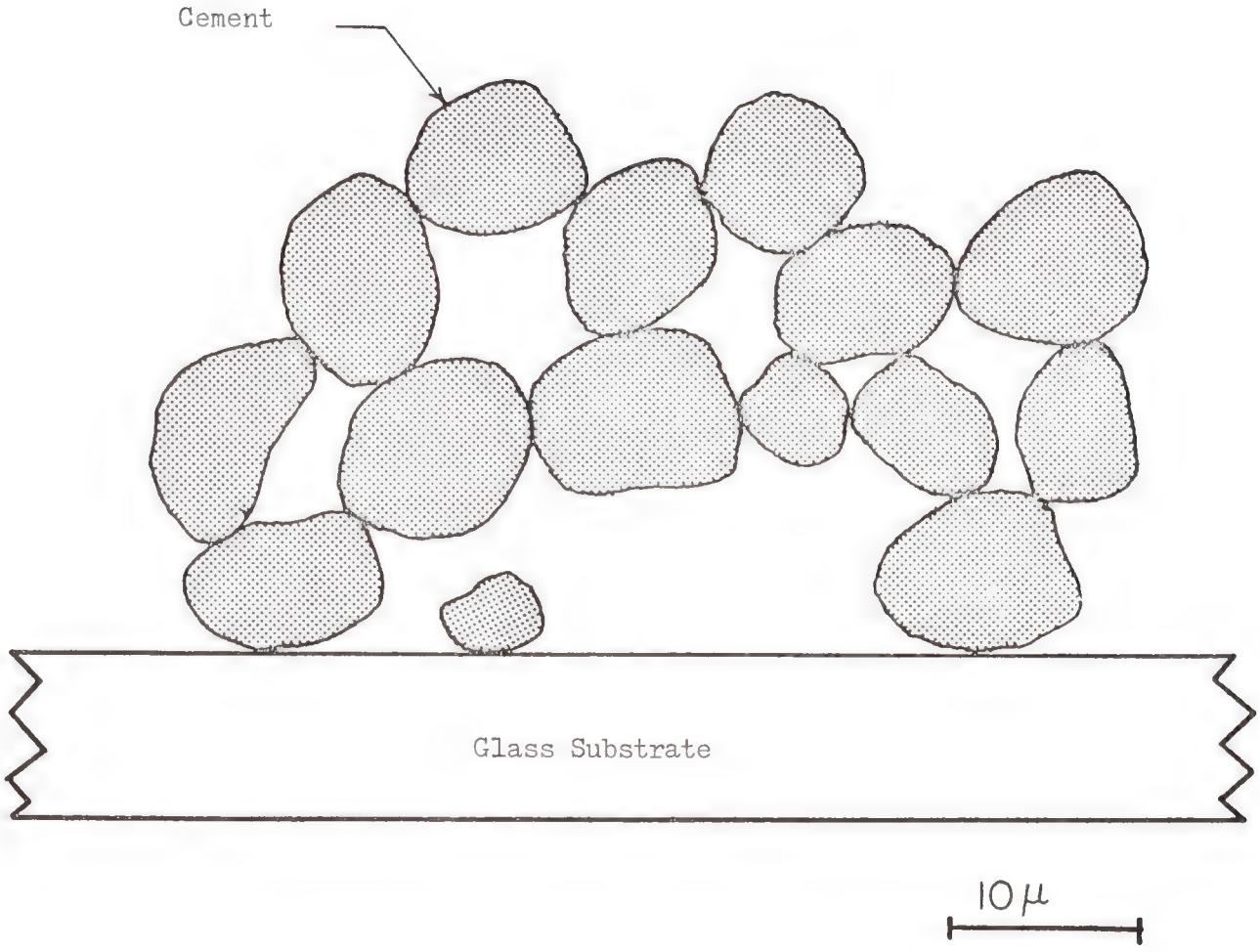

Figure 146. Interface Region Immediately After Consolidation (20)
(See Hadley's (20) Figures 43, 44, 47, and 48)

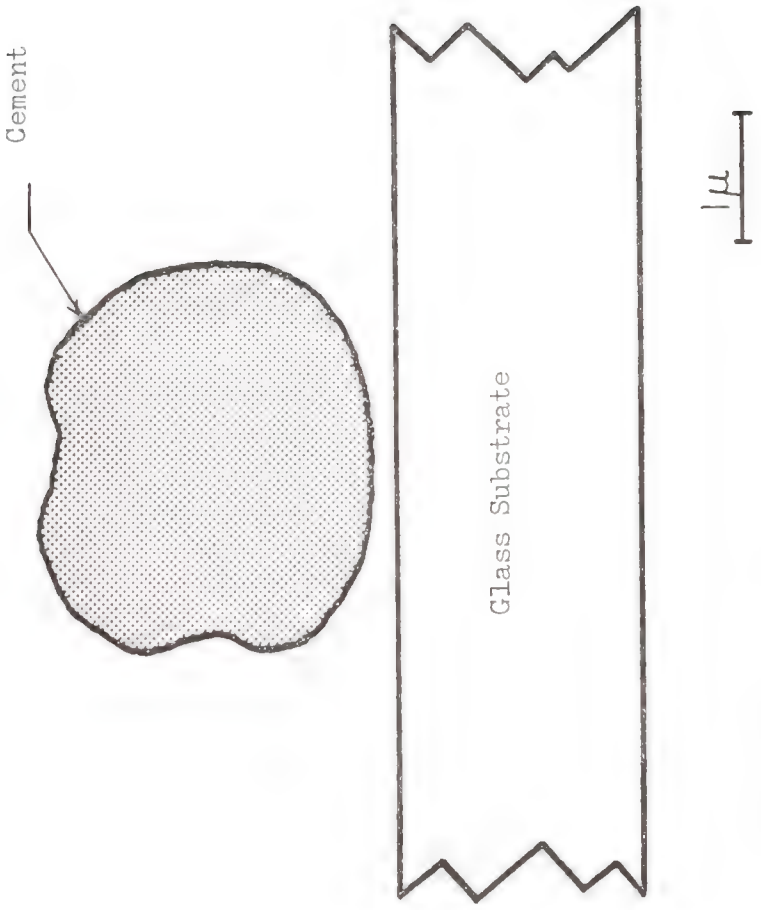

Figure 147. Cement Grain at Interface

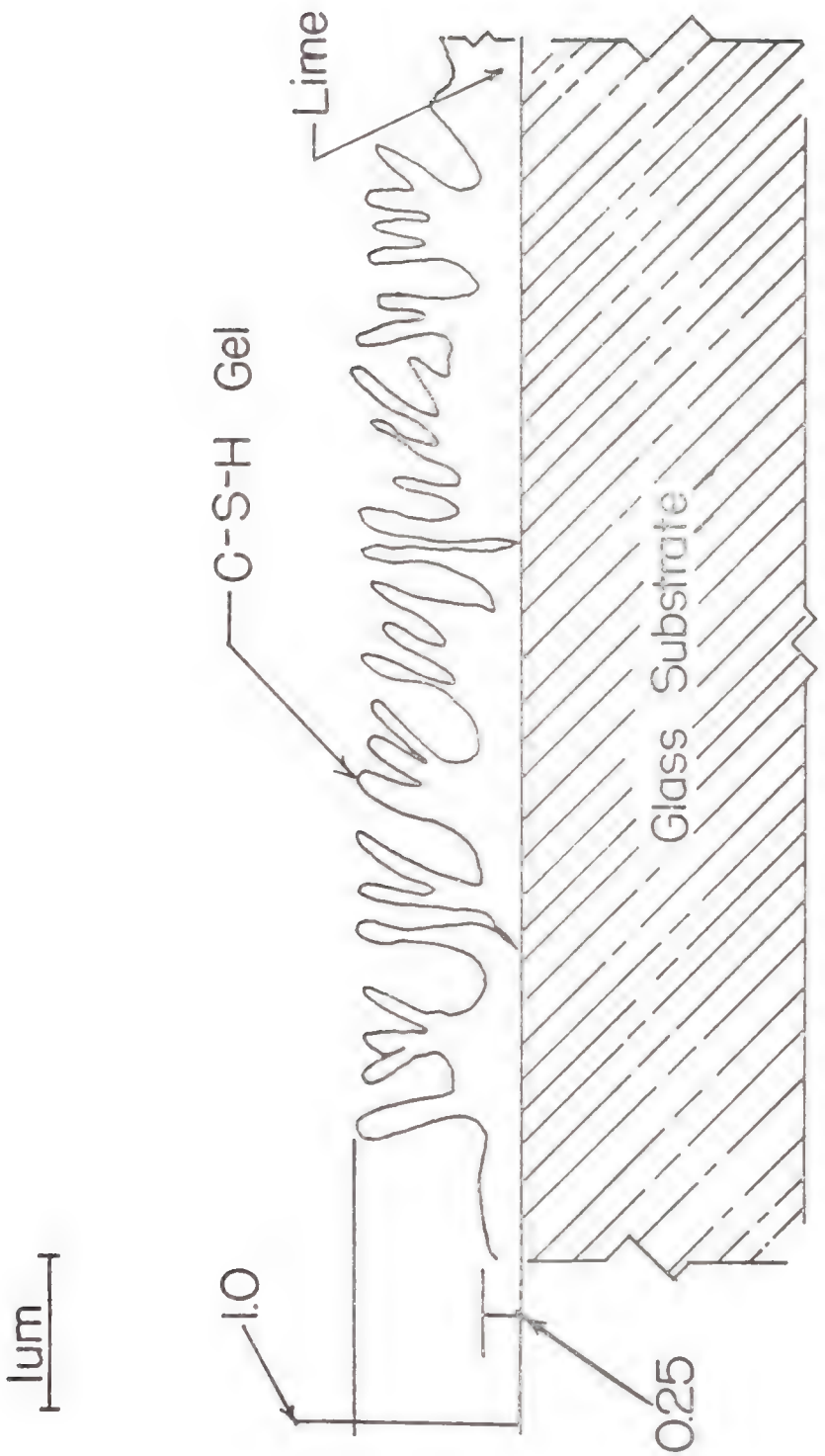

Figure 148. Typical Duplex Film on Substrate
(Reference Figures 7, 8, and 10)

lum

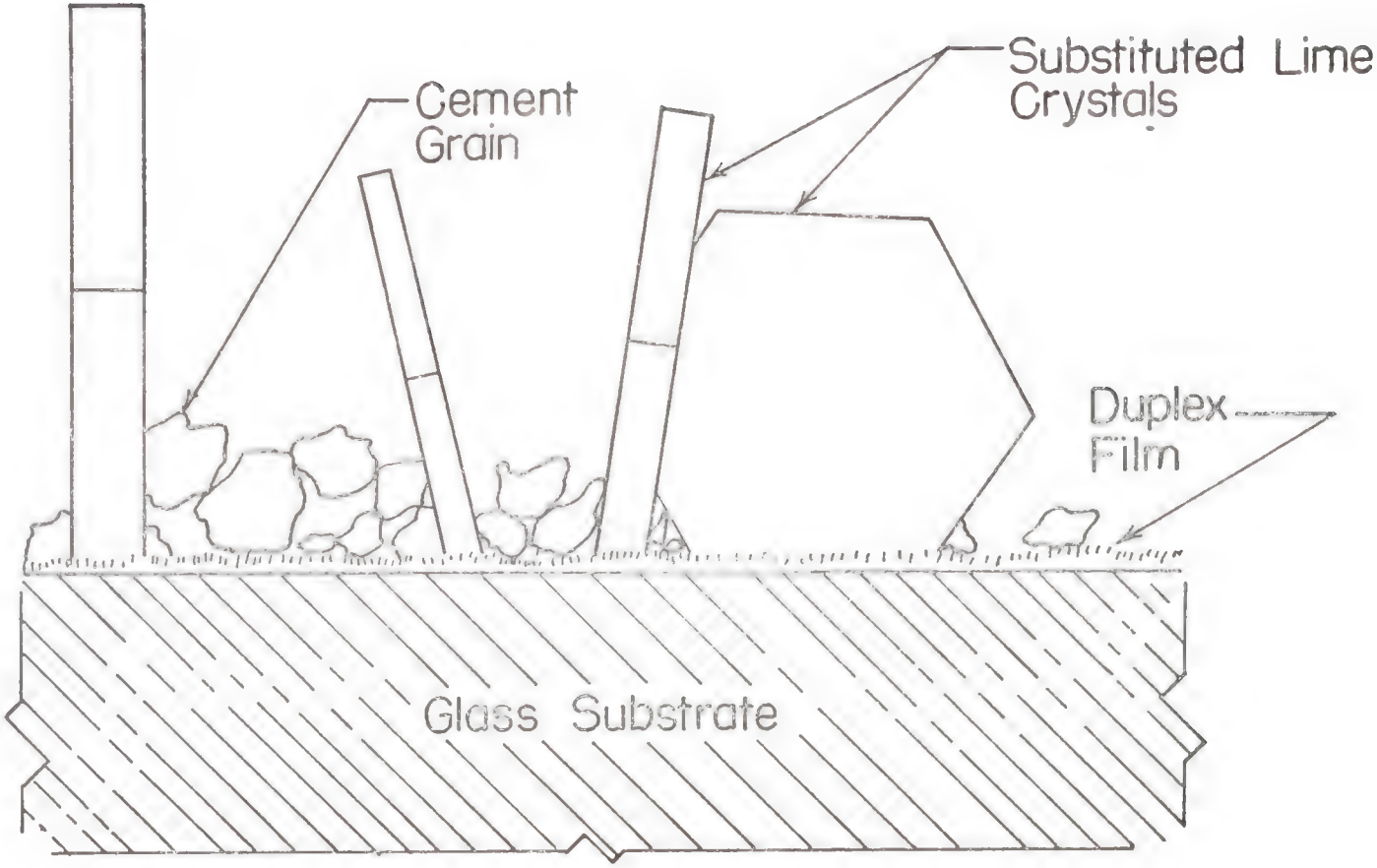

Figure 149. Morphology of the Interface at One Day
(Reference Figures 19, 25, 26, 27, 59,
60, 61, and 62)

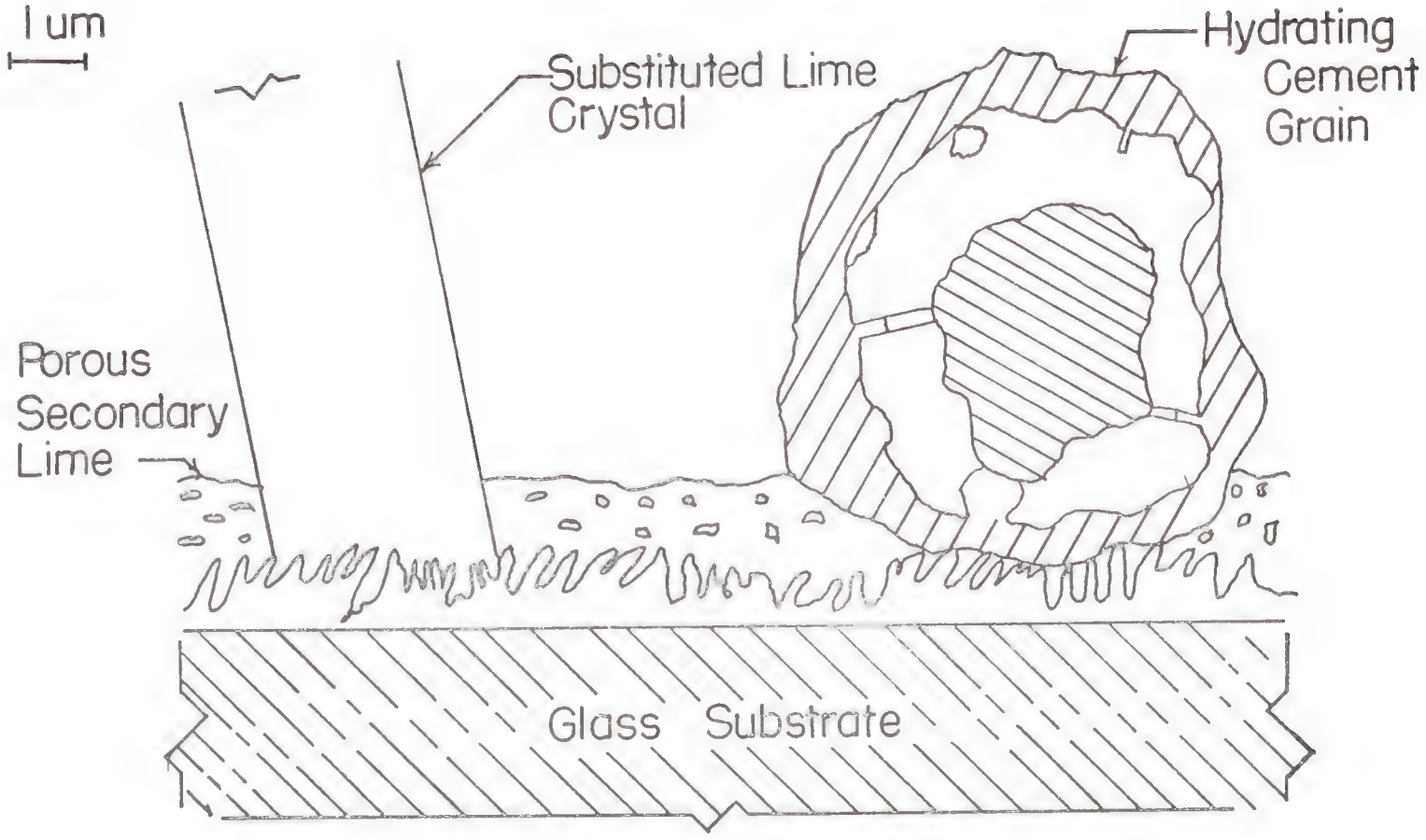

Figure 150. Developing Microstructure at Three Days
(Reference Figures 52, 53, 54, 55, 78, 80, 81, 84, 86, and 87)

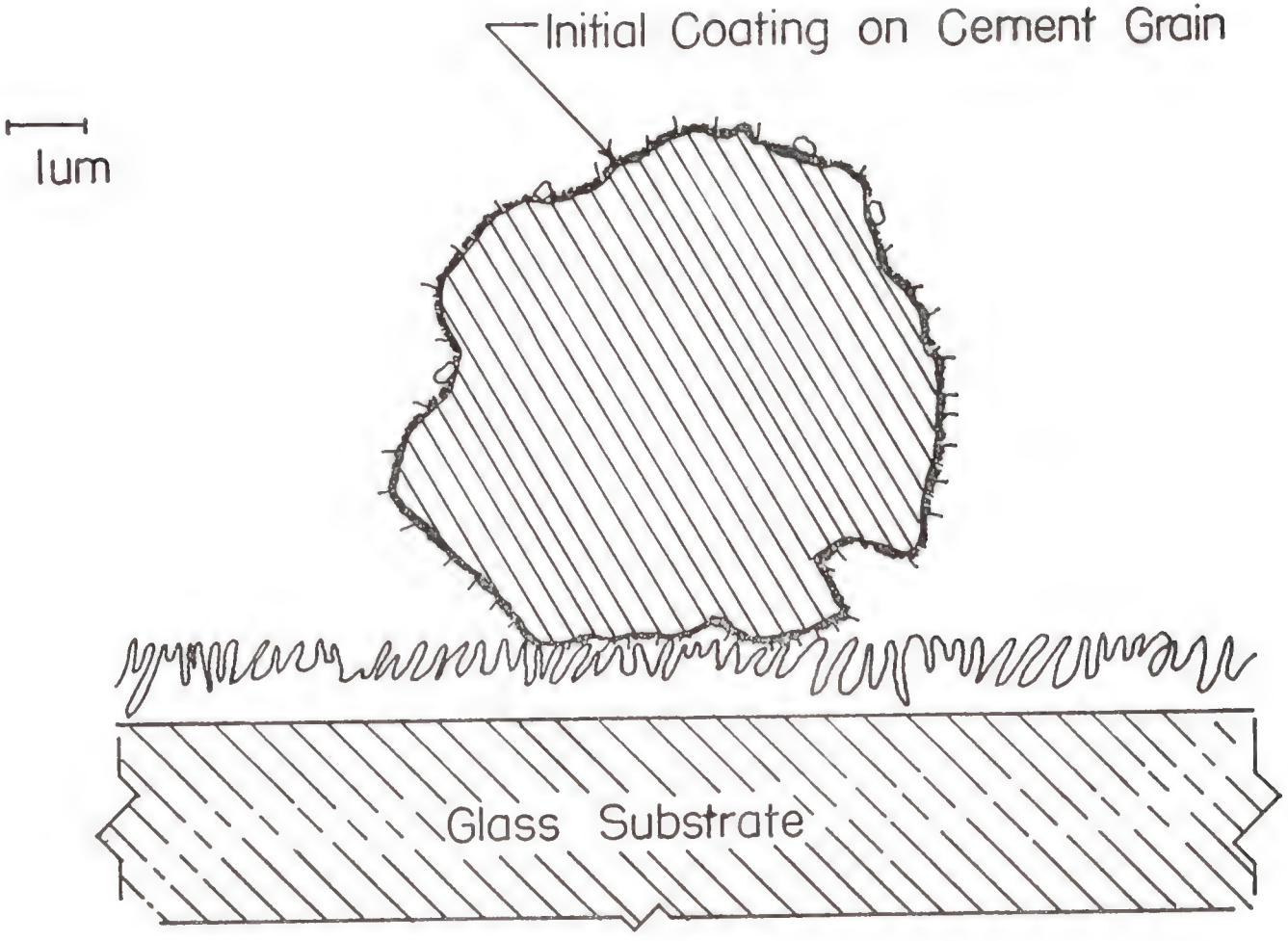

Figure 151. Cement Grain and Coating After About One Hour of Hydration (Reference Hadley's (20) Figures 45, 46, 49, and 50)

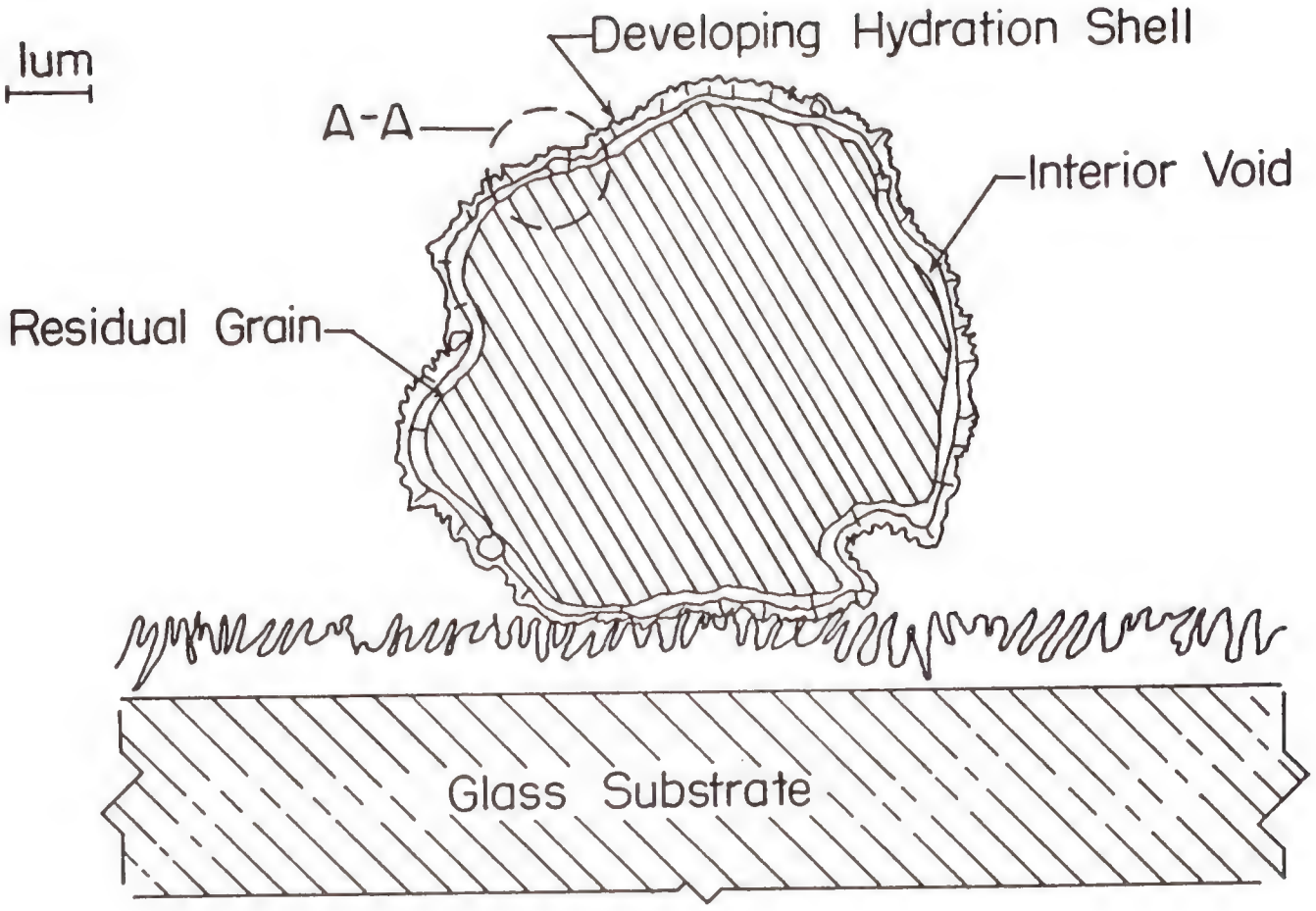

Figure 152. Hadley Grain Hydration After One Day
(Reference Figures 28-50)

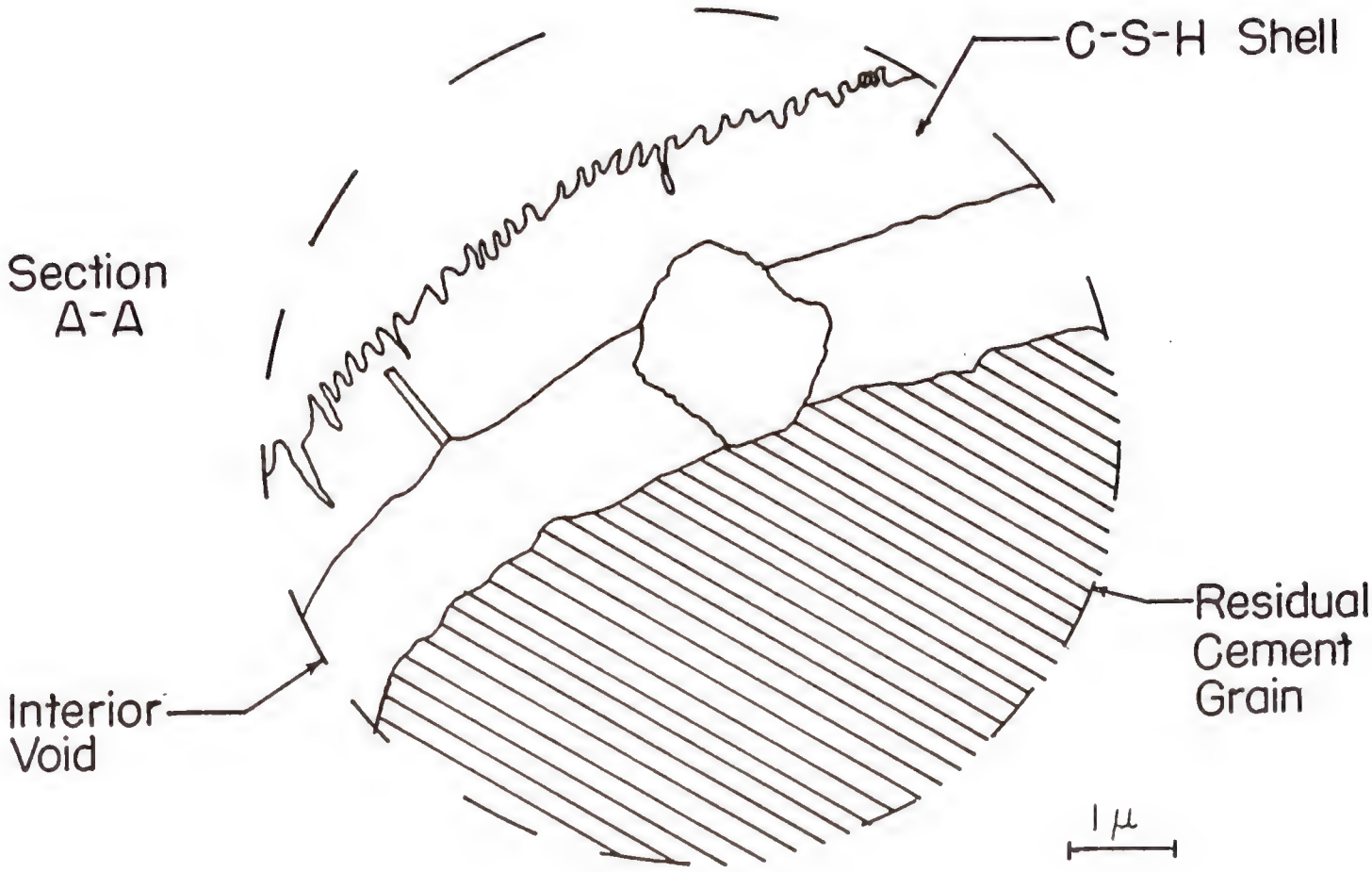

Figure 153. Close-up View of Developing Residual Shell, Void Space, Residual Grain at One Day (Reference Figures 34, 36, 43, 44, 46, 47, 48, and 50)

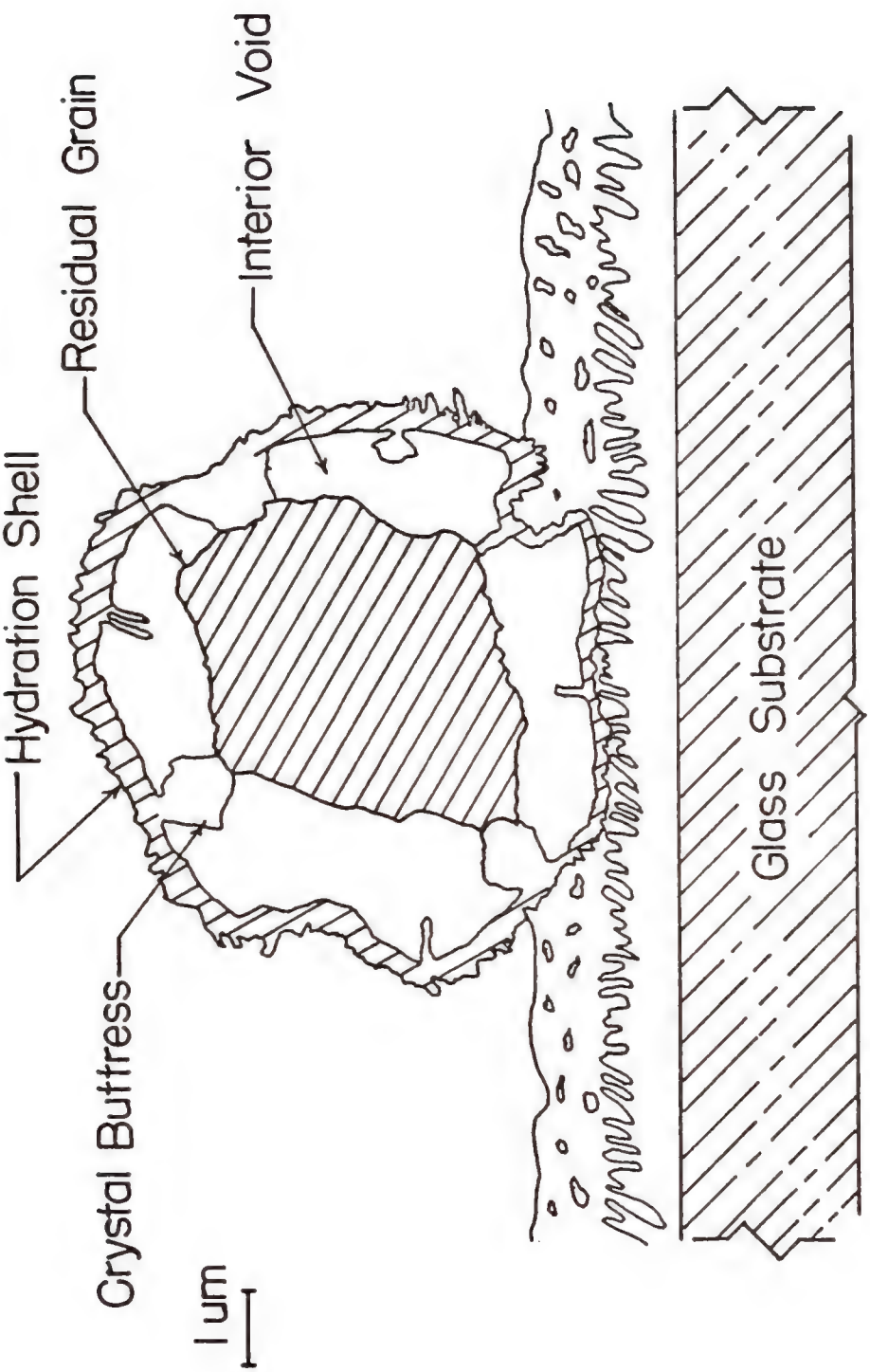

Figure 154. Cement Grain Hydration at Three Days
(Reference Figures 72, 79, 84, and 87)

Figure 155. Low Magnification View of Polished Cement Control Specimen (A5003C1)

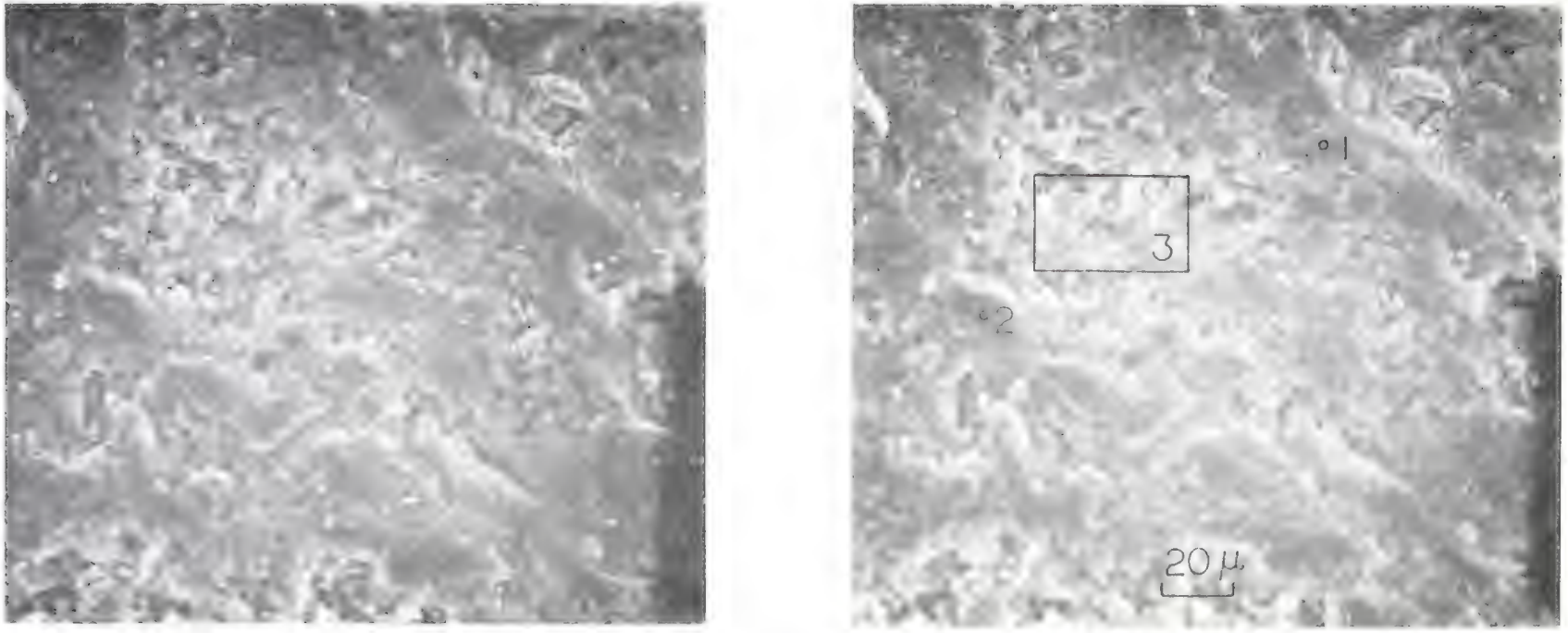

Figure 156. Stereomicrograph of Polished Specimen (A500302)

No.	C/S	C/A	C/$\bar{S}$
1	3.20	338.33	99.71
2	2.83	270.98	64.99
3	3.13	76.60	33.40

Figure 157. Air Bubble Filled by Abraded Hydration Products (A5007C1)

Figure 158. Seven-Day Control Specimen Polished Transverse to the Long Axis (A5007C2)

Figure 159. Enlarged View of Figure 158 (A5007C3)

Figure 160. Polished Fourteen-Day Control Specimen (A5014C1)

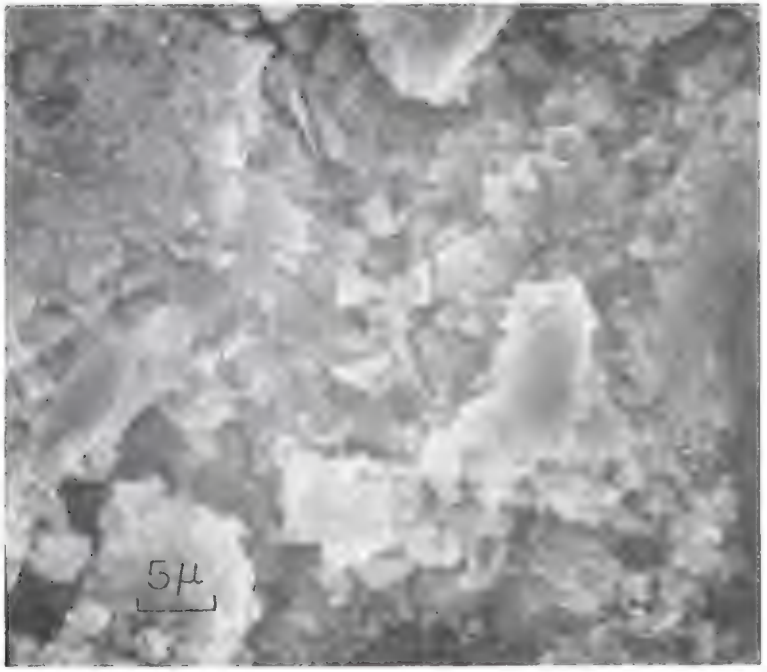

Figure 161. Enlargement of Figure 160 Showing the Lack of Typical Hydration Products (A5014C2)

Figure 162. Low Magnification Micrograph of Twenty-Eight-Day Specimen (A5028C1)

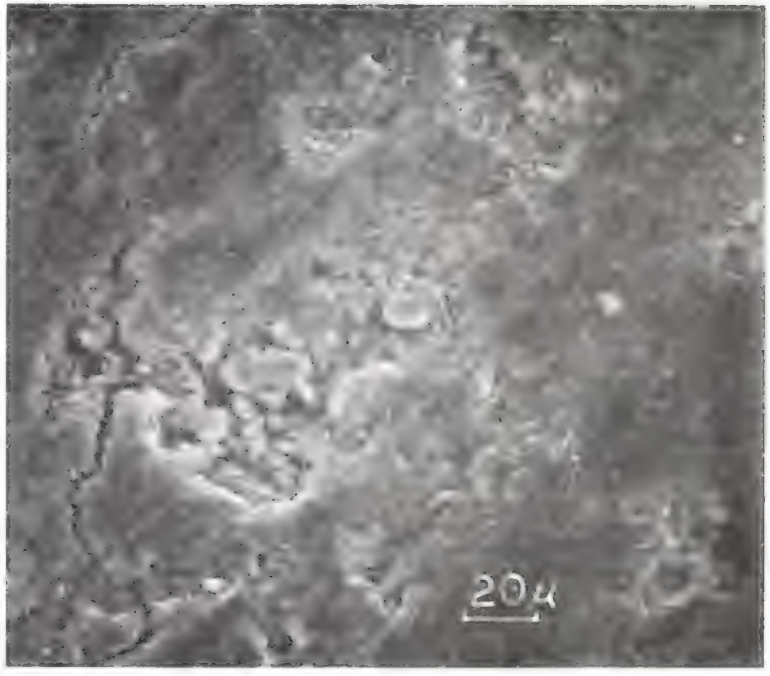

Figure 163. Twenty-Eight-Day Polished Specimen Showing High Flat Zones and Irregular Subsided Areas (A5028C2)

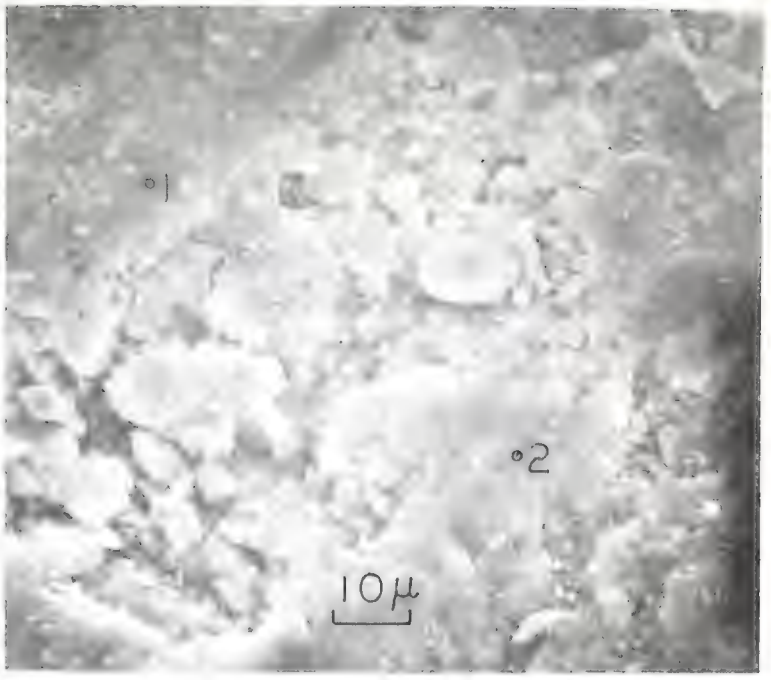

Figure 164. High Flat Zones Appear to be Composed of C-S-H and $Ca(OH)_2$ (A5028C3)

No.	C/S	C/A	C/$\bar{S}$
1	2.21	53.09	37.00
2	43.25	No A	251.25

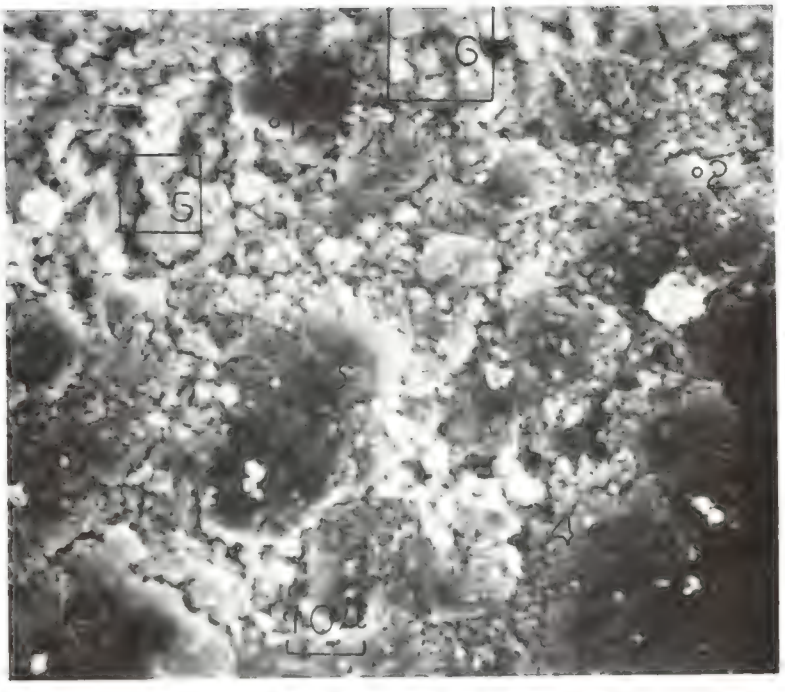

Figure 165. Elemental Composition of Polished Control Specimen (A6501C3)

No.	C/S	C/A	C/$\bar{S}$
1	55.74	1519.50	189.24
2	6.77	98.44	38.44
3	4.29	81.23	28.27
4	11.62	6.22	112.25
5	7.74	76.54	30.98
6	4.48	80.07	39.28

Figure 166. Photo-Mosaic of Fourteen-Day-Old Fractured Control Specimen (A5014F)

No.	C/S	C/A	C/$\bar{S}$
1	10.85	360.52	No $\bar{S}$
2	134.62	No A	541.56

20 μm

20 µm

Figure 167. Photo-Mosaic of Hydration Products Just Under the Duplex Film of a Fourteen Day Paste Interface (A5014P)

20 μm

20 μm

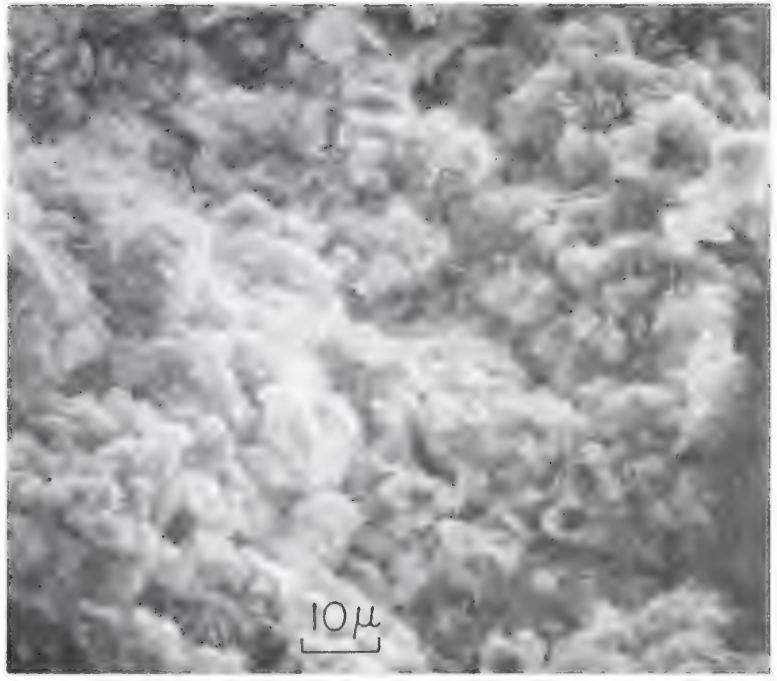

Figure 168. Fracture Surface of One-Day-Old Paste (A5001F7)

Figure 169. Hadley Grains with Portion of Fractured Residual Shell Remaining Attached (Enlargement of Grain in Lower Right of Figure 168) (A5001F5)

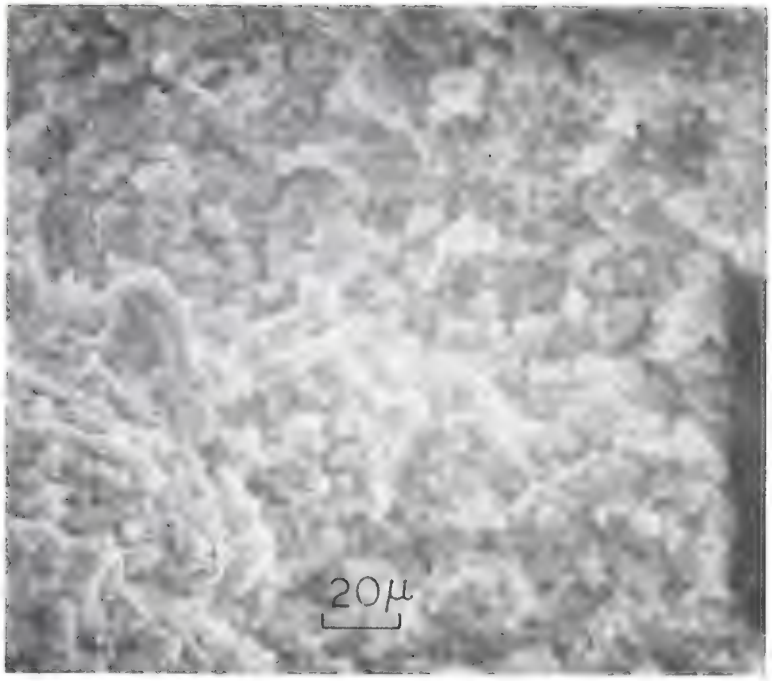

Figure 170. Fracture Surface of One-Day-Old Paste (A5001F9)

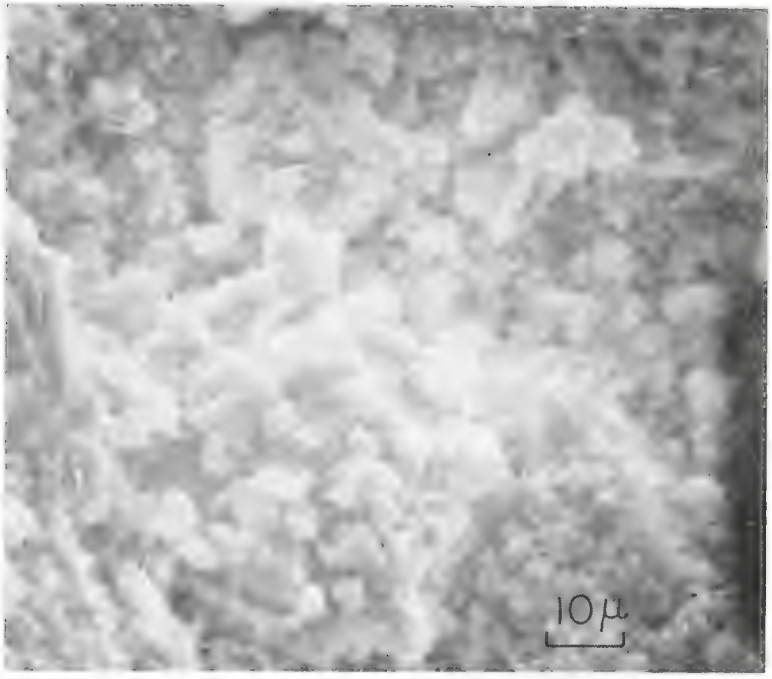

Figure 171. Fracture Surface of One-Day-Old Paste (A5001F10)

Figure 172. Hadley Grain with Residual Shell and Residual Grain (A5001F2)

Figure 173. Residual Shell with Only a Small Amount of Interior Residual Material (A5001F8)

Figure 174. Fracture Surface of Three-Day-Old Paste (A5003F1)

Figure 175. Higher Magnification View of Three-Day-Old Paste Fracture Surface (A5003F4)

No.	C/S	C/A	C/$\bar{S}$
1	8.22	5.08	7.62

Figure 176. One of a Very Few "Williamson Grains" (A5003F8)

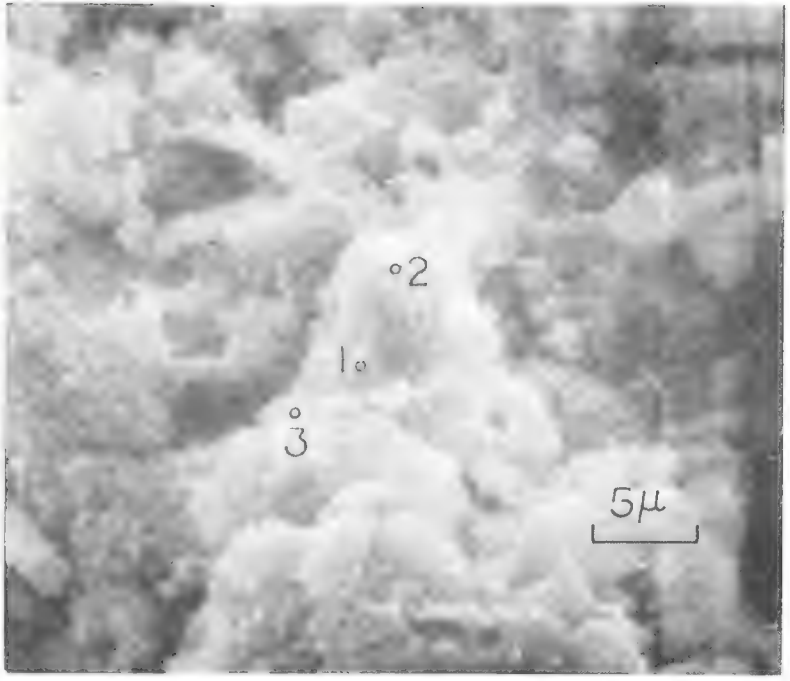

Figure 177. Hadley Shell and Williamson Grain in Close Proximity (C6503F3)

No.	C/S	C/A	C/S̄
1	1.51	52.61	84.18
2	1.56	13.14	58.57
3	1.95	35.52	35.71

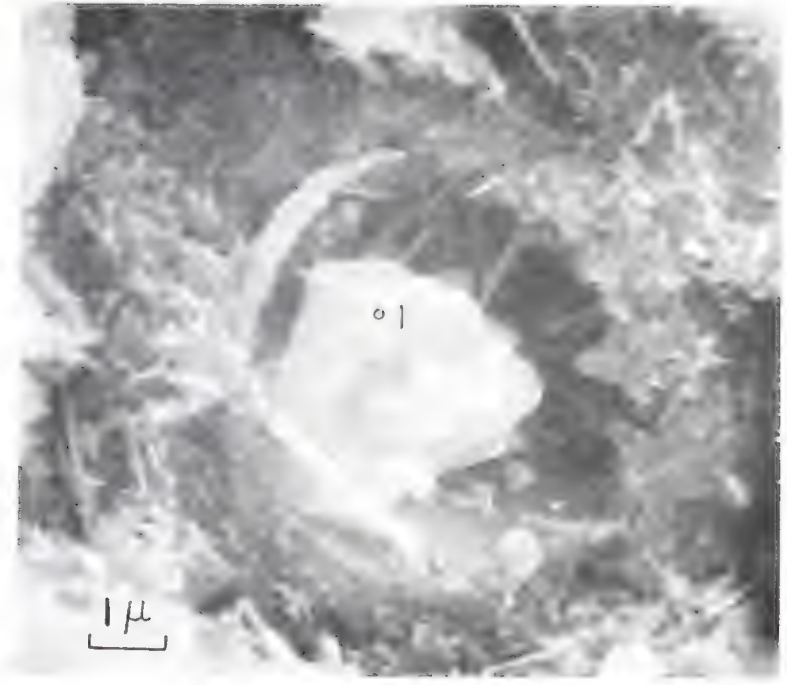

Figure 178. Hadley Grain Showing Both Interior Platelets and Needles (A5007F1)

No.	C/S	C/A	C/$\bar{S}$
1	2.32	51.29	39.48

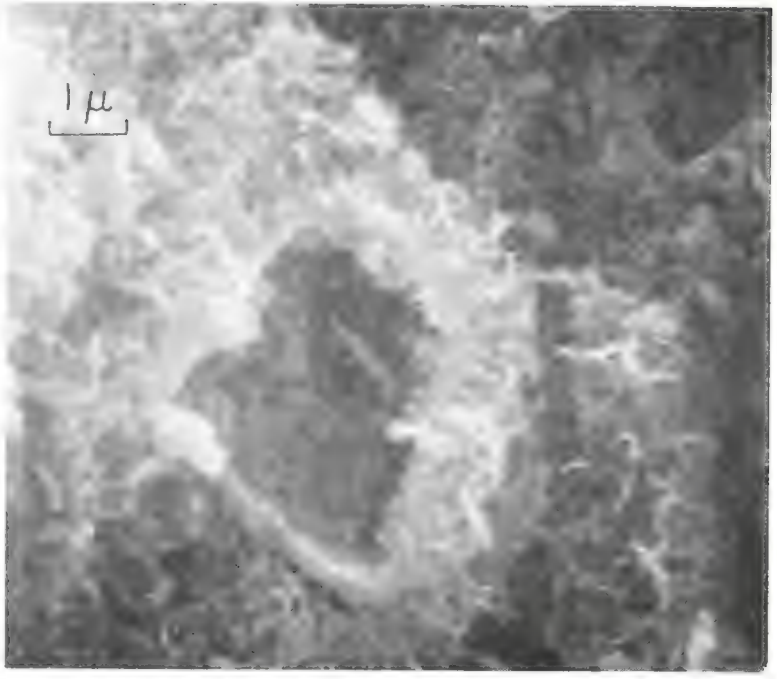

Figure 179. Empty Residual Shell (A5007F4)

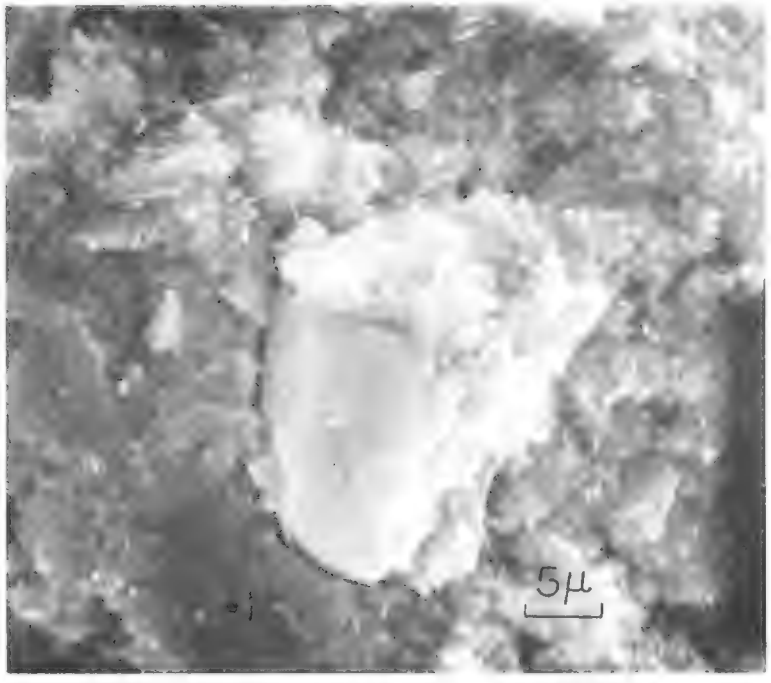

Figure 180. Cement Grain Encapsulated by Relatively Pure Lime (A5014F1)

No.	C/S	C/A	C/$\bar{S}$
1	176.38	No A	373.13

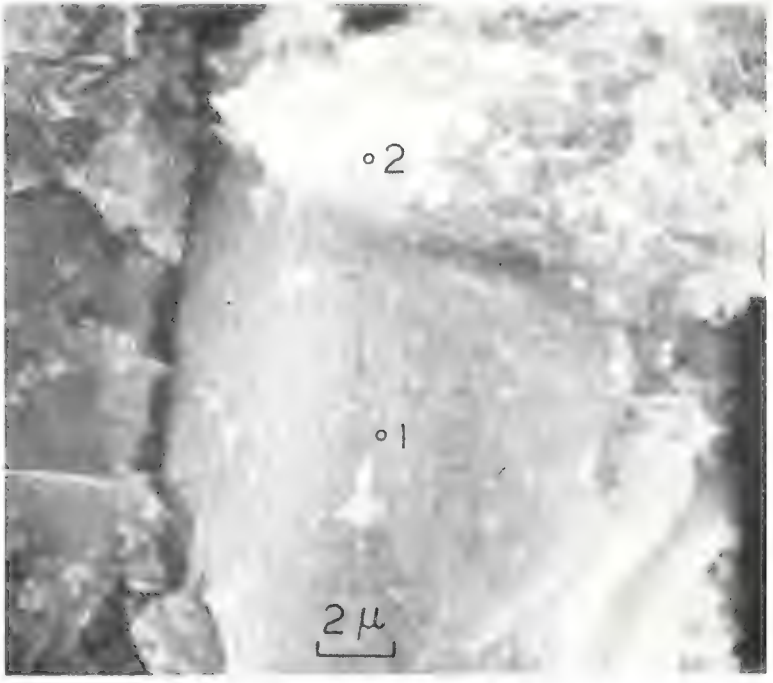

Figure 181. Close-up View of Cement Grain Shown in Figure 181 (A5014F2)

No.	C/S	C/A	C/$\bar{S}$
1	2.61	19.18	16.26
2	1.97	61.46	38.47

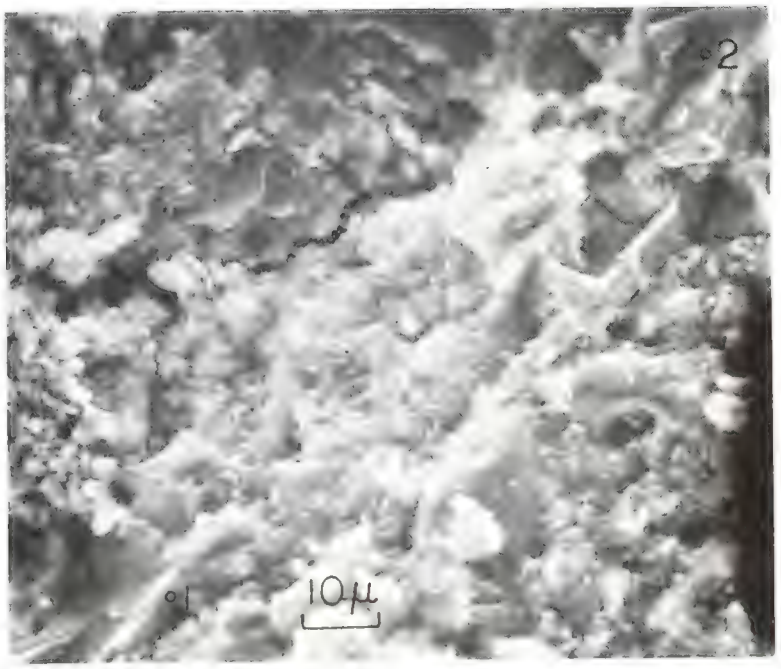

Figure 182. Cement Grains, Encapsulating Lime, and Empty Shells in a Twenty-Eight-Day-Old Paste Fracture Surface (A5028F1)

No.	C/S	C/A	C/$\bar{S}$
1	12.56	No A	178.97
2	26.68	No A	111.95

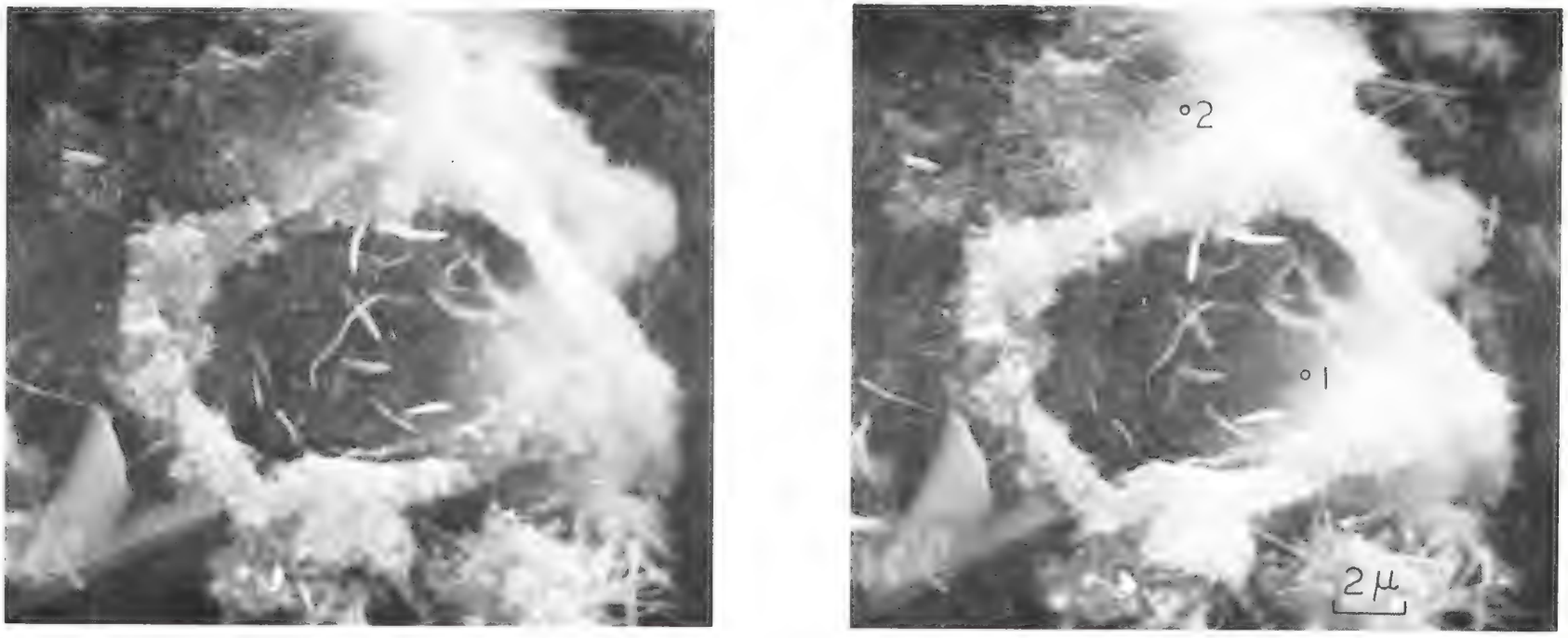

Figure 183. Stereomicrograph of Residual Shell with Interior Platelets (A6501F5)

No.	C/S	C/A	C/$\bar{S}$
1	5.52	No A	No $\bar{S}$
2	4.64	No A	No $\bar{S}$

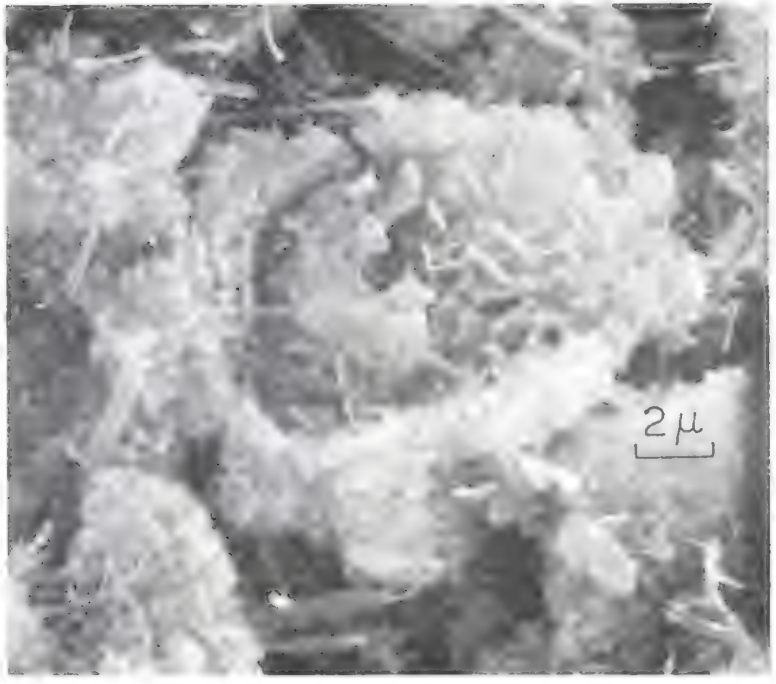

Figure 184. Interior Platelets Growing on Residual Shell (A6501F6)

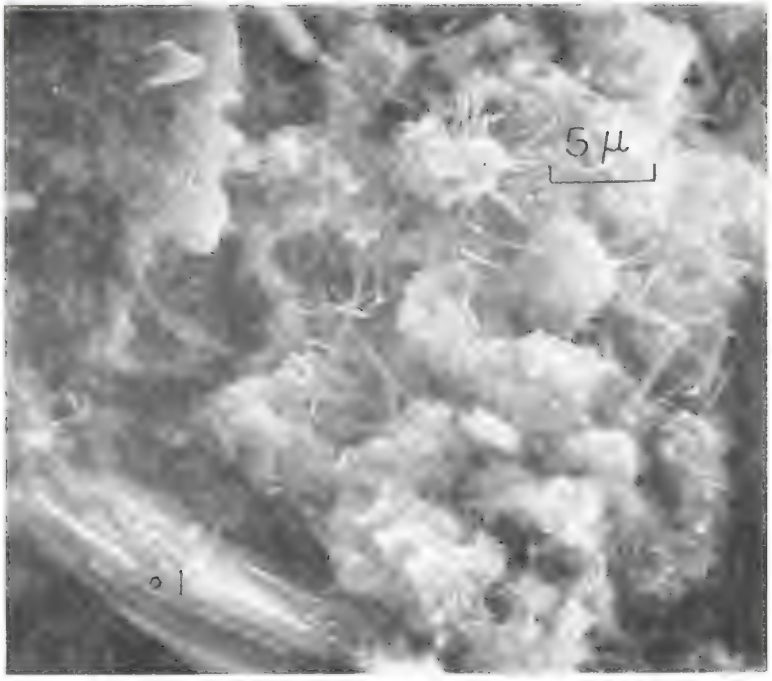

Figure 185. Lime Crystal Showing Good Cleavage Planes and Hexagonal Angles with a Few Empty Residual Shells (A651F3)

No.	C/S	C/A	C/$\bar{S}$
1	21.14	No A	No $\bar{S}$

Figure 186. Encapsulating Lime with Void Residual Shell Beneath It (A6503F1)

No.	C/S	C/A	C/$\bar{S}$
1	35.44	No A	446.80

Figure 187. Residual Shell with Smooth Interior Component (A6501F4)

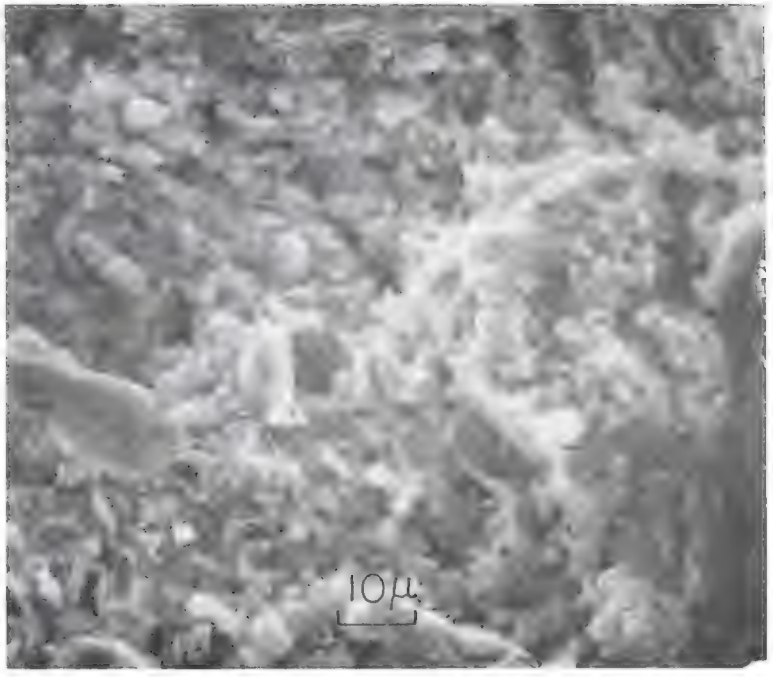

Figure 188. Fracture Surface of Three-Day-Old Specimen (B5003F2)

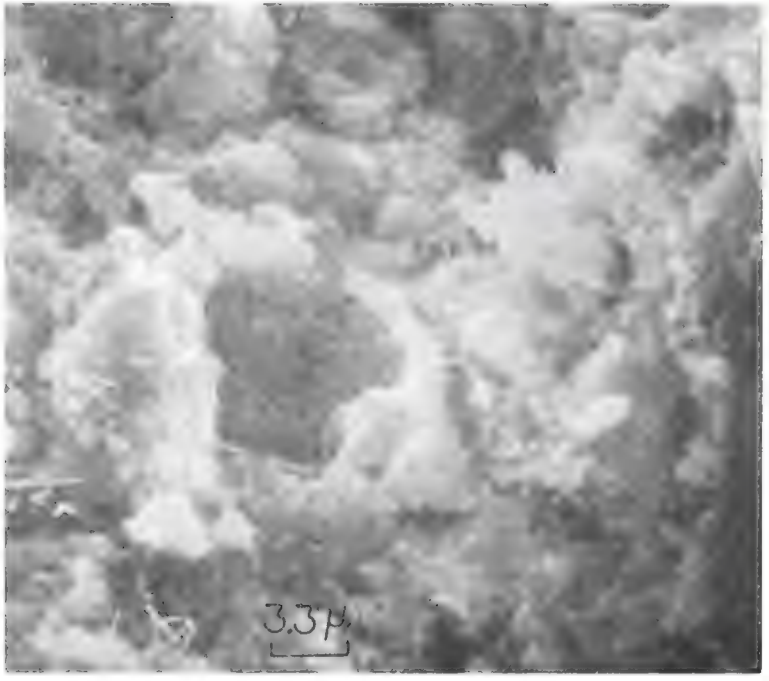

Figure 189. Close-up View of Central Residual Shell in Figure 188 (B5003F1)

Figure 190. Apparent Hadley Grain and Williamson Grain Adjacent to Each Other (B5003F6)

No.	C/S	C/A	C/$\bar{S}$
1	2.05	No A	No $\bar{S}$

Figure 191. High Magnification of Inner and Outer Product of Williamson Grain Shown in Figure 190 (B5003F7)

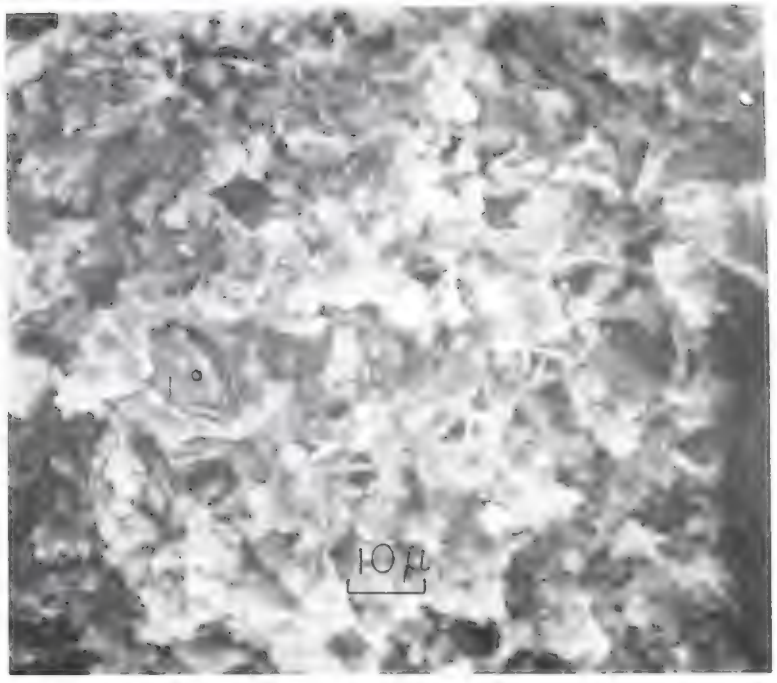

Figure 192. Fracture Surface of Three-Day-Old Paste (C5003F1)

No.	C/S	C/A	C/$\bar{S}$
1	4.45	No A	No $\bar{S}$

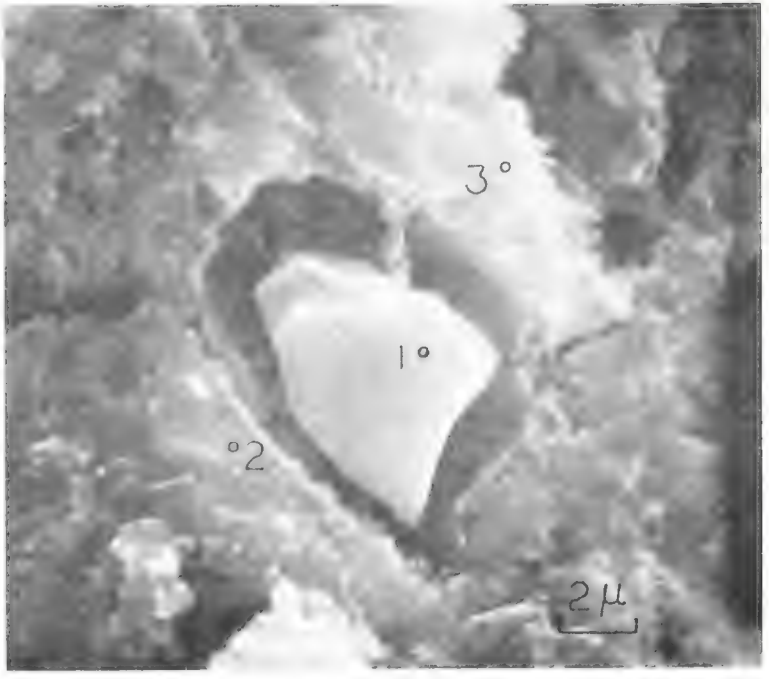

Figure 193. Residual Grain Exhibiting an Extremely Clean Surface (C5003F2)

No.	C/S	C/A	C/$\bar{S}$
1	3.73	No A	No $\bar{S}$

Figure 194. Residual Shell with Smooth Interior (C5003F3)

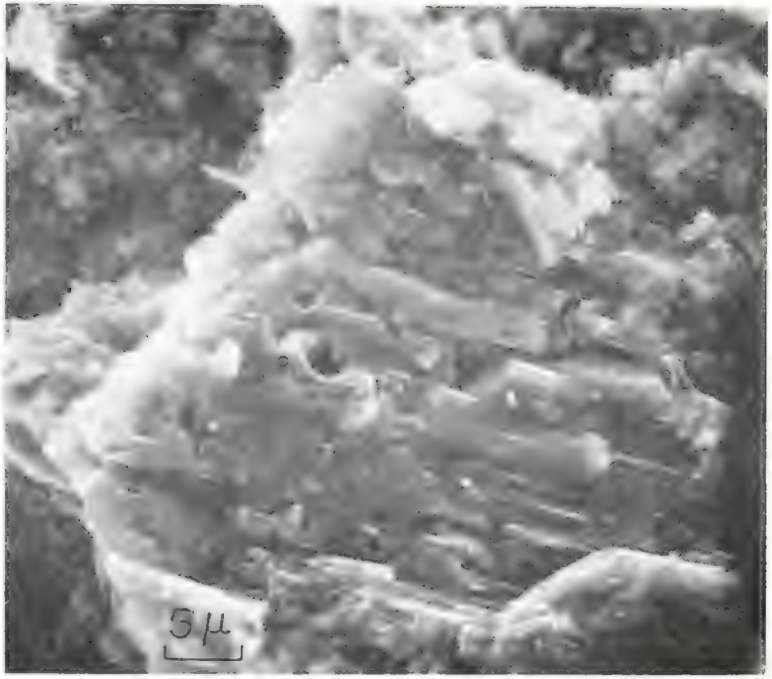

Figure 195. Lime Showing Areas of Encapsulation and Good Cleavage (C5003F4)

No.	C/S	C/A	C/$\bar{S}$
1	7.83	No A	No $\bar{S}$

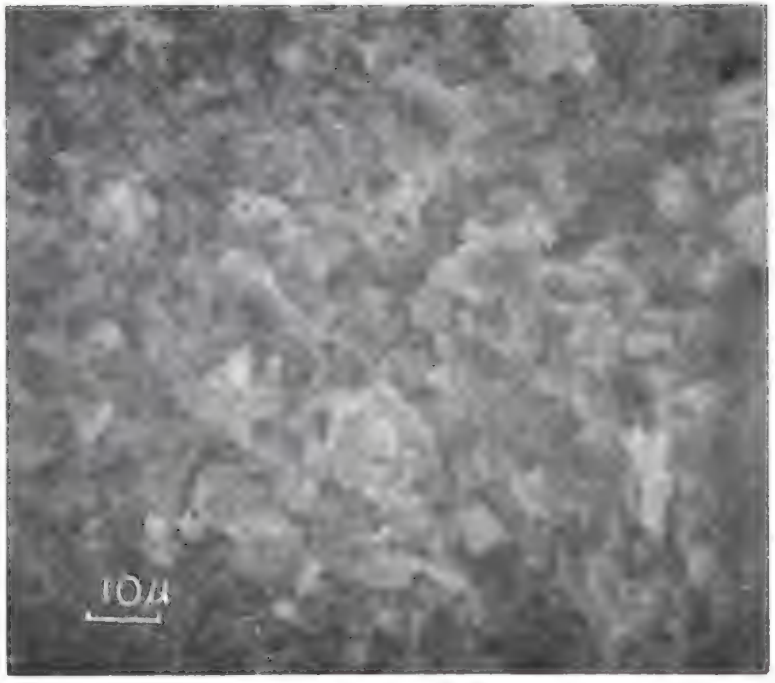

Figure 196. Fracture Surface of Three-Day-Old Paste (D5003F5)

Figure 197. Close-up View of Hadley Grain Appearing in the Lower Left Portion of Figure 196 (D5003F3)

No.	C/S	C/A	C/$\bar{S}$
1	2.99	No A	No $\bar{S}$

Figure 198. Close-up View of Hadley Grain Appearing in the Center of Figure 196 (D5003F4)

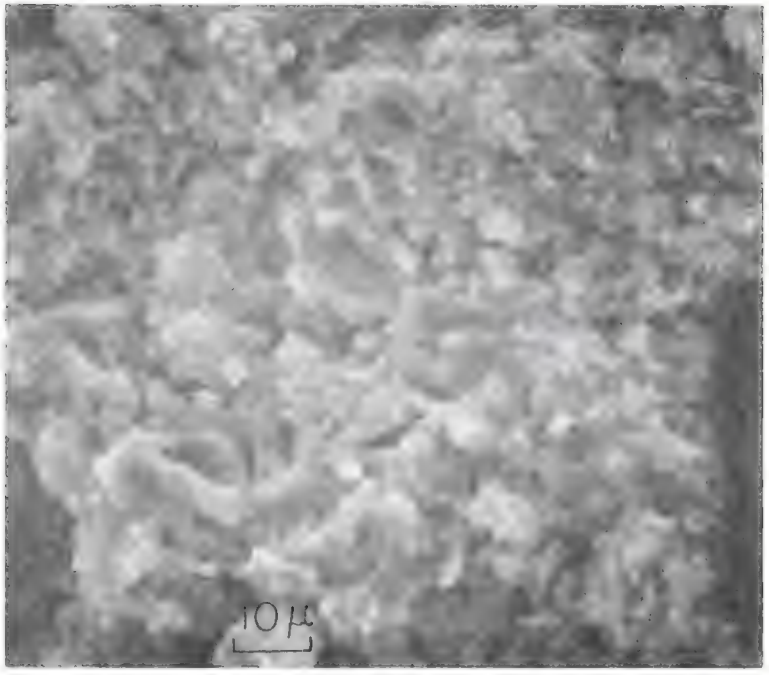

Figure 199. Fracture Surface Showing Many Empty Residual Shells (D5003F6)

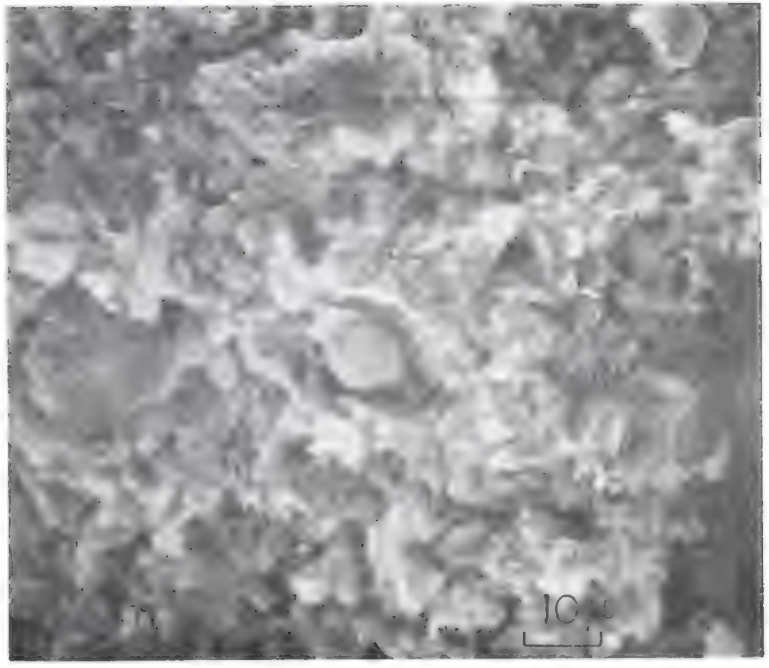

Figure 200. Fracture Surface Showing Residual Shells and an Obvious Hadley Grain (D5003F1)

Figure 201. Enlargement of Hadley Grain Appearing in the Center of Figure 200 (D5003F2)

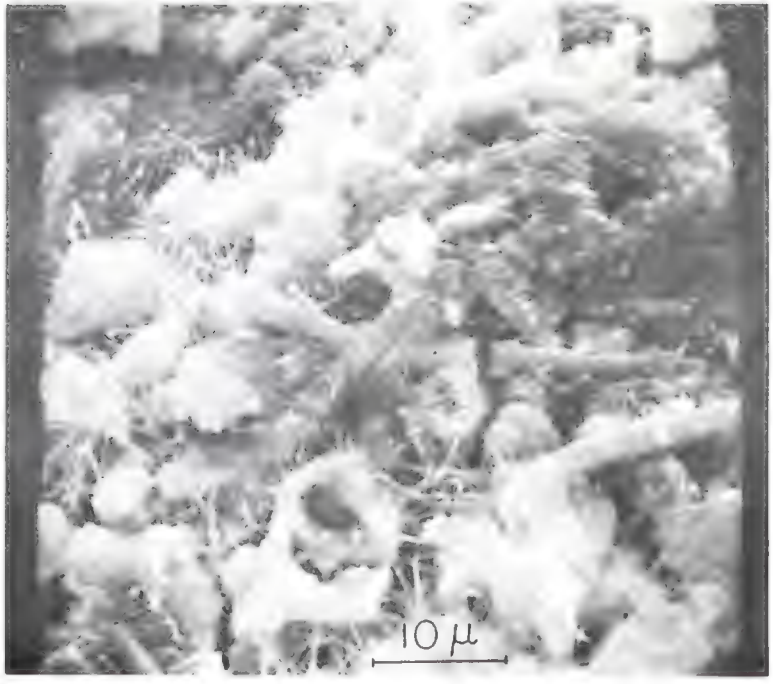

Figure 202. Micrograph from Diamond's Earlier Work Showing Vacant Residual Shells (w/c = 0.60, Hydrated three days)

Figure 203. Ottawa Sand Grains at Low Magnification (Sand--2)

KCα Counts

No.	Si	Ca	Mn
1	Particle charged and "jumped-off" specimen stub		
2	57166	No Ca	48
3	Particle charged and ...		
4	34444	1497	26
5	10328	78	14

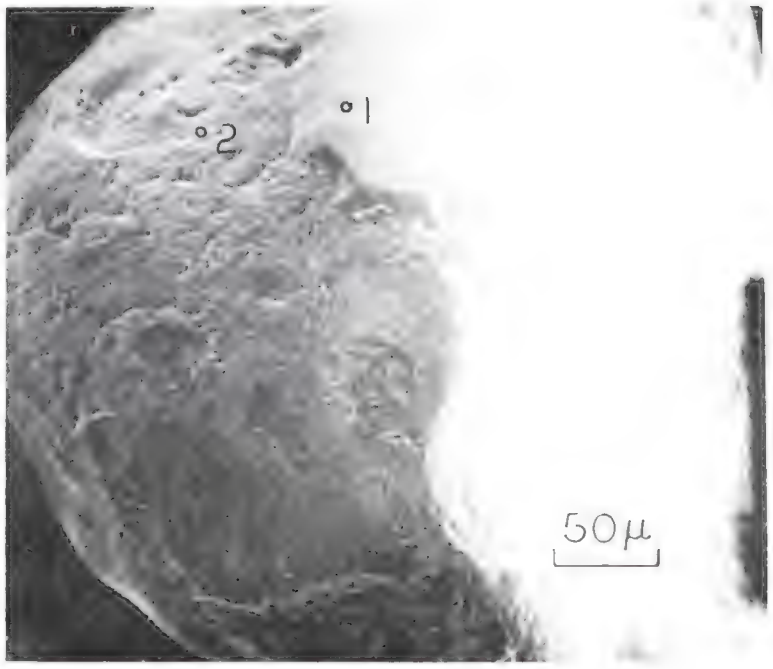

Figure 204. Region of Smooth and Jagged Topography Occur on the Sand Grain (Sand--3)

Kα Counts

No.	Al	Si
1	No Al	44912
2	2595	42218

Figure 205. General View of Broken Topography on Sand Grain (Sand--4)

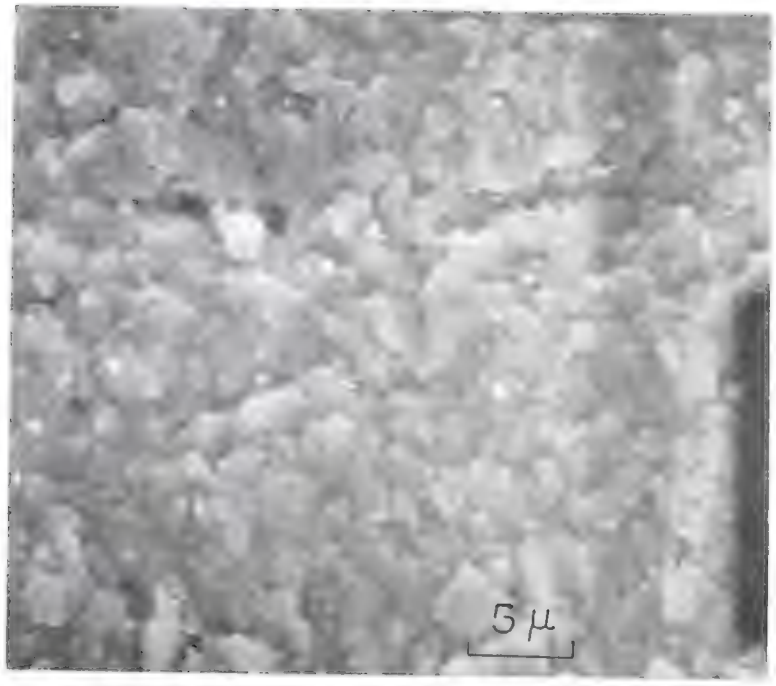

Figure 206. Enlargement of Broken Topography Shown in Figure 205 (Sand--5)

Figure 207. High Magnification View of Broken Topographic Region (Sand--6)

Figure 208. Flat, Smooth, Blocky Structures with Parallel Striations (Sand--7)

Figure 209. Dished-out Region and Polygonal Crack Patterns (Sand--8)

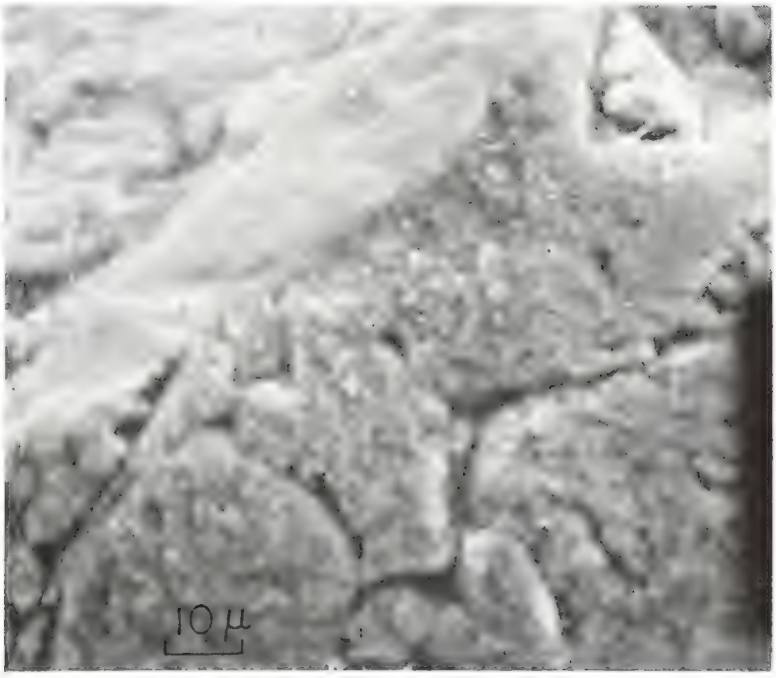

Figure 210. Dished-Out Region Appears Smooth and Polygonal Cracks Seem Deep (Sand--9)

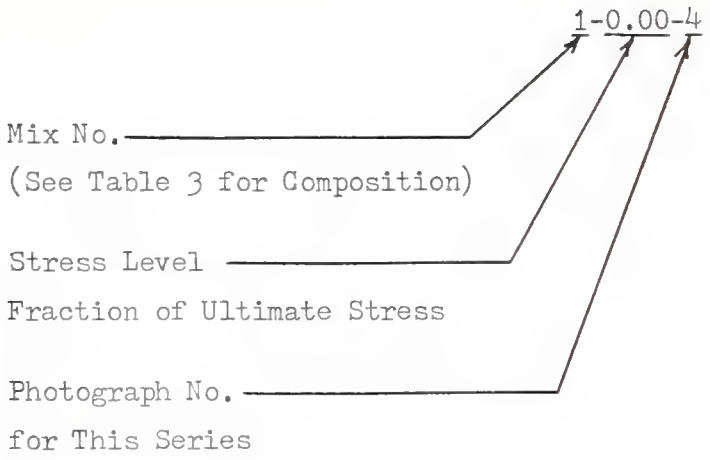

For Example: 3-0.60-5

Means a specimen made from Mix No. 3 subjected to 0.60 of its ultimate strength.

Figure 211. Coding Key for Type III, Mortar, Specimens

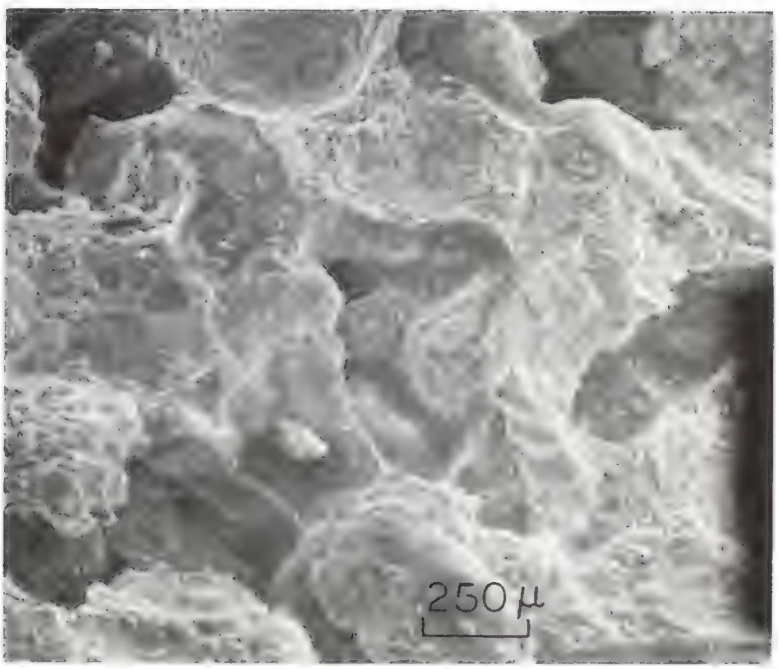

Figure 212. Poorly Consolidated High Porosity, 60% Aggregate Volume Fraction Specimen (2-0.00-4)

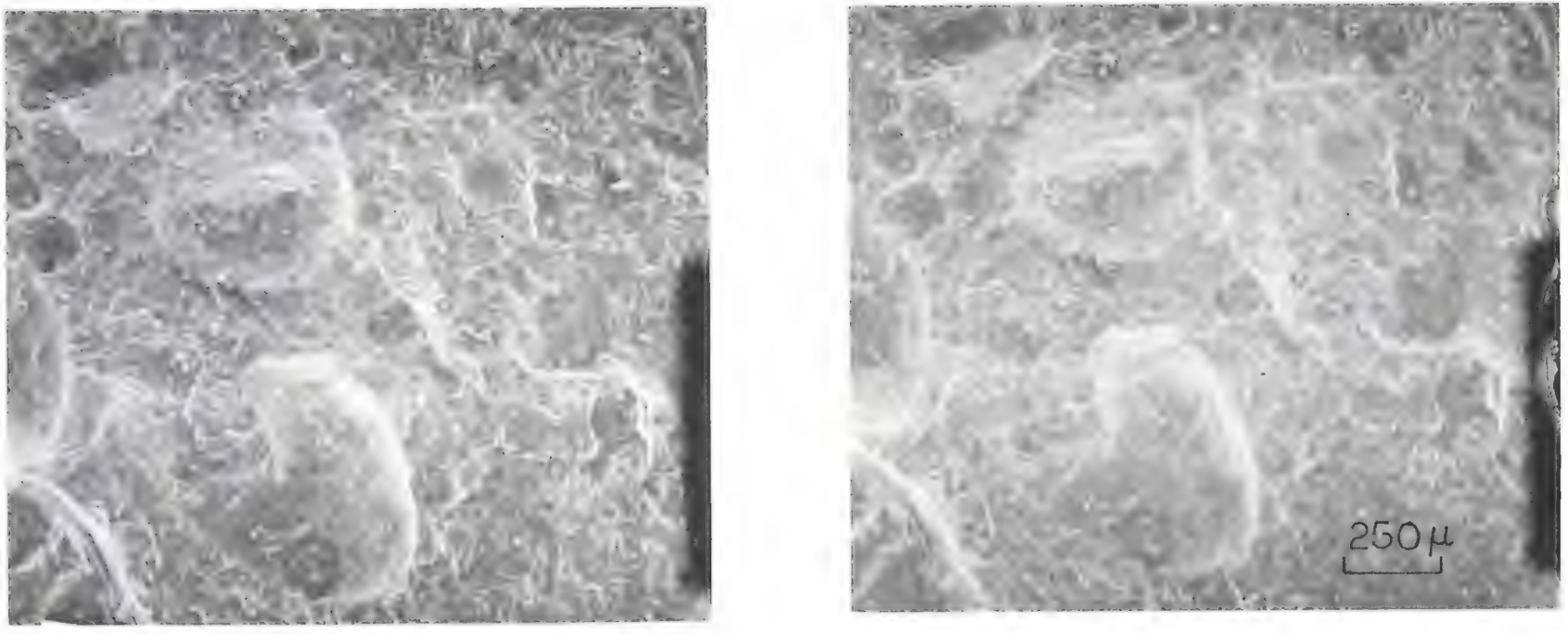

Figure 213. Stereomicrograph of Fractured Mortar Surface (1-0.00-16)

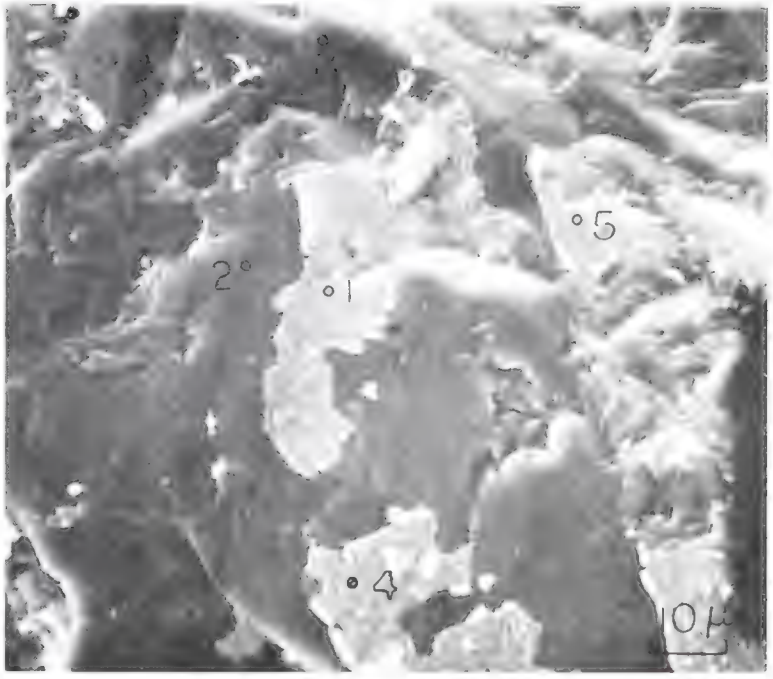

Figure 214. Duplex Film on Flat Sand Surface (1-0.00-1)

No.	C/S	C/A	C/$\bar{S}$
1	0.15	No A	No $\bar{S}$
2	0.13	No A	No $\bar{S}$
3	0.12	No A	No $\bar{S}$
4	0.15	No A	No $\bar{S}$
5	0.14	No A	No $\bar{S}$

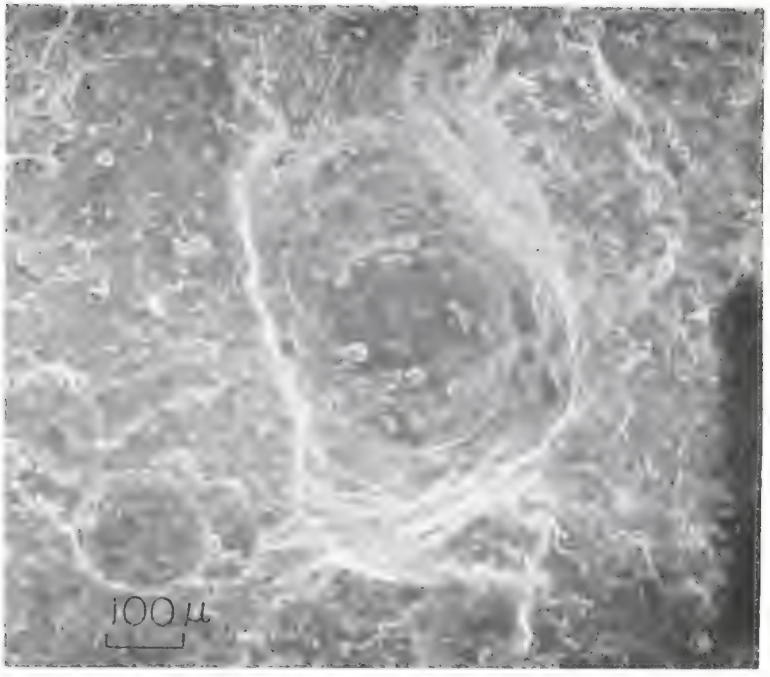

Figure 215. Low Magnification View of Grain Socket (1-0.00-7)

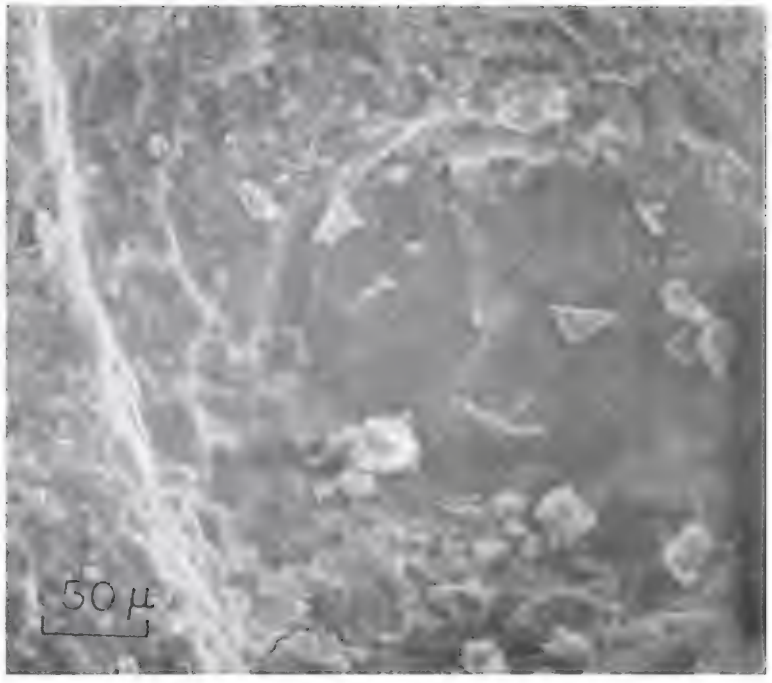

Figure 216. Enlarged View of Duplex Film in Grain Socket Shown in Figure 215 (1-0.00-8)

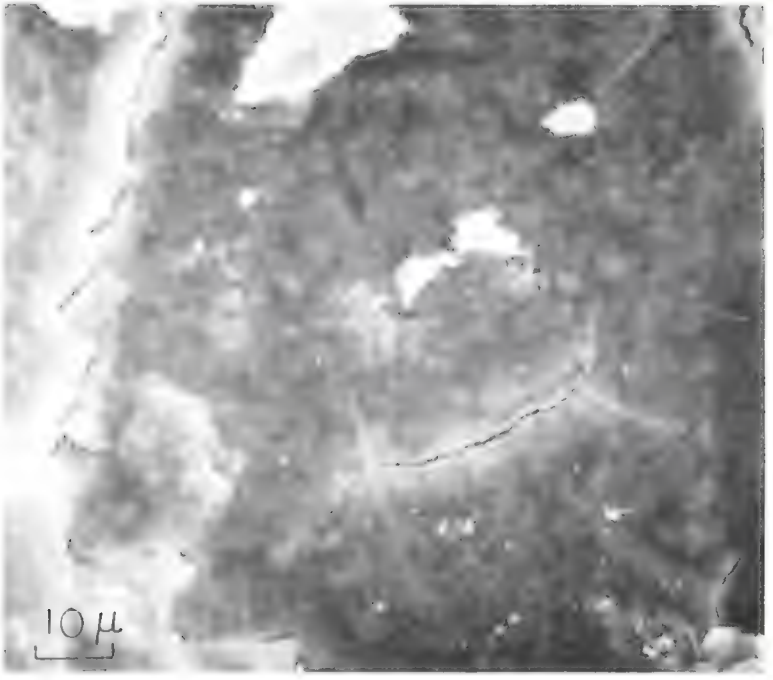

Figure 217. Duplex Film Underlain by Linear Features and Exhibiting Several Windows (Figure 215 Enlargement) (1-0.00-9)

Figure 218. Low Magnification View of Grain Socket (1-0.00-10)

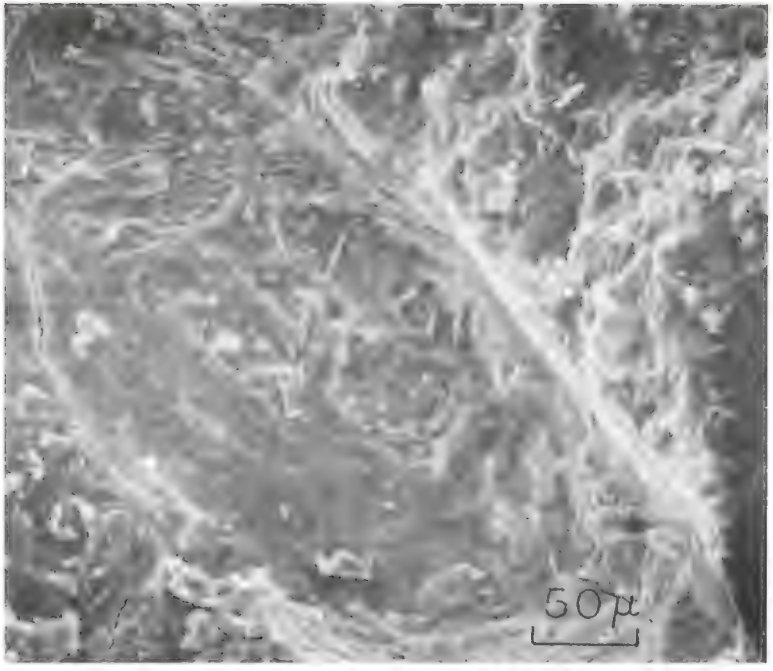

Figure 219. Grain Socket with Duplex Film, Secondary Lime, and Platey Crystals (Figure 218 Enlarged (1-0.00-11)

Figure 220. Secondary Lime and Edge-on Crystals Appearing in Figure 218 (1-0.00-12)

No.	C/S	C/A	C/$\bar{S}$
1	53.85	186.25	250.79
2	3144.52	466.53	226.51
3	37.09	251.35	No $\bar{S}$
4	11.73	123.17	0.12

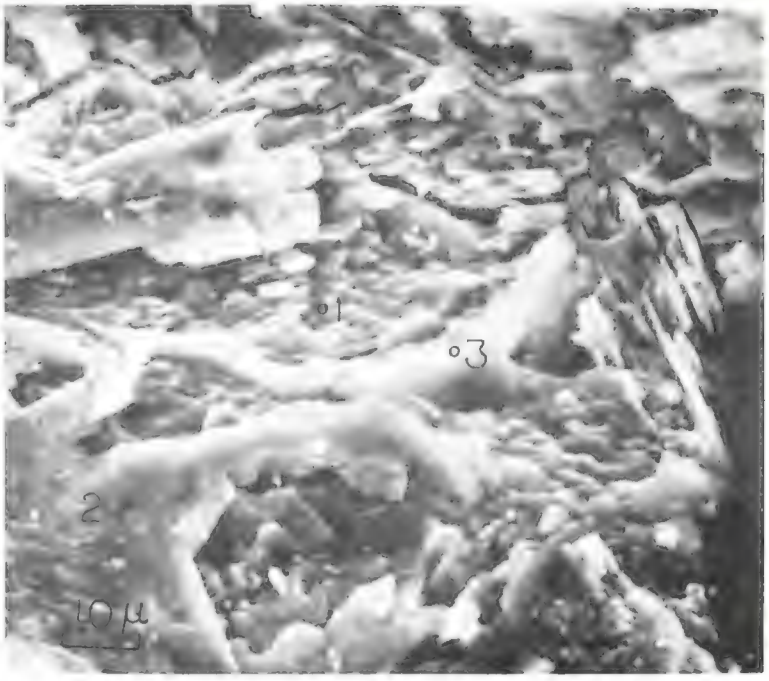

Figure 221. Additional View of Material Underlying the Duplex Film (Figure 218 Enlargement) (1-0.00-14)

No.	C/S	C/A	C/$\bar{S}$
1	8.14	124.21	45.05
2	17.60	143.11	104.03
3	6.94	0.19	47.03

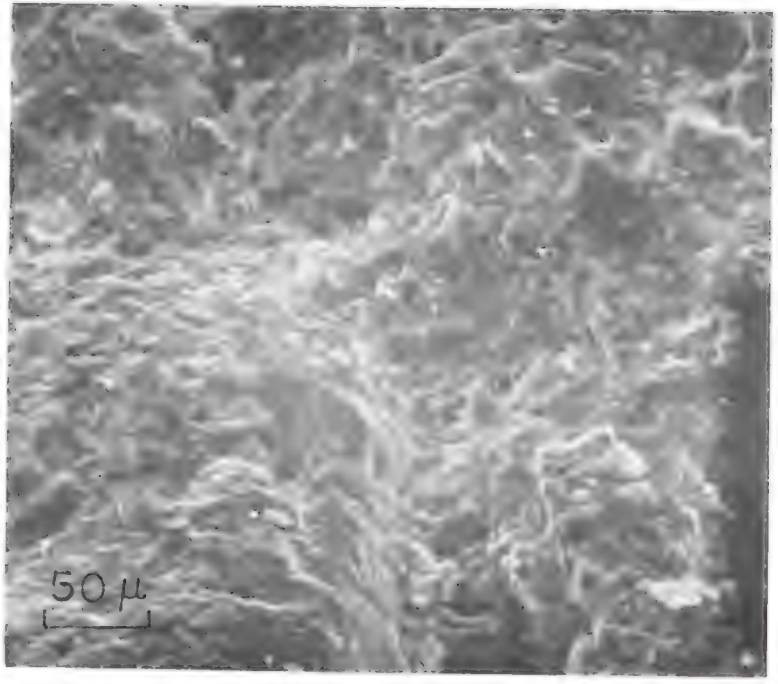

Figure 222. Crack at the Paste-Aggregate Interface in a Previously Unloaded Specimen (1-0.00-19)

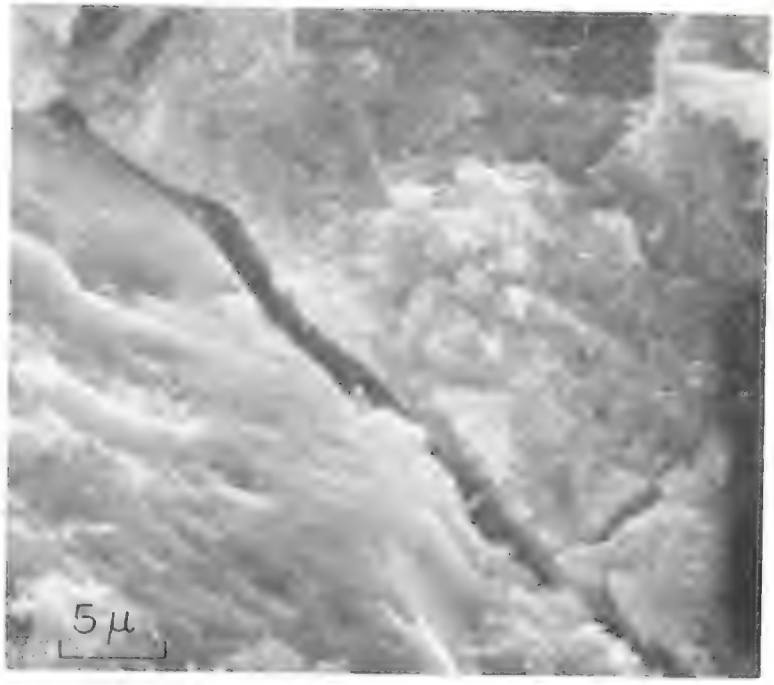

Figure 223. Enlargement of Interfacial Crack in Unloaded Specimen (1-0.00-20)

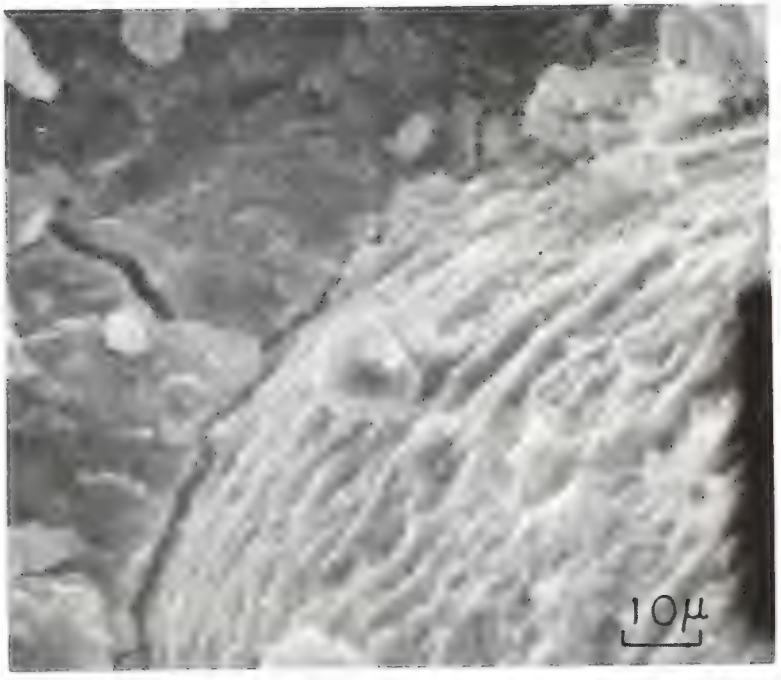

Figure 224. Enlargement of Crack in Unloaded Specimen (1-0.00-21)

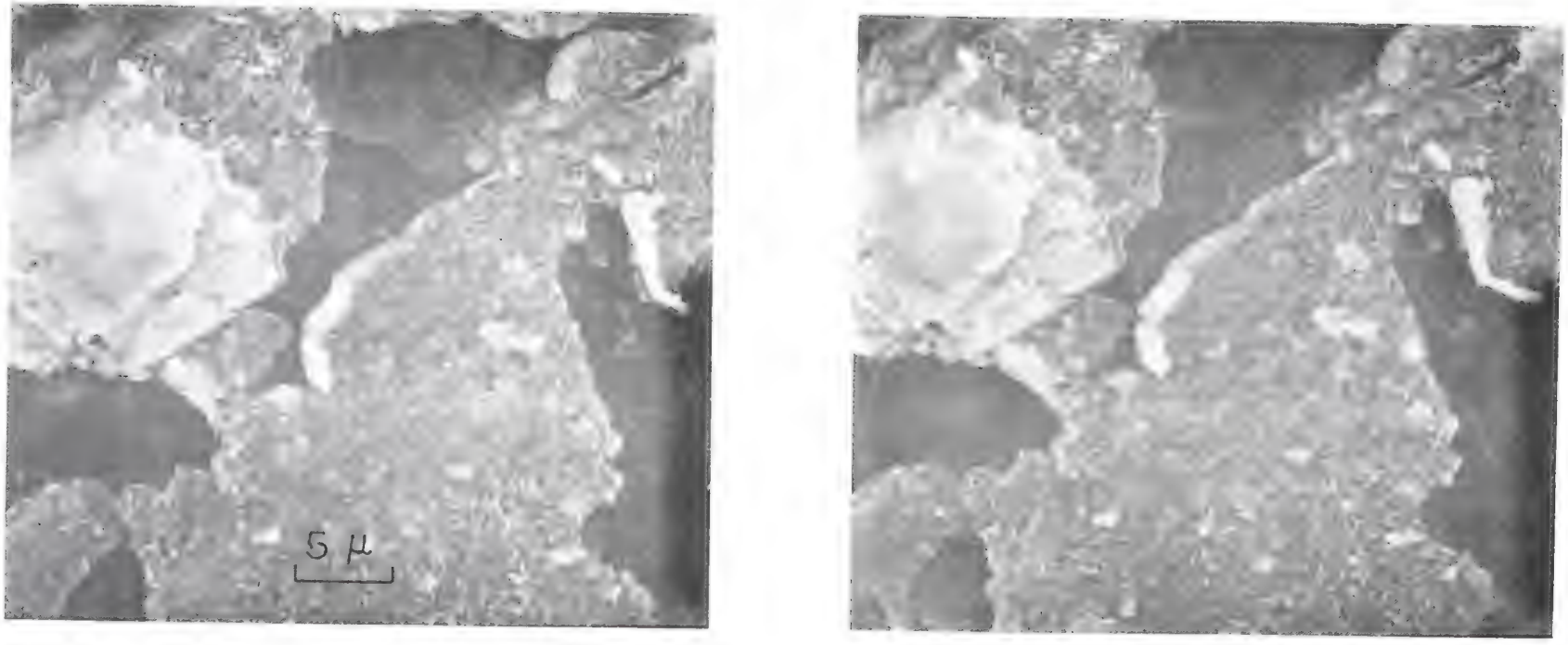

Figure 225. Stereomicrograph of Duplex Film on Sand Grain (1-0.30-6)

Figure 226. Enlargement of Duplex Film Shown in Figure 225 (1-0.30-4)

No.	C/S	C/A	C/$\bar{S}$
1	0.22	No A	No $\bar{S}$

Figure 227. Enlargement of Duplex Film Showing the Foreshortened Nature of the C-S-H (1-0.30-5)

No.	C/S	C/A	C/$\bar{S}$
1	0.14	No A	No $\bar{S}$

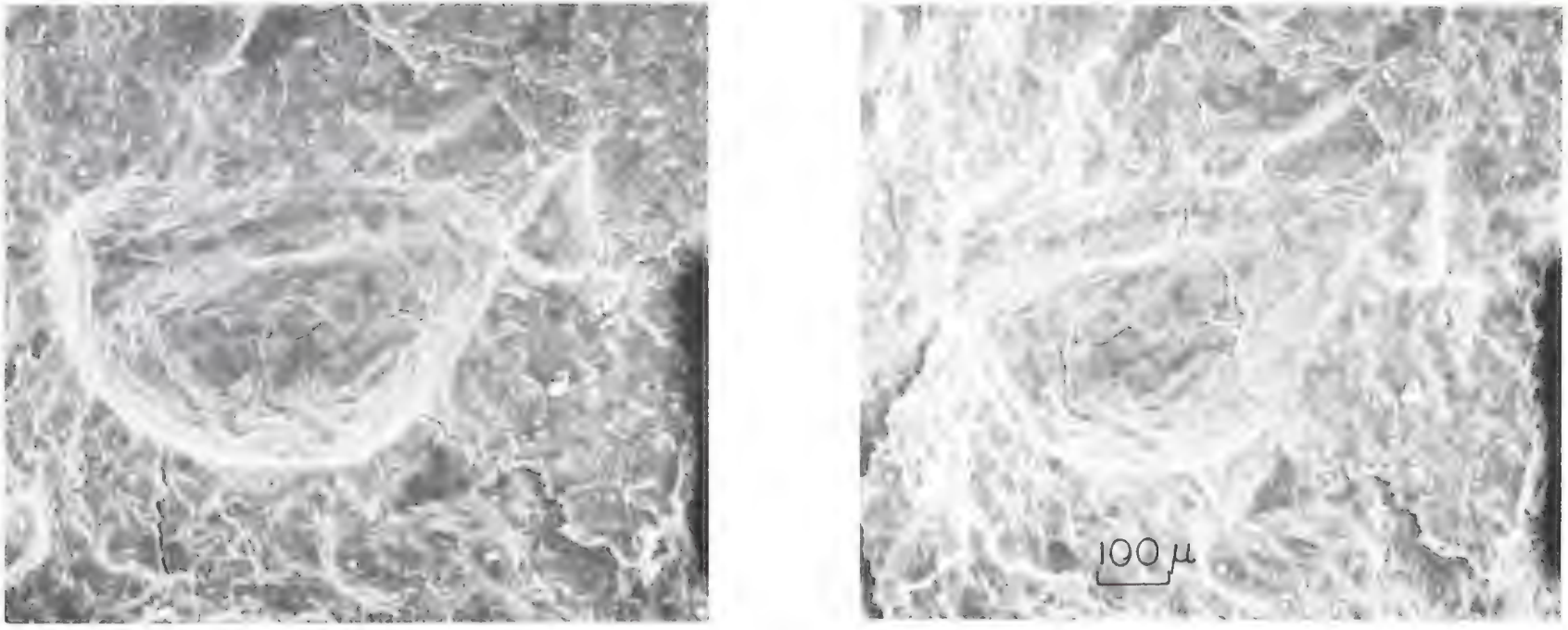

Figure 228. Stereomicrograph of Sand Grain Socket (1-0.30-9)

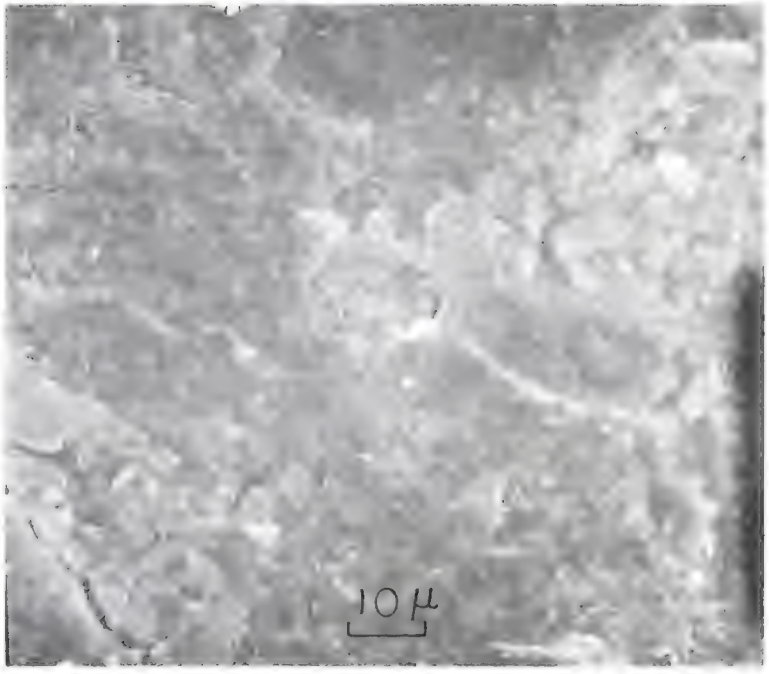

Figure 229. Undulating Duplex Film Reflecting the Topography of the Sand Grain Surface From Which It Separated (1-0.30-7)

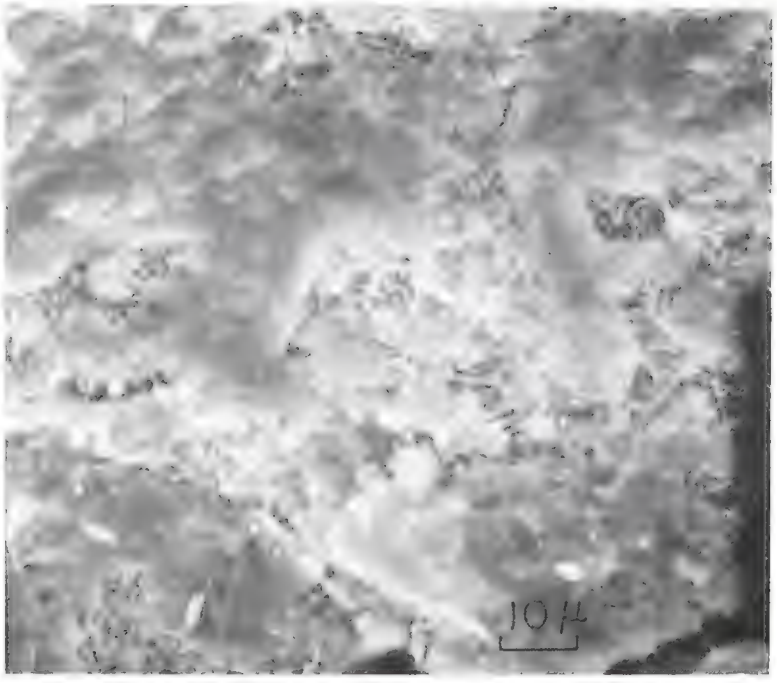

Figure 230. Duplex Film Apparently Underlain by Acicular Ettringite Crystals (1-0.30-8)

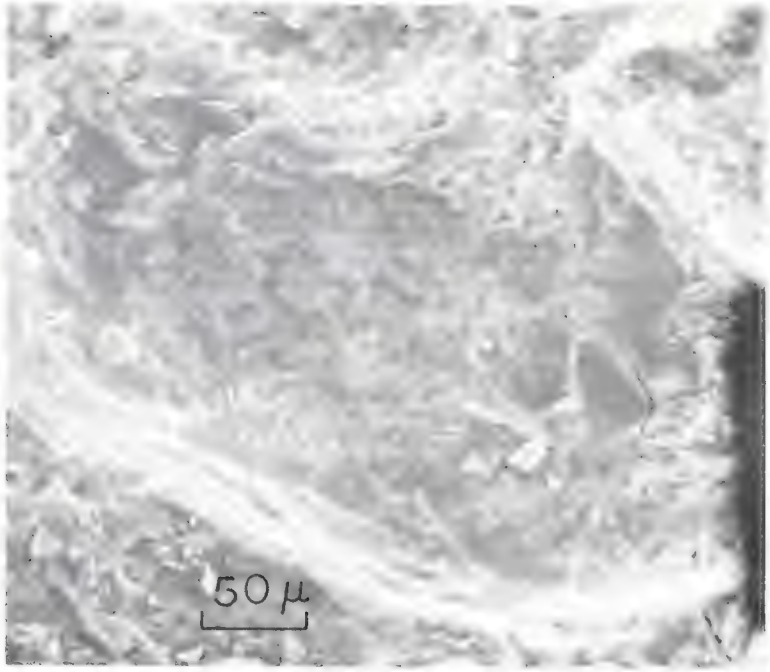

Figure 231. Duplex Film in a Grain Socket Reflecting the Underlying Linear Features (1-0.30-2)

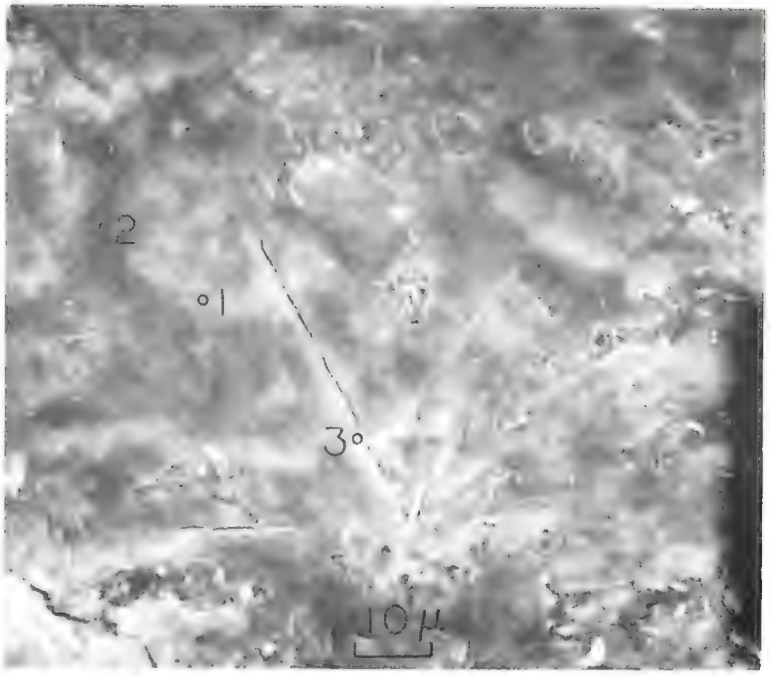

Figure 232. Enlargement of an Area Showing Underlying On-Edge Crystals (Enlargement of Figure 231)

No.	C/S	C/A	C/$\bar{S}$
1	12.44	No A	76.63
2	9.60	No A	46.06
3	13.25	No A	138.85

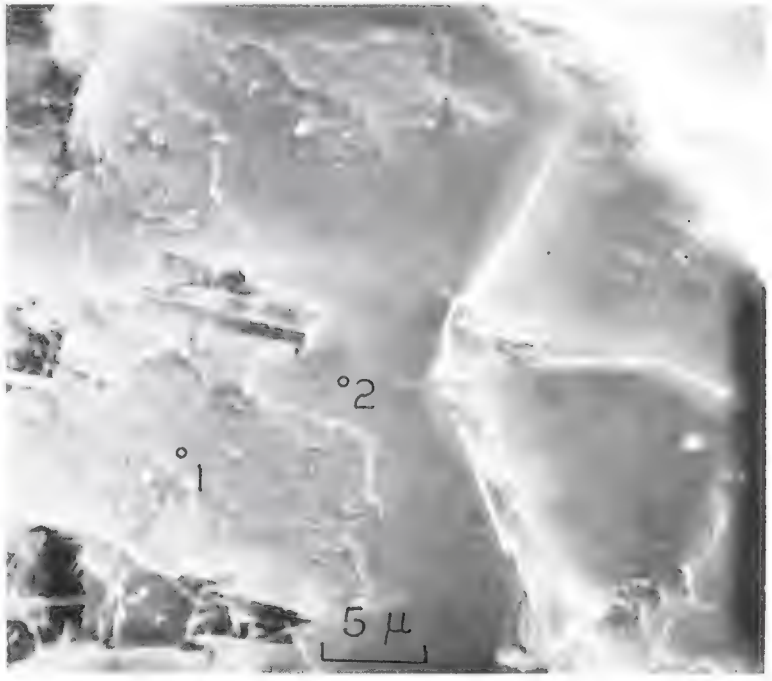

Figure 233. Duplex Film and Underlying Secondary Lime (1-0.30-1)

No.	C/S	C/A	C/$\bar{S}$
1	25.85	No A	92.04
2	12.49	No A	78.55

Figure 234. Secondary Lime Layer Appears to be Replaced by Ettringite Needles Between the Paste and Duplex Film (1-0.30-11)

Figure 235. Ettringite Needles Filling Interfacial Void (1-0.30-12)

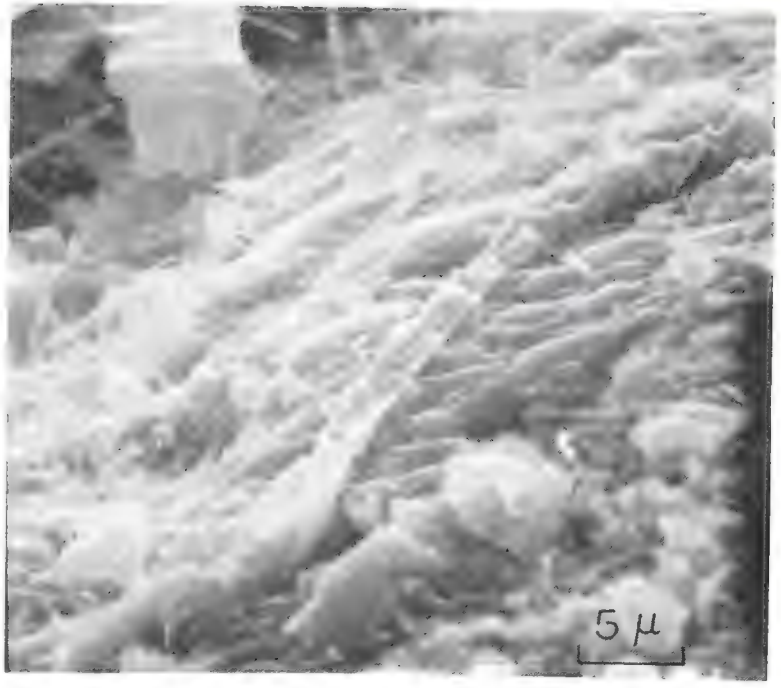

Figure 236. Close-up View of Duplex Film on Irregular Sand Surface (1-0.30-13)

Figure 237. Mode of Mechanical Bonding or Interlock (1-0.30-10)

No.	C/S	C/A	C/$\bar{S}$
1	0.11	No A	No $\bar{S}$

Figure 238. Crack Following Paste-Aggregate Interface (1-0.60-2)

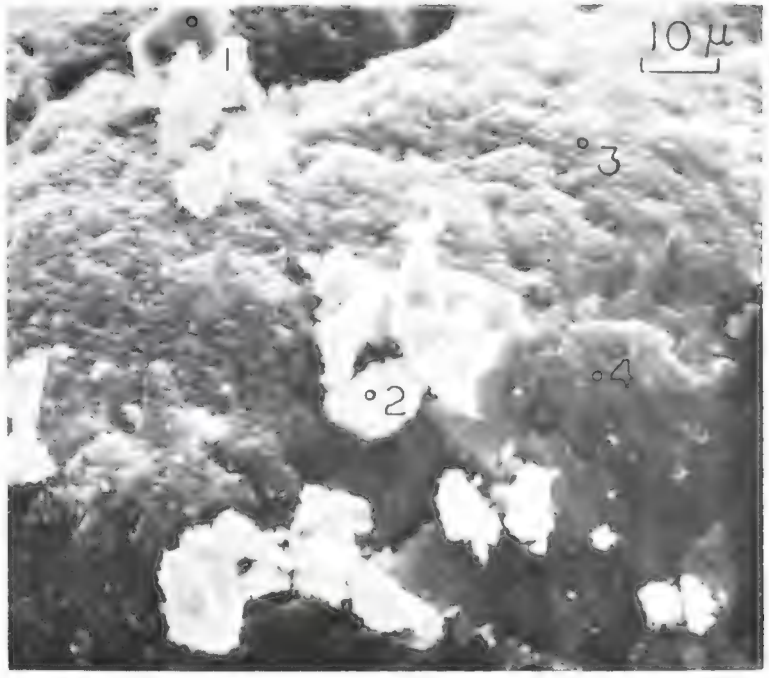

Figure 239. Hydration Products Remaining on Sand Grain (1-0.60-3)

No.	C/S	C/A	C/$\bar{S}$
1	2.38	No A	No $\bar{S}$
2	0.51	7.47	33.04
3	0.12	No A	No $\bar{S}$
4	0.12	No A	No $\bar{S}$

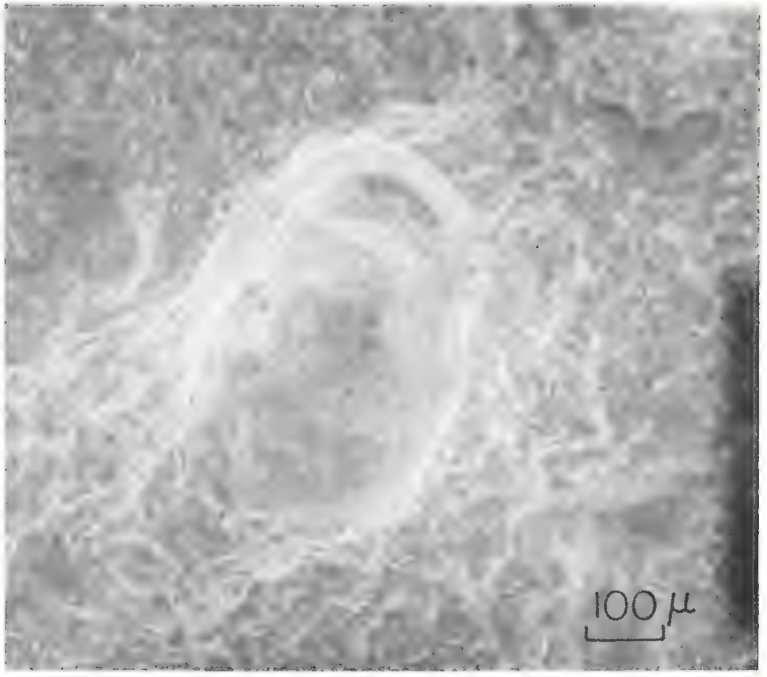

Figure 240. Low Magnification View of Sand Grain in Cement Paste (3-0.00-7)

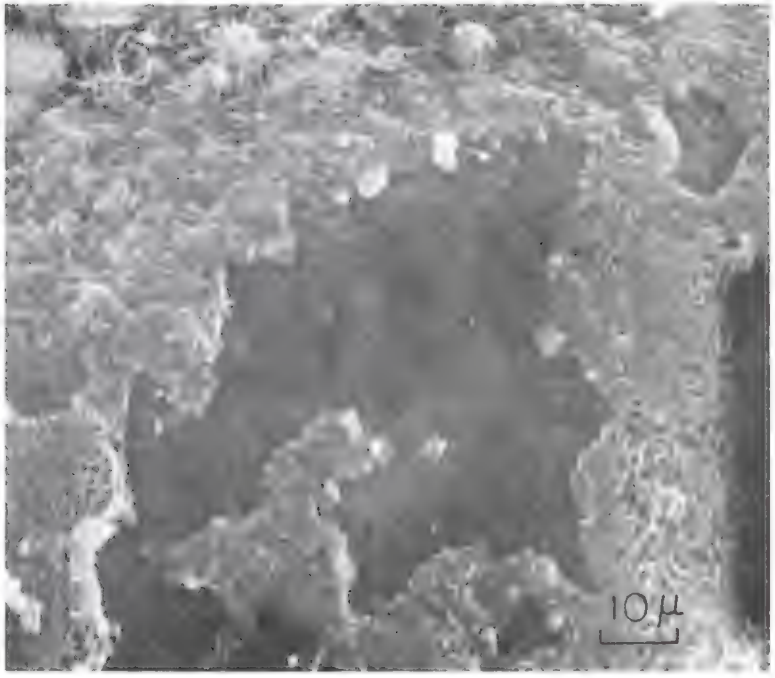

Figure 241. Duplex Film on Sand Grain (3-0.00-8)

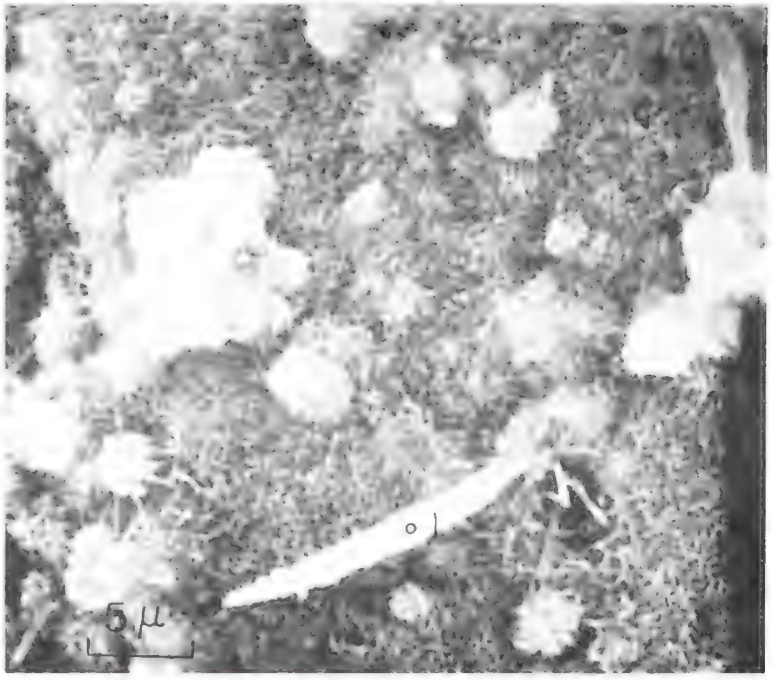

Figure 242. Duplex Film, Small Cement Grains, and an On-Edge Crystal on a Sand Grain Surface (3-0.00-6)

No.	C/S	C/A	C/$\bar{S}$
1	0.44	No A	118.52

Figure 243. Aggregation of Cement Grains Encapsulated by Lime on a Sand Grain (3-0.00-11)

Figure 244. General View of Massive Lime on Duplex Film (3-0.00-4)

Figure 245. Enlargement of Massive Lime on Duplex Film (3-0.00-2)

Figure 246. Enlargement of Duplex Film and Massive Lime Contact (3-0.00-1)

No.	C/S	C/A	C/$\bar{S}$
1	2.72	109.67	38.81

Figure 247. Sand Grain Socket at Low Magnification (3-0.00-12)

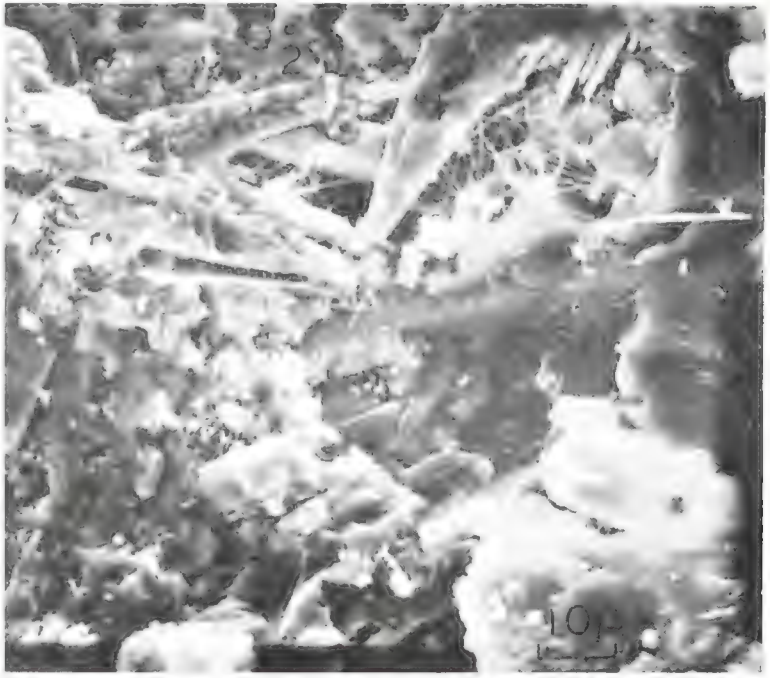

Figure 248. Various Familiar Structures at Bottom of Grain Socket Shown in Figure 247 (3-0.00-13)

No.	C/S	C/A	C/$\bar{S}$
1	15.55	No A	300.51
2	No S	No A	No $\bar{S}$

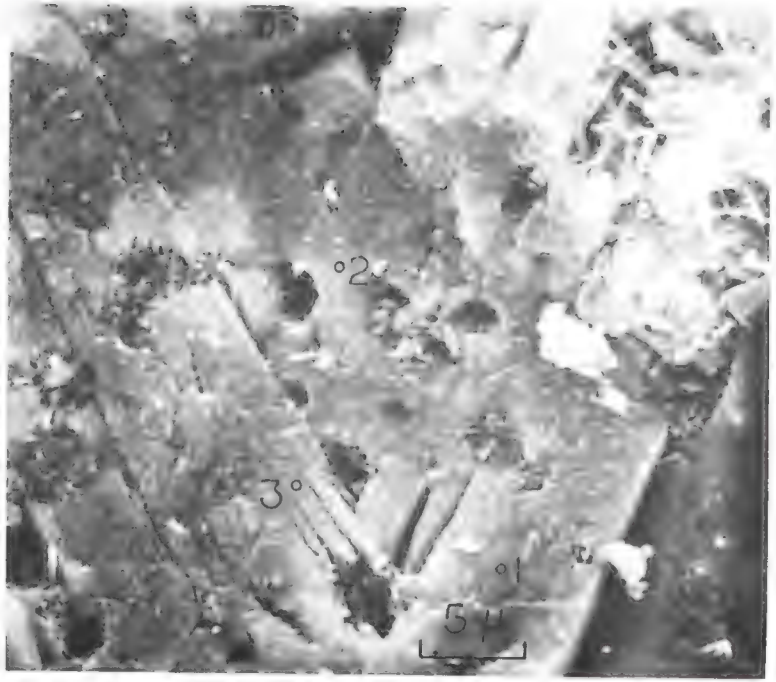

Figure 249. Secondary Lime and Lime with Good Cleavage at Bottom of Grain Socket (3-0.00-14)

No.	C/S	C/A	C/$\bar{S}$
1	19.89	No A	No $\bar{S}$
2	121.72	1021.84	No $\bar{S}$
3	89.19	170.92	No $\bar{S}$

Figure 250. High Magnification of Secondary Lime Shown in Figure 249 (3-0.00-15)

Figure 251. Residual Shell in Mortar Specimen Near the Aggregate Surface (3-0.00-9)

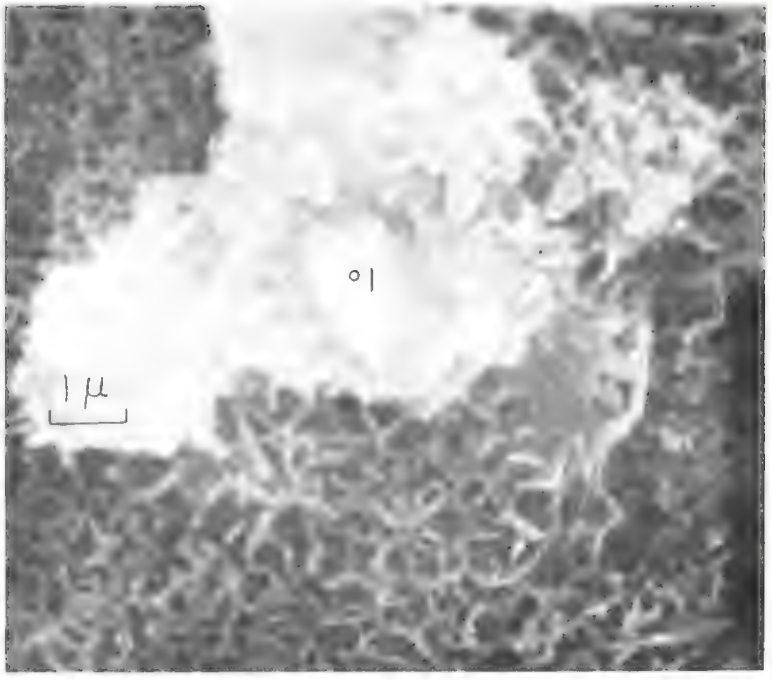

Figure 252. Possible Hadley Grain on Duplex Film Exhibiting a Reticulated Network C-S-H Gel (3-0.00-5)

No.	C/S	C/A	C/$\bar{S}$
1	0.88	No A	74.48

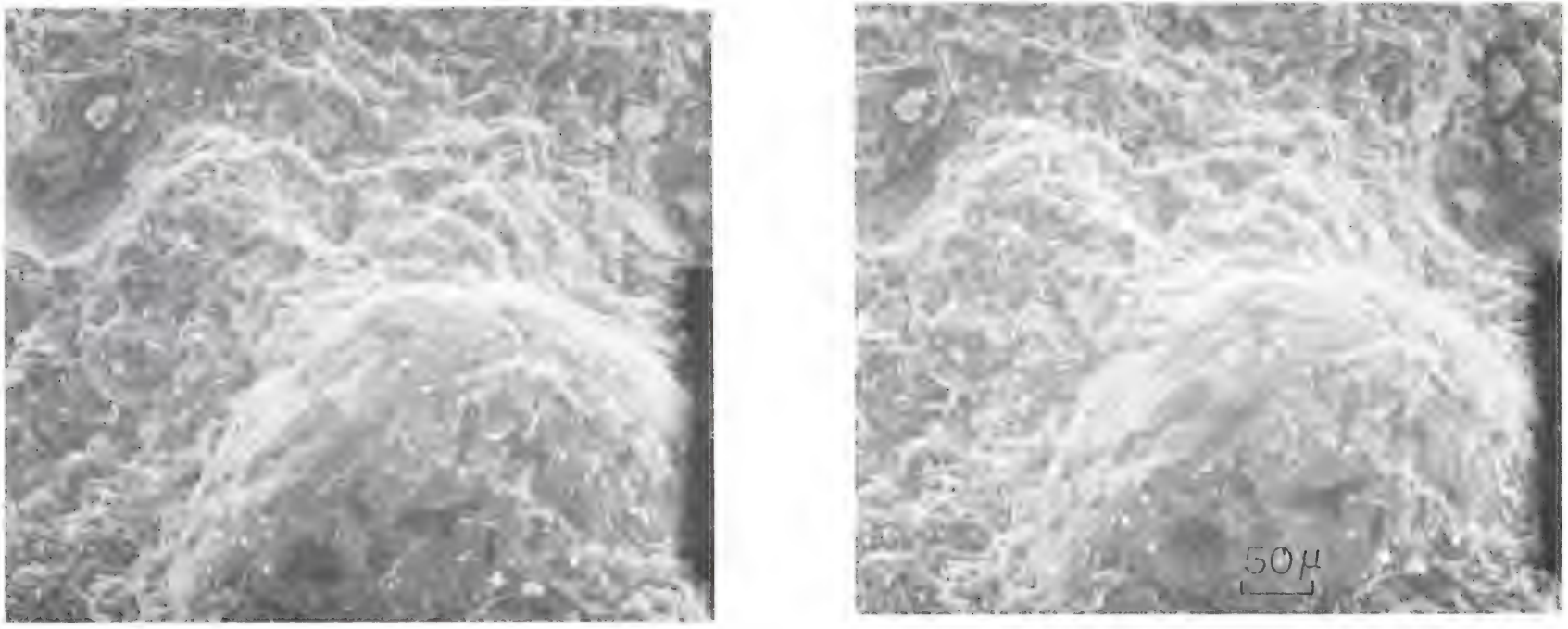

Figure 253. Stereomicrograph of Sand Grain in Paste Matrix (3-0.30-4)

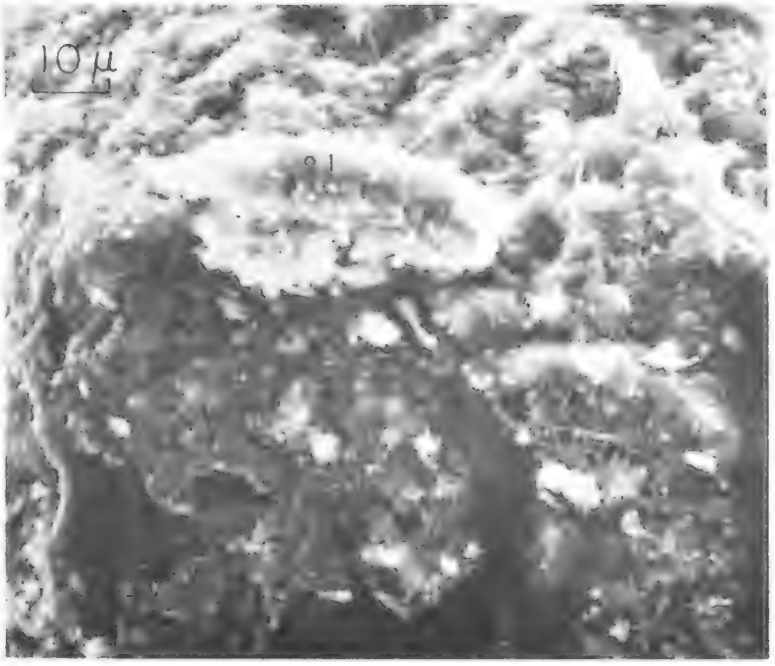

Figure 254. Hydration Products on Sand Grain (3-0.30-2)

No.	C/S	C/A	C/$\bar{S}$
1	1.91	0.19	0.12

Figure 255. Enlargement of Duplex Film--Aggregate Separation Shown in the Center of Figure 254.

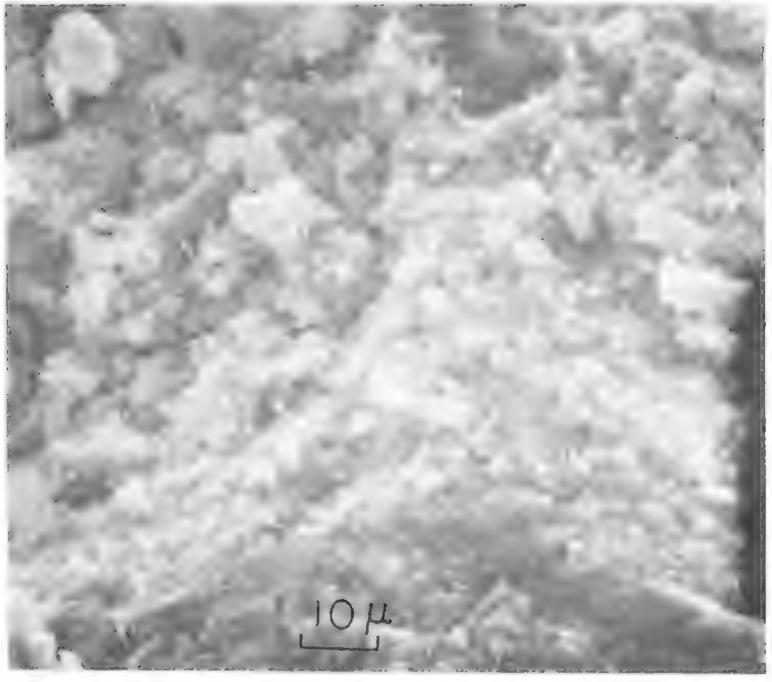

Figure 256. Duplex Film with Adhering Small Cement Grains on Sand Grain (3-0.30-7)

Figure 257. Crack Immediately Behind the Duplex Film (3-0.30-6)

Figure 258. Bottom of Sand Grain Socket (3-0.30-9)

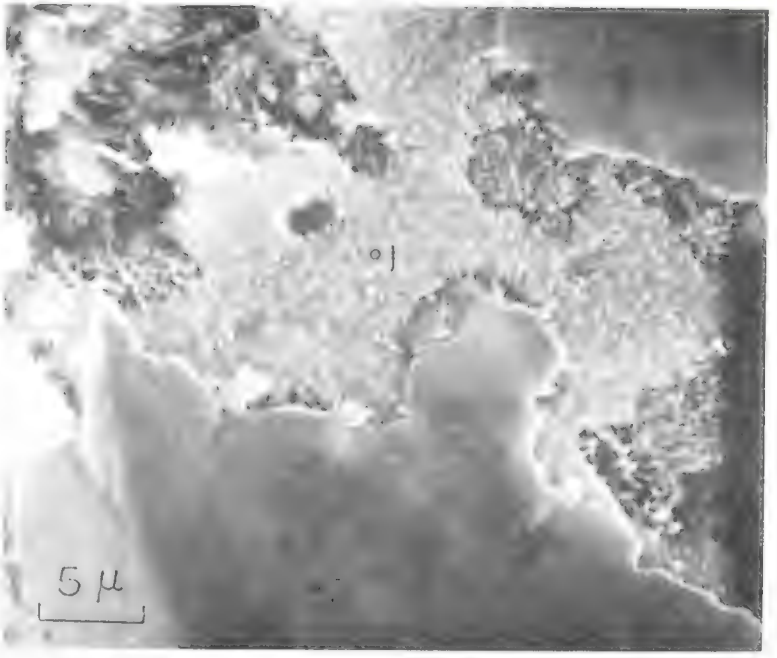

Figure 259. Enlargement of Figure 258 Showing Secondary Lime and Duplex Film (3-0.30-8)

No.	C/S	C/A	C/$\bar{S}$
1	40.68	No A	No $\bar{S}$
2	7.94	1206.99	64.10
3	26.14	682.74	1377.97

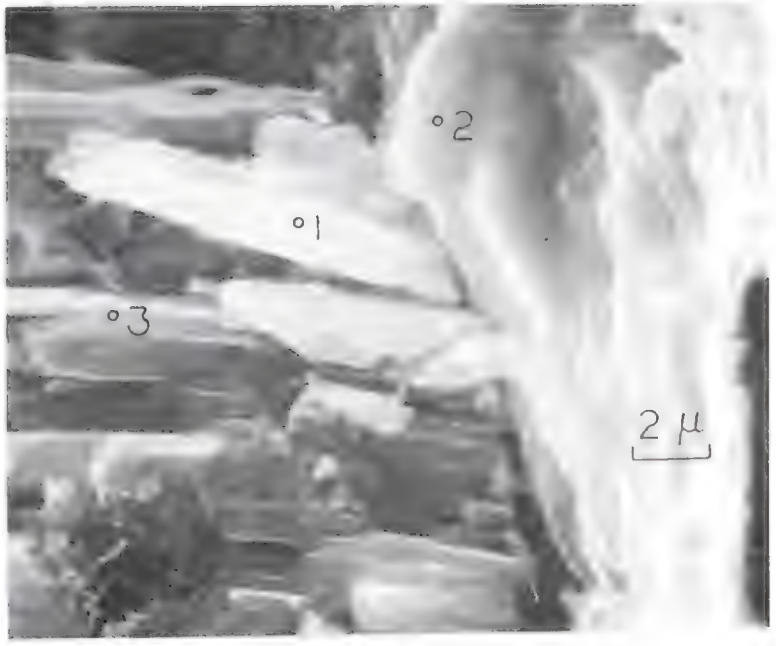

Figure 260. Massive Lime Beginning to Separate from the Paste-Aggregate Interface (3-0.30-1)

No.	C/S	C/A	C/$\bar{S}$
1	2.09	No A	0.12
2	0.36	No A	61.73
3	8.04	No A	97.98

Figure 261. Microcrack Propagating Around Aggregate and On Into the Paste (3-0.30-10)

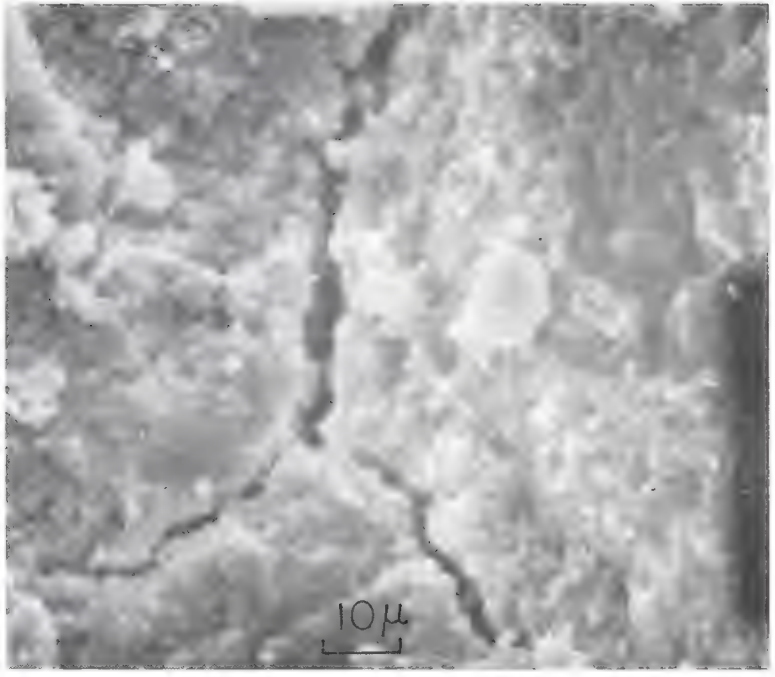

Figure 262. Branched Crack Near the Aggregate Surface (3-0.30-11)

Figure 263. Microcrack Following the Aggregate Outline (3-0.60-2)

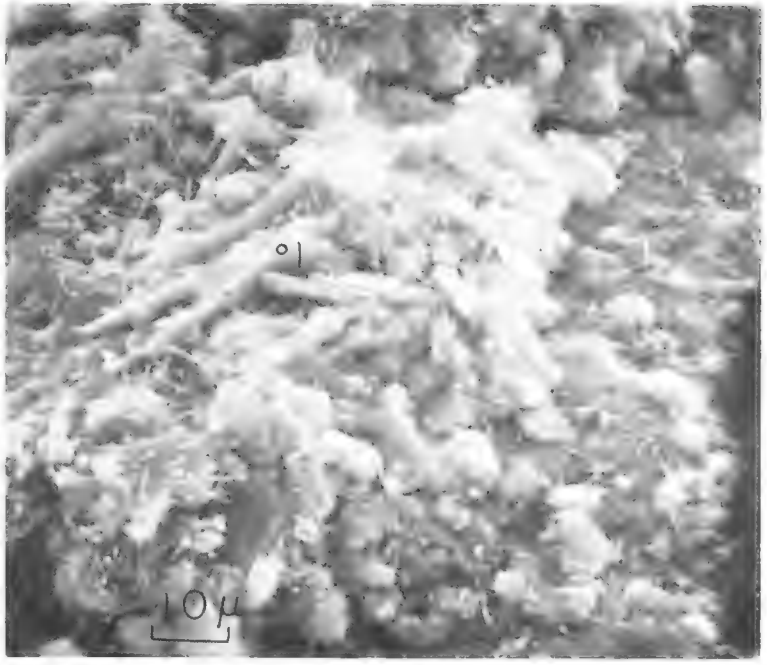

Figure 264. Enlarged View of Cement Grain Aggregation Shown in Figure 263 (3-0.60-1)

No.	C/S	C/A	C/$\bar{S}$
1	13.16	565.08	214.97

Figure 265. Small Hadley Grain on Duplex Film (3-0.60-3)

No.	C/S	C/A	C/$\bar{S}$
1	0.11	19.43	14.97

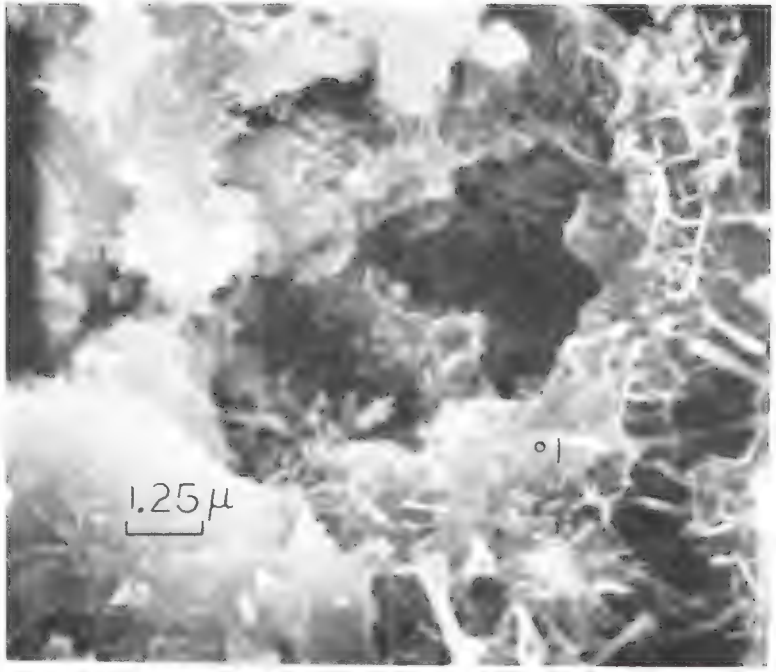

Figure 266. Residual Shell Near Aggregate Surface (3-0.60-4)

No.	C/S	C/A	C/$\bar{S}$
1	4.59	0.19	17.00

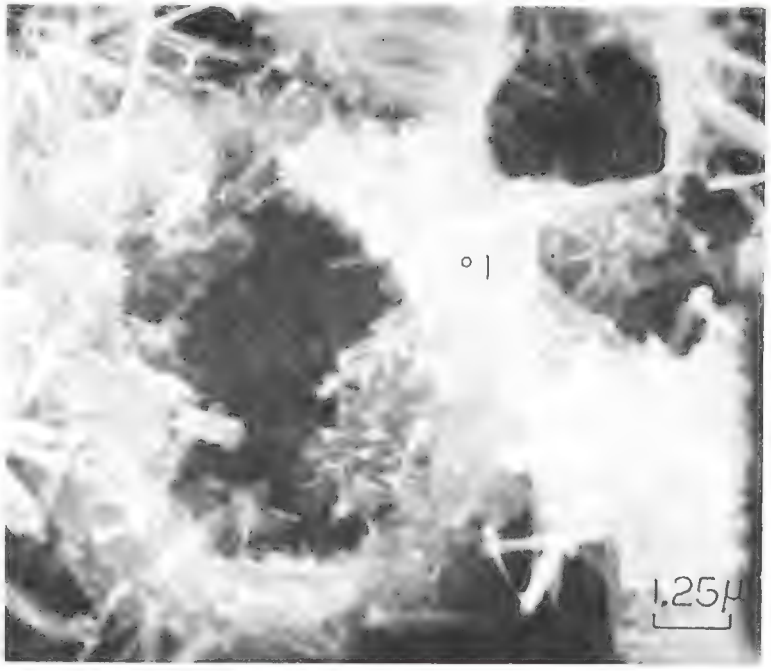

Figure 267. Residual Shells Near Aggregate Surface (3-0.60-5)

No.	C/S	C/A	C/$\bar{S}$
1	0.11	31.66	15.35

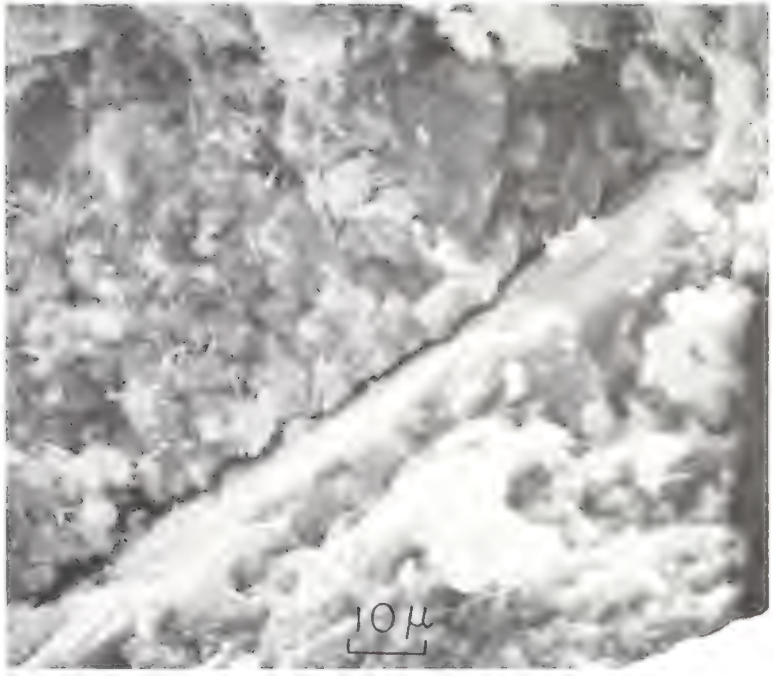

Figure 268. Crack Passing Between Massive Lime and Duplex Film (3-100-1)

Figure 269. Close-up View of Massive Lime Separation from Duplex Film (3-100-2)

Figure 270. Photo-Mosaic of Cracks Occurring Around a Sand Grain in a 3-0.00 Mortar

3-0.00-M-26

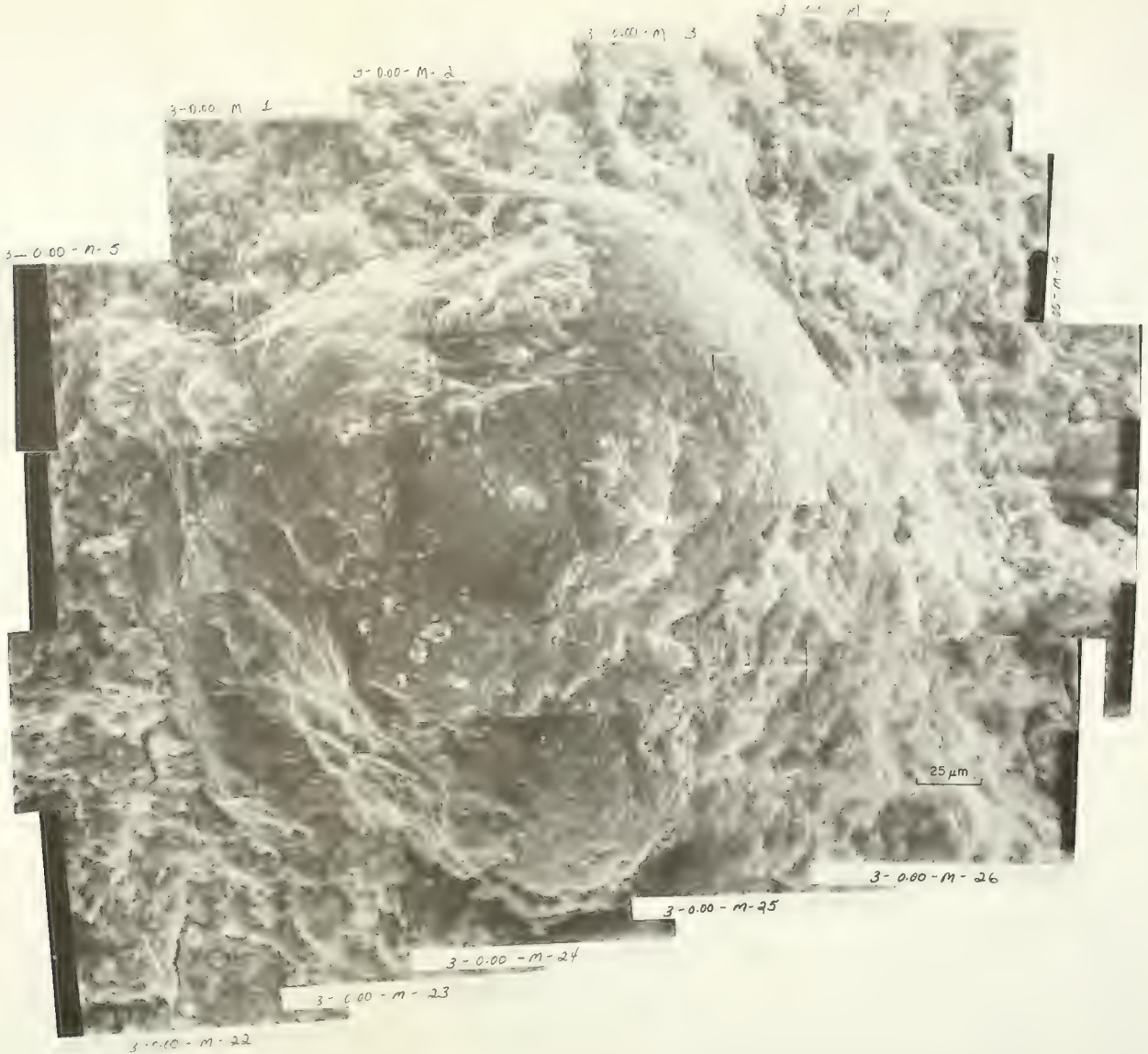
3-0.00-M-1
3-0.00-M-2
3-0.00-M-3
3-0.00-M-4
3-0.00-M-5
25 µm
3-0.00-M-22
3-0.00-M-23
3-0.00-M-24
3-0.00-M-25
3-0.00-M-26

Figure 271. Photo-Mosaic of Cracks Occurring Around a Sand Grain in a 3-0.60 Mortar

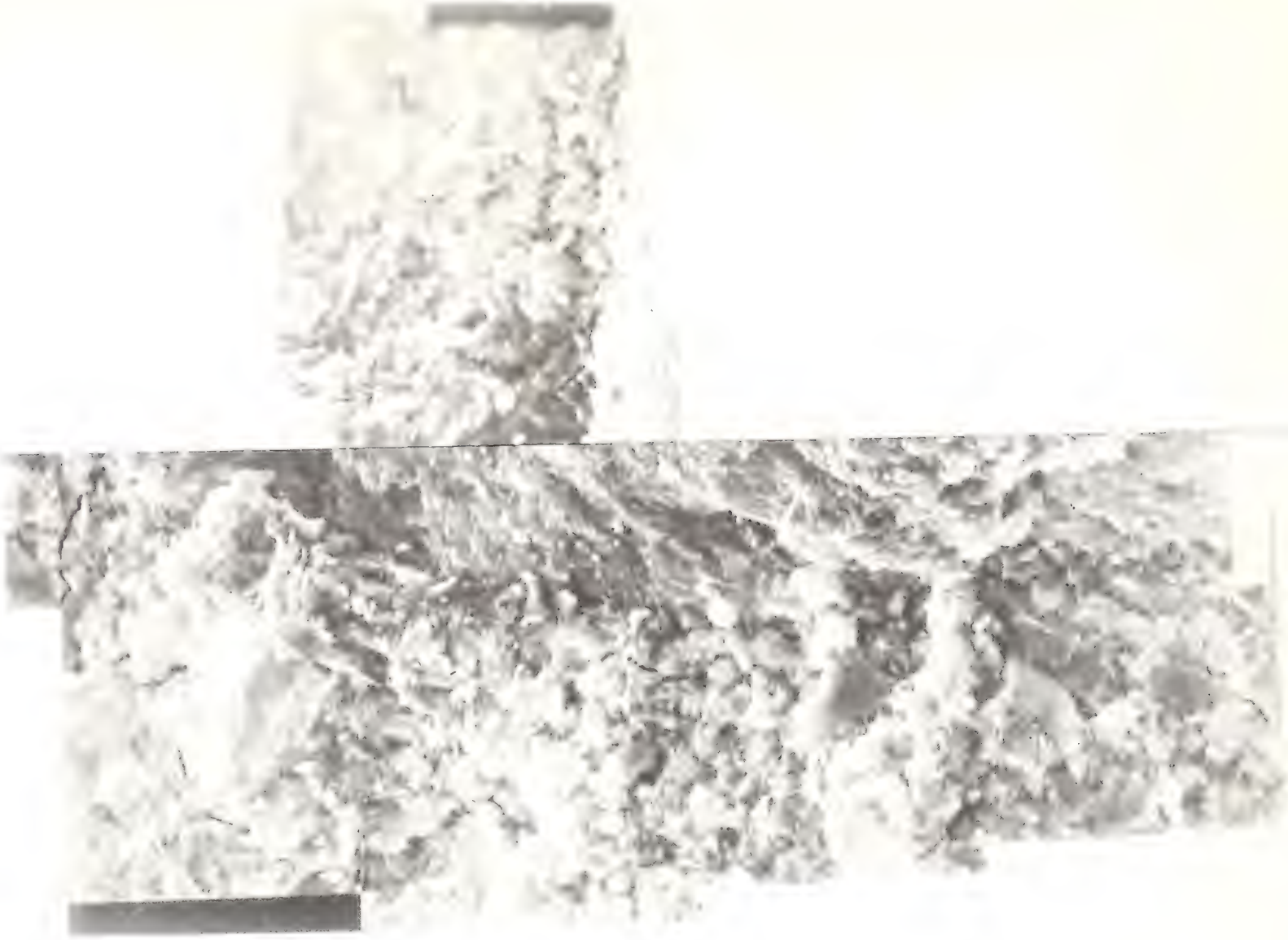

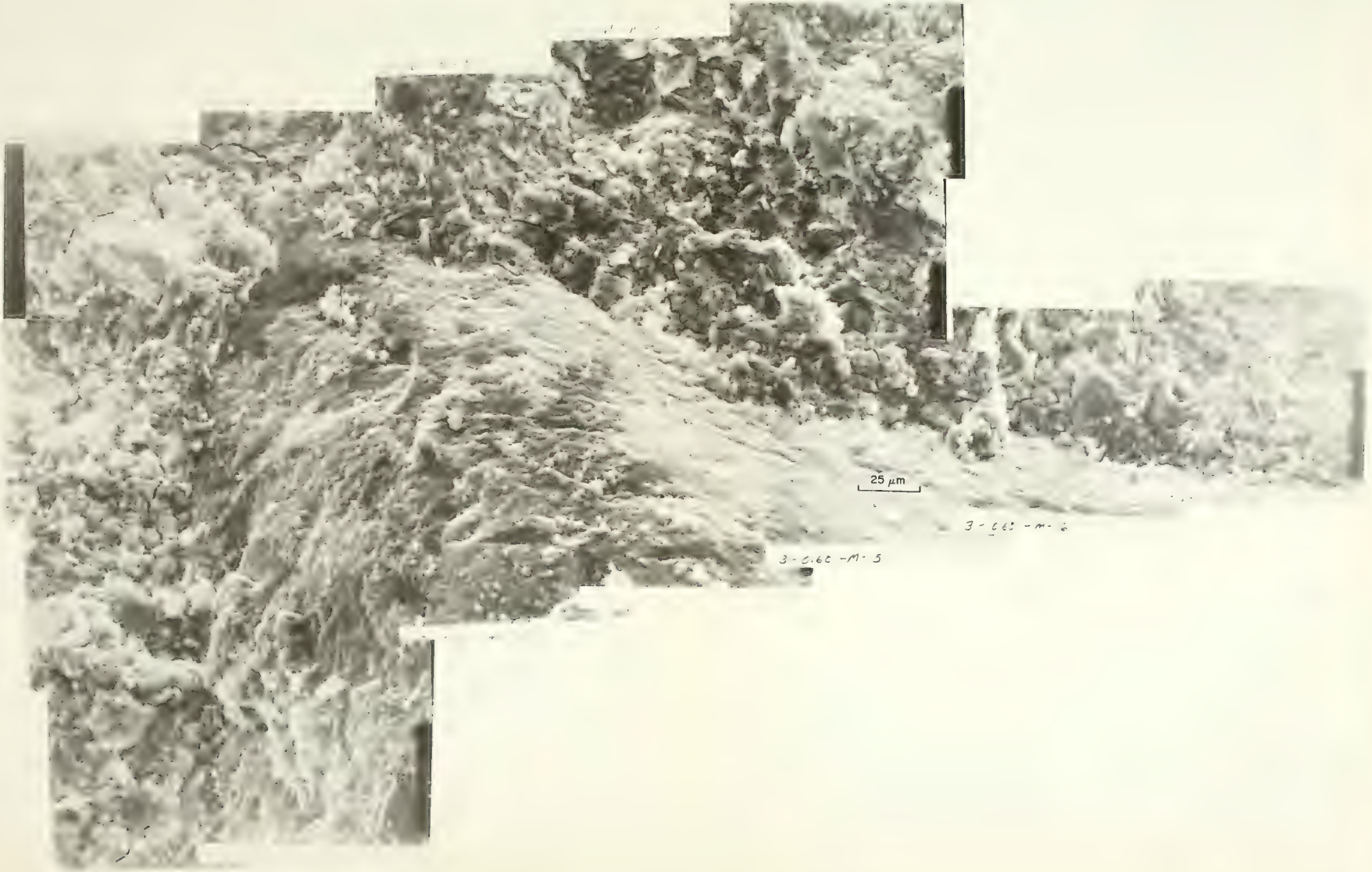
25 µm
3-C.6C-M-5

Figure 272. Photo-Mosaic of Interfacial Cracks
in a 1-0.00 Specimen

25 μm

25 μm

Figure 273. Photo-Mosaic of Interfacial Cracks in a 1-0.60 Specimen

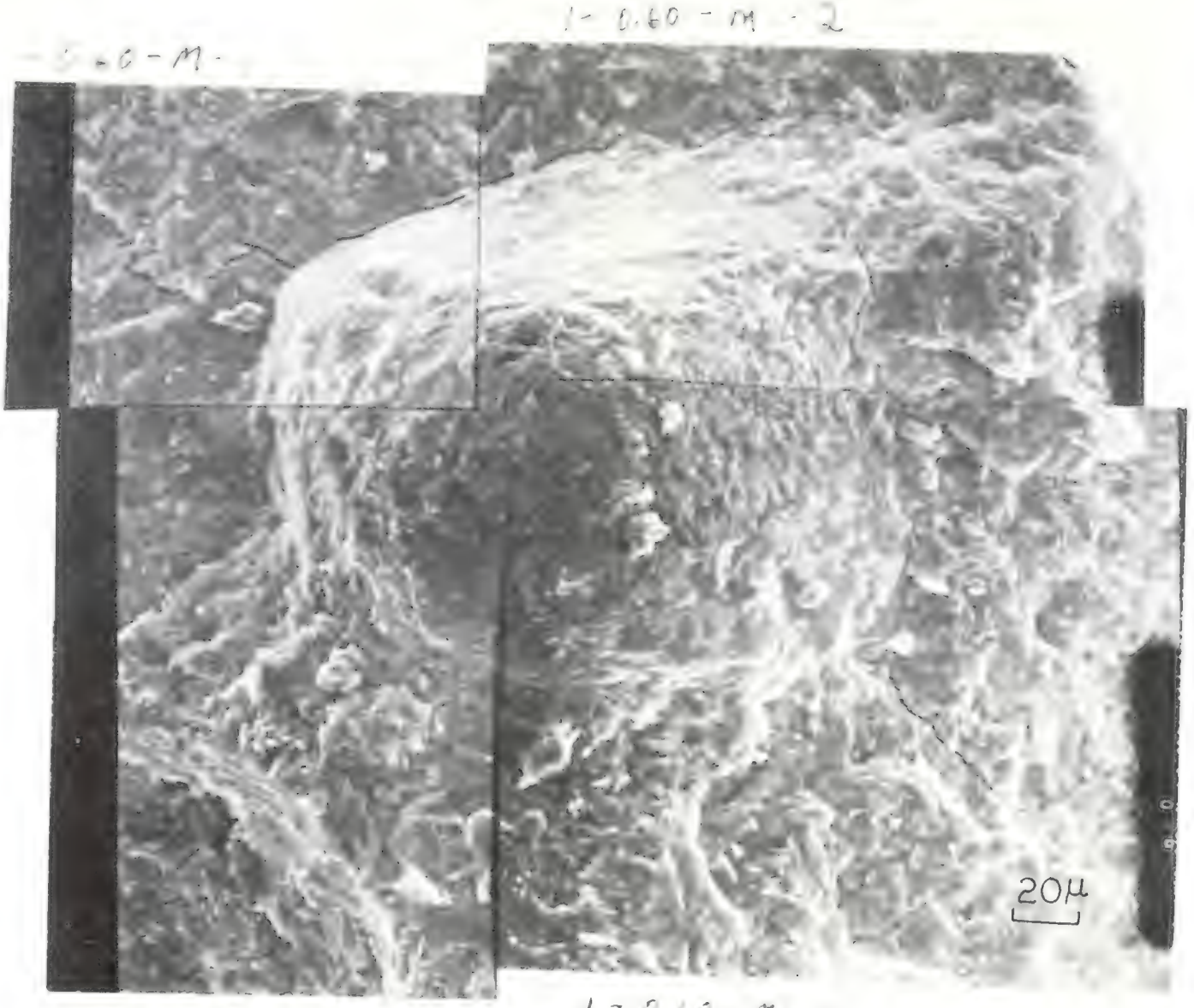
1-0.60-M-2
1-0.60-M-3
20μ

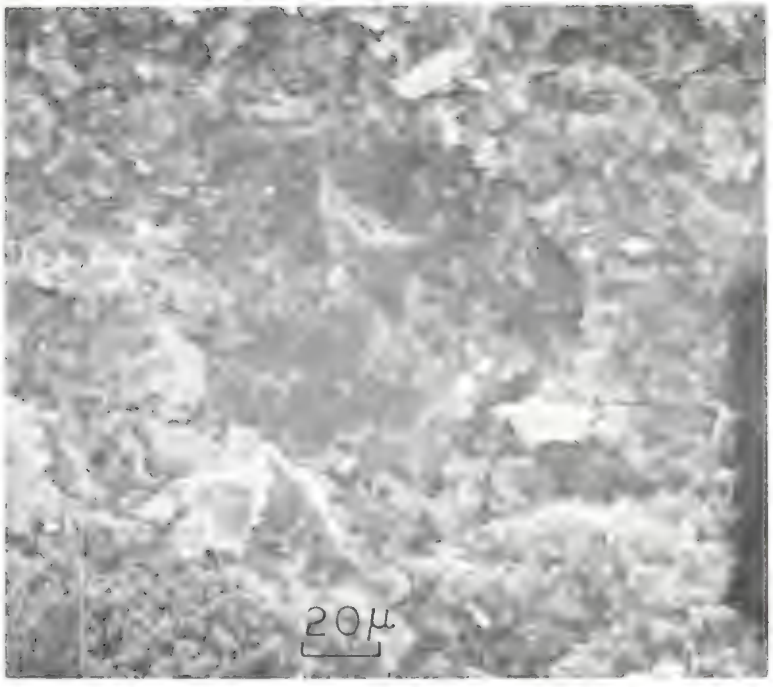

Figure 274. Sand Grain at the Mortar-Glass Interface of a Specimen Similar to the Type I Specimen (MA3201-1)

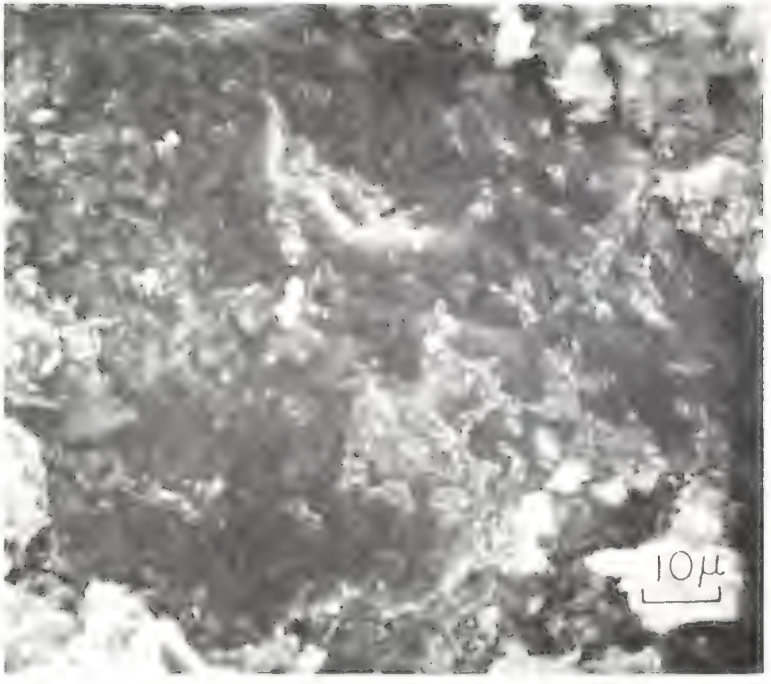

Figure 275. Enlargement of Figure 274 Showing the Crack Location and Hydration Products on the Sand Grain (MA3201-3)

Figure 276. Interfacial Cracks Occur in Mortars Subjected to Shrinkage Only

MA 3201-6

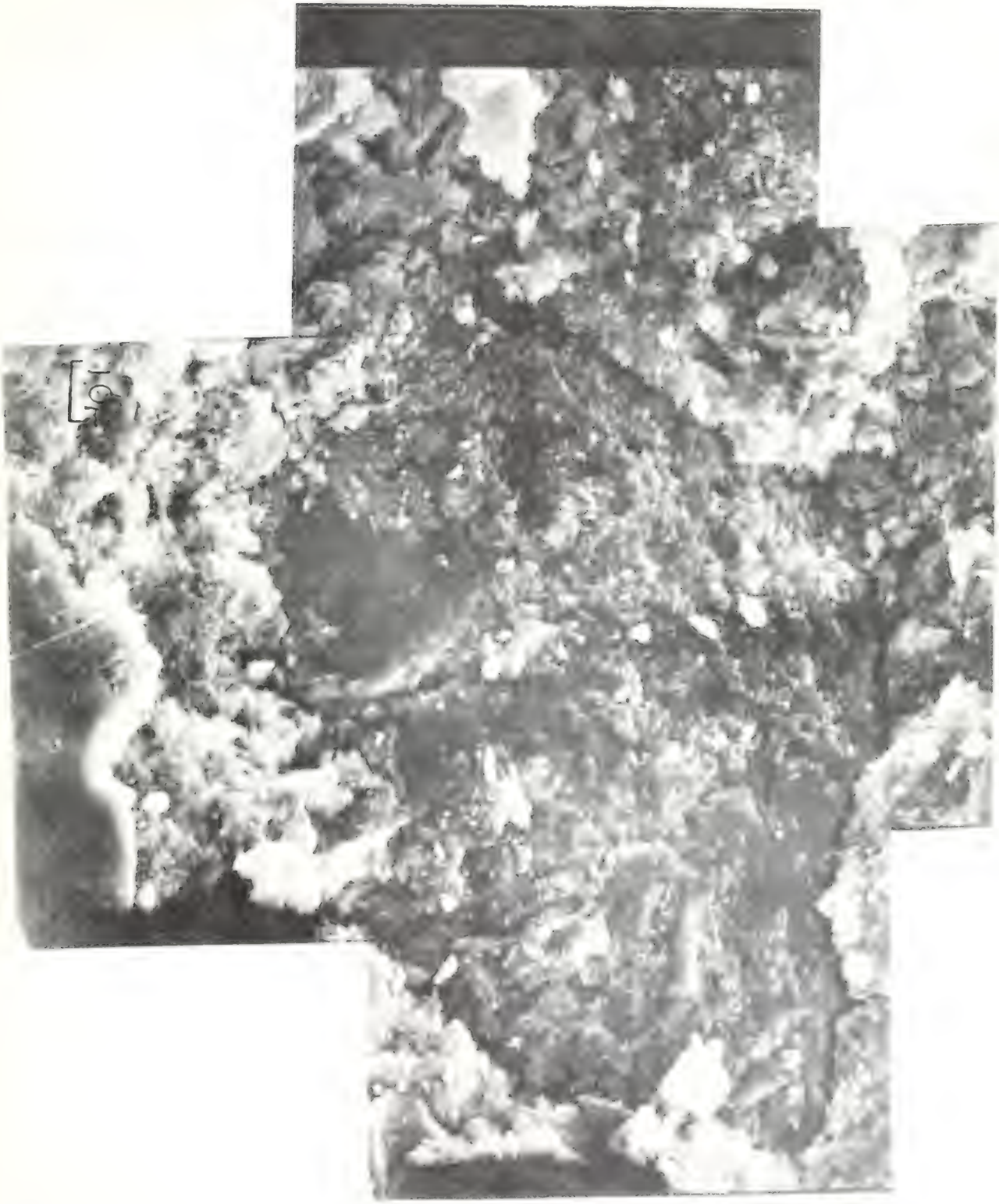

MA 3201-6

MA 3201-6

MA 3201-6

MA 3201-6

Figure 277. Typical Large Crack Resulting From Unstable Crack Propagation at Failure (1-1.00)

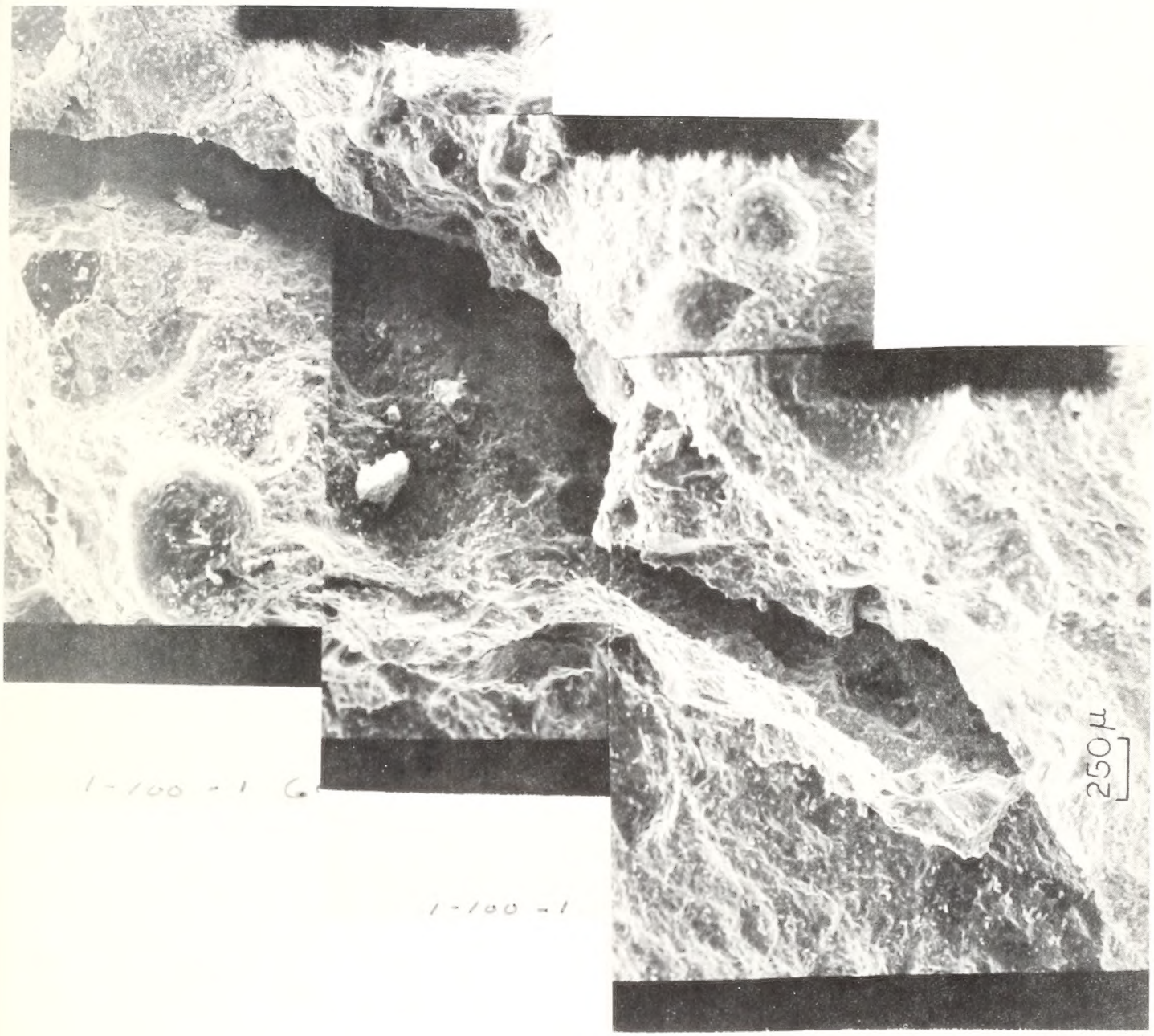

1-100-1 60X

COVER DESIGN BY ALDO GIORGINI